REACTION KINETICS
OF NICKEL AND IRON DROPS
WITH FLOWING GASES

by

Arthur Robert Palmer

A Thesis submitted to the University of London
for the degree of Doctor of Philosophy

January, 1971

ABSTRACT

The kinetics of heterogeneous reactions at high temperatures were studied by exposing electro-magnetically levitated drops of nickel and iron to flowing gases.

The rates of reduction of nickel-oxygen alloys in hydrogen and the rate of solution of oxygen in pure nickel showed that the transport of solute atoms in liquid metals under these conditions is much more rapid than other workers had suggested.

Gaseous products are formed by the combination of adsorbed atoms on the surface of the liquid metal. The surface activity of solutes is therefore of primary importance. Overall reaction rates can be controlled by the kinetics of these surface reactions when the concentration of an adsorbed reactant is low. In the oxidation of sulphur from nickel-sulphur alloys, the rate can become chemically controlled when the surface concentration of either oxygen or sulphur is low.

During the oxidation of iron-carbon and nickel-carbon alloys, the change in rate-control at carbon concentrations below about 0.4% is due to a decrease in the rate of the chemical reaction at the metal surface, which is in turn caused by the low concentration of adsorbed carbon atoms. The evidence does not support the earlier hypothesis that the slow diffusion of dissolved carbon to the metal surface controls the reaction rate.

The carbon monoxide "boil" has been shown to be independent of the formation of metal oxides. When iron-carbon drops react with oxygen diluted with helium, the "boil" can occur at supersaturations of carbon monoxide estimated to be below 10 atmospheres.

Acknowledgements

The writer would like to express his gratitude to Professor F.D. Richardson, F.R.S., of the Royal School of Mines for valuable guidance and stimulating discussions throughout the work.

Thanks are due to Mr. L.E. Leake who had constructed much of the apparatus for controlling the gas flows and who assisted in making the high-speed cine films.

The writer is greatly indebted to the Management of Atlas Steels Company of Welland, Ontario and to the Board of Directors of the parent company, Rio Algom Mines Ltd. of Toronto, Ontario, for permitting the long leave and providing financial support for the research and for the writer.

CONTENTS

Page

I. INTRODUCTION

The research which will be described in this thesis began with the purpose of investigating an anomaly in phase nucleation. Other workers had shown that carbon monoxide bubbles could nucleate in drops of liquid iron-carbon alloy in the absence of any solid phase. Supersaturation of the gas was calculated to be less than 100 atmospheres but theoretical estimates showed that pressures of 10,000 atmospheres should be necessary.

Electro-magnetically levitated drops of a nickel-oxygen alloy were reduced in hydrogen but this experimental system failed to produce the expected bubbles of water vapour. Examination of the reasons revealed that solutes such as oxygen were transported in the liquid metal much more rapidly than earlier workers had suggested. It appeared that the surface of the liquid metal and the adsorption of solutes on it might be important in heterogeneous reactions. Experiments on the oxidation of nickel-sulphur alloy drops showed that a chemical reaction between adsorbed species could be the rate-controlling step when a gas reacts with a dissolved element.

Alloys of carbon in nickel or iron were oxidised to determine whether surface chemical reactions were also important in decarburisation. The conditions at the time of the carbon monoxide "boil" reaction were of special interest in view of the original purpose of the research.

Because of the changing course of the research, it is not possible to present a literature survey of the whole field comprehensively and concisely and Section II instead describes the origins of the project. Particular attention is given to the decarburisation reaction which not only is

crucial to the manufacture of steel but also continues to pose problems of great theoretical interest in the field of high-temperature chemistry.

The methods used in calculating mass transport rates are set out in Section V, in which experiments to measure empirical constants are also described. Some ways of improving the methods of calculation are also proposed.

Notes:

All temperatures not otherwise designated are in degrees Centigrade.

All compositions of liquid and solid metals are given as weight percent. The same units apply in considerations of thermodynamic equilibrium.

In abbreviating 'Argon', the permitted alternative 'Ar' has been used to avoid confusion with the general symbol 'A' for an unspecified gas in mass transport theory.

The reference 'Distin' which appears frequently and without a number has been used for brevity and should be read as including his co-authors Hallett and Richardson (1).

II BACKGROUND TO THE RESEARCH

1. General

As recently as the early years of this century, the refining of the blast-furnace product to steel was little understood in scientific terms. Pioneers such as Herty in the 1920's began studying the changes that occur in the steel furnace and in the following decades, Schenck and notably Chipman investigated the physical chemistry of steelmaking reactions in the laboratory.

Attention focussed at first on thermodynamics: energy balances and the conditions for equilibrium. More recently, the kinetics of reactions have claimed more interest and physical chemistry has been supplemented by the theory of transport phenomena.

2. Work at the Royal School of Mines

Investigations in the early 1950's relating to metal refining were concerned mainly with reactions between slags and metals in crucibles. When the field of research expanded to include reactions between liquid metals and gases, the technique of electromagnetic levitation of metal drops was adopted.

The application of this phenomenon of levitation to solid and liquid metals was proposed in Germany in the 1920's but its development as a laboratory technique had to await the 1950's, when Okress and others in the USA began to explore its possibilities. Peifer (3) reviewed this development and described current equipment and its applications. Toop and Distin in their doctoral theses discussed control variables and some of the varied work employing the technique (1,2).

Levitation has the unique advantage of supporting a metal drop out of contact with any other liquid or solid phase. Interactions with crucible materials are eliminated and a large area of metal, in relation to its weight, is presented for reaction with the gas stream.

Toop (2) exploited this advantage in studying oxidation

equilbria and kinetics with nickel and copper drops. He found that the rate of oxidation of liquid copper appeared to be controlled by a slow chemical reaction at the phase interface but Glen (4) later showed how traces of silicon in the metal could oxidise to form a film which retarded reactions at the surface. Forster (5) took precautions to remove such films and studied reactions of copper and nickel with oxygen and sulphur. The rates of sulphurising, desulphurising and deoxidising copper were controlled by gaseous diffusion but a slow chemical reaction appeared to control the rate of oxidation of copper by CO_2, at least at temperatures up to 1500°C.

Hallett (6) made some studies of the fume formation from iron-carbon alloy drops. His calculations of the supersaturation of carbon monoxide when the "boiling" action began gave values as high as 100 atmospheres.

Distin investigated the processes of decarburisation and recarburisation with iron drops, the rate of vaporisation of iron and the rate of sulphur loss from iron/sulphur alloys in reactive and inert gases.

Because of the special relevance of decarburisation to the research to be described, other work on this basic reaction of steelmaking will be surveyed before Distin's work is discussed in more detail.

3, Decarburisation of Liquid Iron-Carbon Alloys

By the late 1950's, the essential thermodynamic data of steelmaking, including activities and interactions of carbon and oxygen in liquid iron (7-9) and the equilibria between these solutes (10-12) had been established. Interest in the reaction kinetics was developing at this time and by about 1961 several writers had discussed and summarised the kinetics of reactions in the open-hearth furnace (13-17). Chemical reaction theory applied to the carbon-oxygen reaction predicted a rate of "carbon drop" that was 10,000 times greater than that observed (14) and the rate-limiting effects of diffusion processes were recognised.

These contributions dealt with reactions between metal and oxidising slag and with the diffusion of carbon monoxide from the metal into bubbles of the same composition (see also ref. 18). The gaseous oxidation of iron-carbon alloys in crucibles was examined by Russian, Japanese and Canadian workers: among the more accessible accounts are those of Niwa and co-workers (19) and of Jamieson and Masson (20), who found that the rate was controlled by a gaseous diffusion step.

Baker, Warner and Jenkins (21) employed levitation in studying the gaseous oxidation reaction and so eliminated the confusing side reactions with slags and crucible walls. When carbon dioxide was used as the oxidant, its rate of diffusion in the gaseous phase was the rate-controlling step. Baker, in co-operation with Ward (22), later experimented with iron-carbon drops falling through pure oxygen and found that a violent 'boil' occurred which was caused by the generation of carbon monoxide within the liquid metal. Hamielec, Lu and MacLean (25) pointed out that Baker's theoretical model of the diffusion process predicted rates lower than those observed. In subsequent papers, Baker revised his calculations of the theoretical rates and confirmed his earlier conclusions (23,24).

In their second paper, Baker, Warner and Jenkins (23) reported that the rate of decarburisation of levitated drops in oxygen began to decrease at a carbon level a little below 1%, at the same time as the carbon monoxide 'boil' occurred. They considered that the transport of carbon in the liquid metal had become the rate-limiting step.

Other workers at this time were decarburising crucible melts with oxygen (26-28), carbon dioxide (29-32) or water vapour (29), with and without inert diluents. Most of them confirmed that gaseous diffusion controlled the reaction rate down to carbon levels below 1%. Some also reported a change of kinetic control

due to the slow diffusion of dissolved carbon (26,28-30) and noted the appearance of oxide at the time of this change (29). The only dissent came from Swisher and Turkdogan (32) who exposed crucible melts to a stream of carbon monoxide and dioxide and considered that the reaction rate was controlled by a slow chemical reaction at the metal surface involving the dissociation of carbon dioxide.

Distin (1) decarburised levitated iron drops with oxygen, carbon dioxide or water vapour and also reported that the gaseous diffusion step controlled the reaction rate down to carbon levels between 0.5 and 1%. There was some evidence that the controlling step changed just as the 'boil' began and Distin commented that iron oxide always appeared at this moment. The gradient in the hypothetical diffusion boundary layer for dissolved carbon was believed to become too low to "drive" the carbon atoms in sufficient numbers to the reaction interface, so that diffusion in the metal phase was then the rate-limiting step. The carbon content at the surface fell to zero and iron oxide could form At this moment the average carbon and oxygen contents of the drop corresponded to conditions of saturation in carbon monoxide at about 40 atmospheres. If it were supposed that small amounts of iron oxide were carried by convection currents into the metal, local supersaturations of 100 atmospheres or more might occur. Indeed, since there was no sudden change in the average oxygen content as the boil began, it appeared that the oxide phase might be nucleating the gas bubbles.

This then was the state of knowledge on decarburisation kinetics when the project began. For the reasoning leading to the initial experimental work we must consider also the difficulty of initiating gas bubbles in a liquid metal.

4. Bubble Nucleation

Most of the literature on nucleation phenomena concerns

solid phases and the few attempts that have been made to predict the conditions for nucleating gas bubbles within liquids, particularly liquid metals, seem to show that nucleation in a truly homogeneous single phase is virtually impossible.

In a small bubble of radius r, the balance of forces due to the surface tension σ and the gas pressure p is such that

$$p = \frac{2\sigma}{r}$$

Then the equilibrium pressure (the supersaturation of the gas in the liquid) must be larger for bubbles of smaller size. Ward (33) estimated that a CO nucleus of molecular dimensions (r = 0.6 nm approx.) requires a supersaturation close to 50,000 atmospheres in the liquid iron.

Supersaturation implies high chemical potential. The free energy is reduced when the dissolved atoms enter a gas bubble but against this there is an increase in interfacial area, requiring an energy increase which is numerically equal, for each unit of area increase, to the surface tension. The decrease in volume free energy is therefore a function of r^3, where 'r' is the bubble radius, whereas the increase in surface free energy is a function of r^2. Below a critical radius, a small increase in bubble size would give a net increase in free energy and could not occur spontaneously. How then is a nucleus to reach a viable size with a radius greater than the critical value?

Bradshaw (34) estimated that the rate of bubble nucleation in liquid iron containing carbon and oxygen would be vanishingly small unless the supersaturation of CO were of the order of 30,000 atmospheres. This treatment necessarily made broad assumptions, in the absence of other data, on the conditions within bubbles that contain only a few molecules of gas.

Baker and Ward (22) considered that a supersaturation of CO estimated at 60 atm. should be sufficient for homogeneous nucleation and quoted Rangue (43) and Bodsworth (44) in support.

Ranque, however, calculated the equilibrium pressure in a bubble with a radius arbitrarily set at one micron as 56 atm. Bodsworth made an almost identical calculation but neither writer claimed that this pressure could cause new bubbles to nucleate homogeneously.

Cahn and Hilliard (35) showed that many assumptions on the nature of a nucleus must be modified when the nucleation of a solid phase within a two-component liquid is being considered but there is apparently no advanced treatment of gas bubble nucleation from a liquid of different composition.

Most writers have resolved these theoretical difficulties by suggesting that gas-filled crevices in a rough furnace hearth or crucible wall could nucleate bubbles heterogeneously. The experiments of Koerber and Oelsen with CO boils in glazed and rough crucibles are often quoted in support of this suggestion (see, for instance, ref. 33).

That CO bubbles should be nucleated in apparently homogeneous levitated drops is therefore of great theoretical interest. Distin's observation that iron oxide may be present does not completely explain the anomaly, since the supersaturation needed to cause nucleation at an oxide/metal interface would be diminished by a factor not greater than three (1b).

5. Initiation of the Project

Further data were sought in support of Distin's conclusion that supersaturation pressures of 100 atm. or less would suffice to nucleate gas bubbles. The reaction to be studied should produce no additional phases such as oxides but should be capable of developing high supersaturation pressures.

In a liquid nickel-oxygen alloy drop, a diffusion coefficient, k_m, for oxygen of the order of 0.03 cm/s was expected, by analogy with Distin's figure for carbon in iron.* The reaction rate for such a drop with flowing hydrogen should quickly become restricted

*See Addendum : p. 9

by slow diffusion of the oxygen to the metal surface and hydrogen should be able to dissolve. For conditions of hydrogen saturation at temperatures a little above the melting point of nickel it can be calculated that

$$P_{H_2O} = 300\,[\%O]_{Ni}$$

If the oxygen concentration were 0.15% a supersaturation pressure of 45 atm. might develop.

These conditions might be induced by exposing nickel-oxygen alloy drops to flowing hydrogen. If the flow were sufficiently rapid, control should shift from transport of gaseous species to transport of dissolved oxygen. Hydrogen should then penetrate the drop while oxygen is still present in the liquid metal.

Addendum: Mass transfer coefficient of oxygen in nickel.

Distin pointed out that the diffusivity of oxygen in liquid iron is not less than one-third of that of carbon and that the mass transfer coefficients would be related to fractional powers of these figures. The viscosity of liquid nickel is not known but is unlikely to differ greatly from that of iron.

III EXPERIMENTAL TECHNIQUES AND MATERIALS

1. Electro-magnetic Levitation

The coils were similar to those employed by other workers at the Royal School of Mines (1,2,4 & 5). Jenkins, Harris and Baker (36) have described coils of this type and discussed the effects of design variables. Power was supplied by a Philips high-frequency generator supplying 6kW at 250 kilocycles per second.

In the simplest experimental apparatus, a reaction tube of silica glass containing the levitated drop in a stream of gas, passes vertically through the coil (2,4,5). This arrangement also simplifies calculations of mass transfer between the drop and the gas stream. The coil must be enlarged to accept a tube of practical size. Because the levitating force decreases sharply as the coil diameter is increased, the sample weight is limited to one gram or less.

Samples of 1.5 to 2 g. were preferred in the work to be described because of the larger weight-to-area ratios and the longer reaction times. Attempts to redesign coils to operate with larger silica tubes were not successful because of the limitations of the power supply. The coil had to be set up inside a reaction vessel, which is shown in Figure 1.

The coil had four or five turns of 1/8-inch copper tubing forming a truncated cone with an included angle close to 60°. The smallest internal diameter was 11.5mm, for nickel drops and 10 mm. for iron drops which were more difficult to levitate. The upper pair of turns of opposite sense were of 11-12 mm. internal diameter.

The high-frequency field both levitates and heats the sample and the two functions cannot be independently controlled, except within very narrow limits (2a). The heating effect would vaporise the common metals if a stream of cooling gas were not supplied. Helium has the highest thermal conductivity among the non-reactive gases and flows of about a litre per minute, impinging

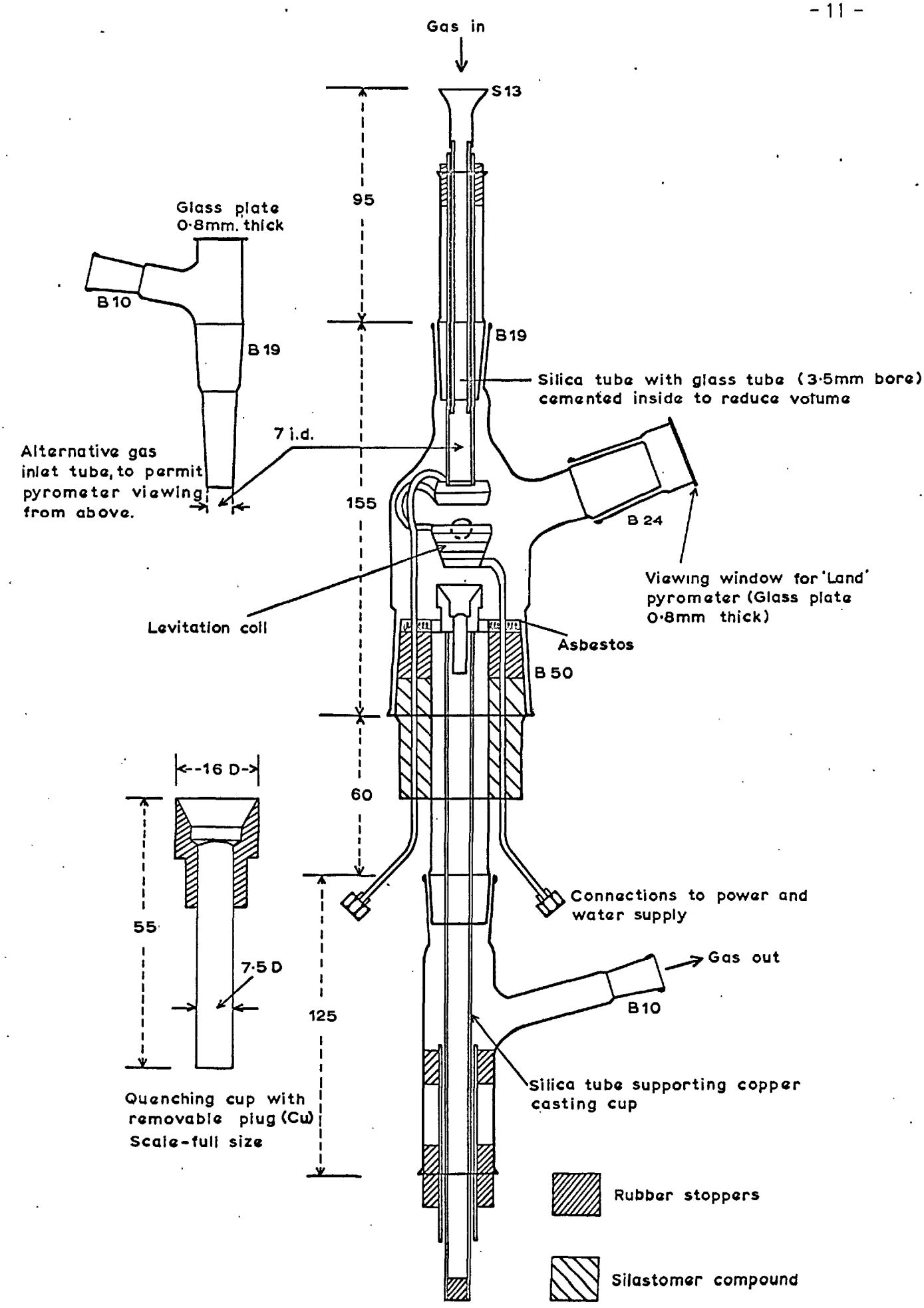

Fig. 1. Details of construction of the levitation cell and its attachments. Scale-half size. (All dimensions given in millimetres)

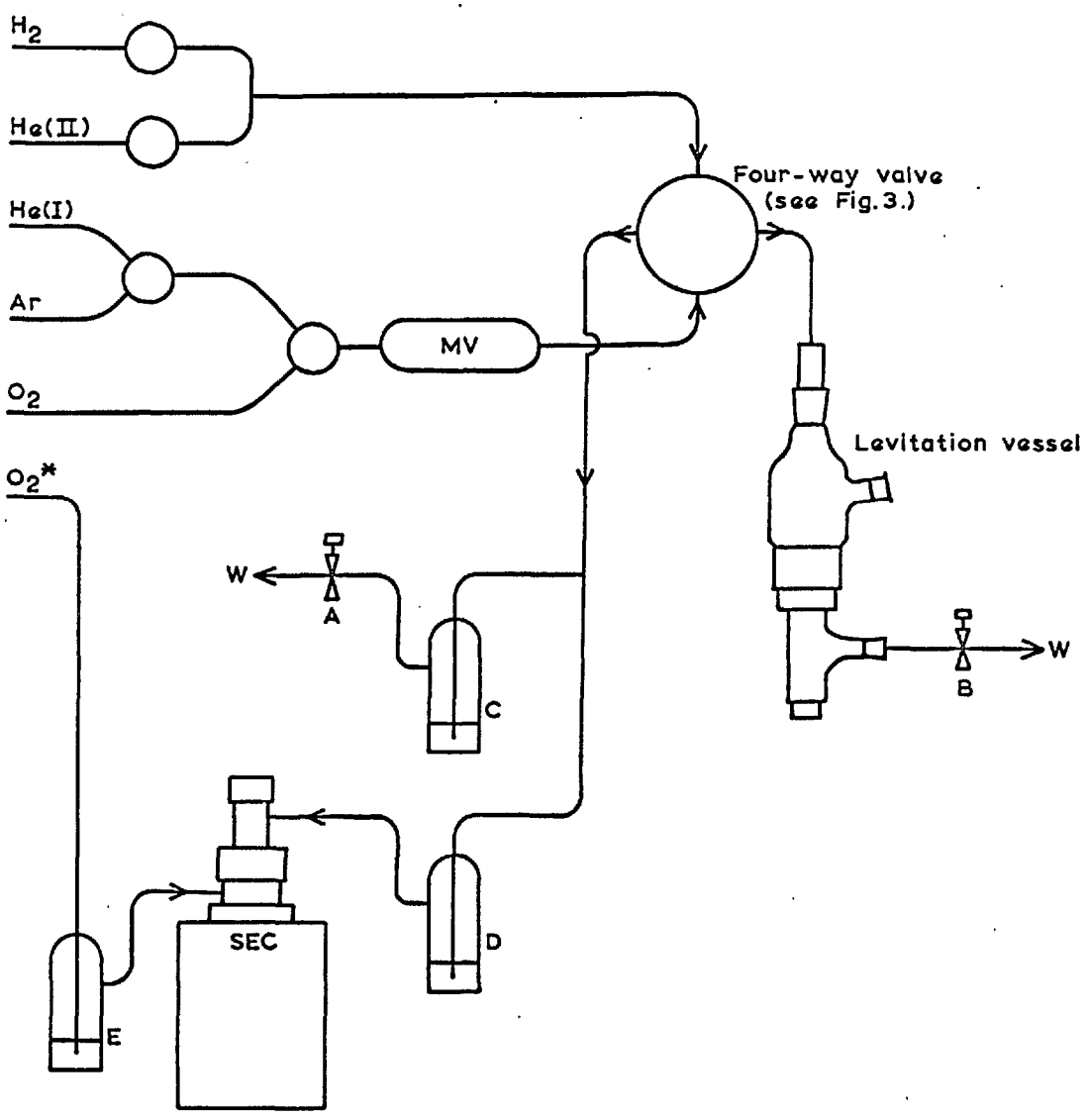

Fig. 2. General arrangement of gas lines and flow controls.

NOTE: All gases except O_2^* are controlled by glass capillary flow-meters

—O—	Two-way stopcocks
⋋O—	Three-way stopcocks
A,B	Screw pinchcocks (on rubber connections)
C,D,E	Glass bubblers containing dibutyl phthalate
MV	Mixing vessel, filled with glass beads
SEC	Solid-electrolyte cell, in wire-wound tube furnace.
W	To waste venting system.

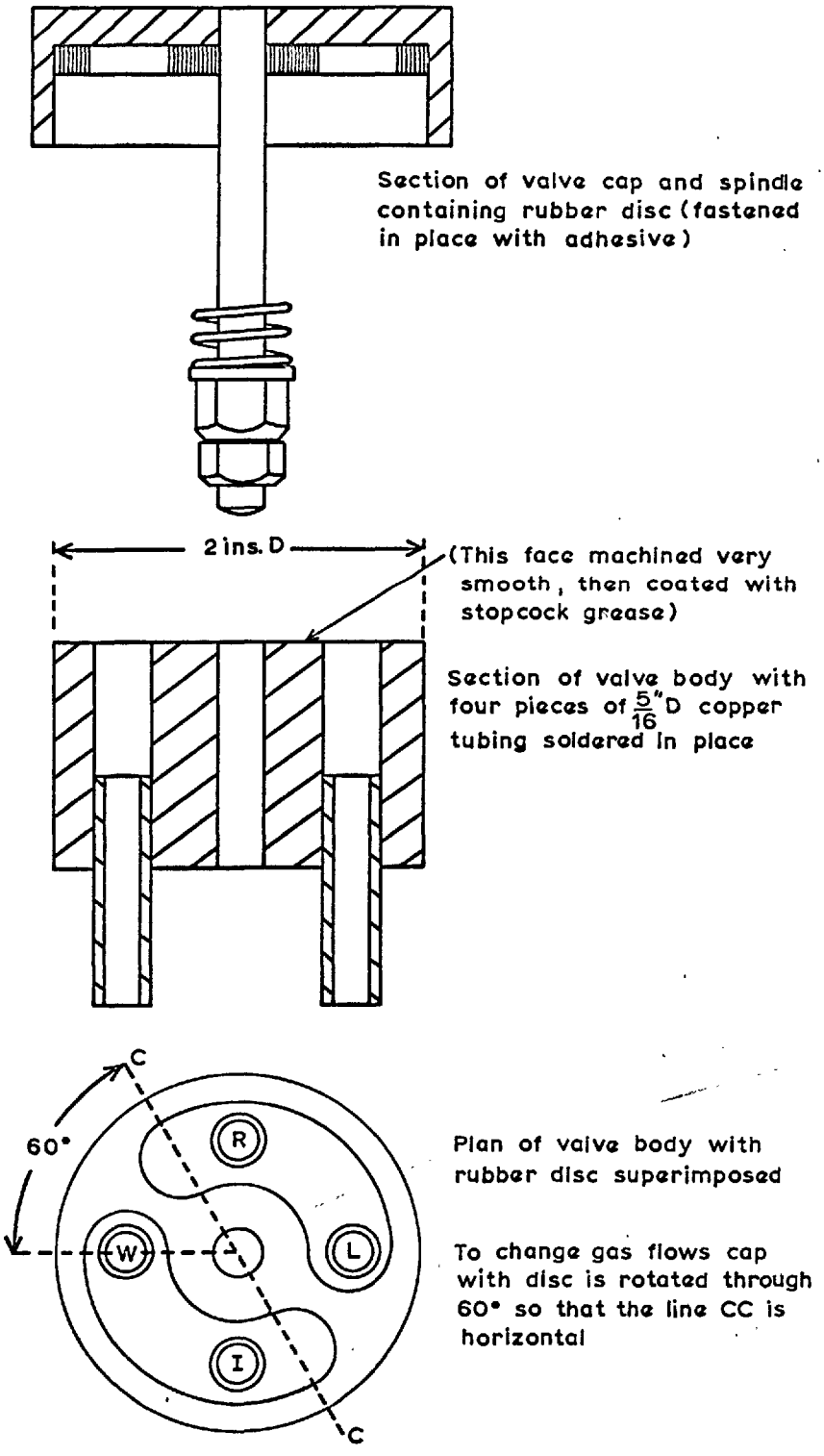

Fig. 3. Four-way valve for rapidly changing gas flows (shown dismantled)

Materials: brass, rubber
Scale: full size
R = Reactive gas
I = Inert gas
L = Levitation vessel
W = To waste

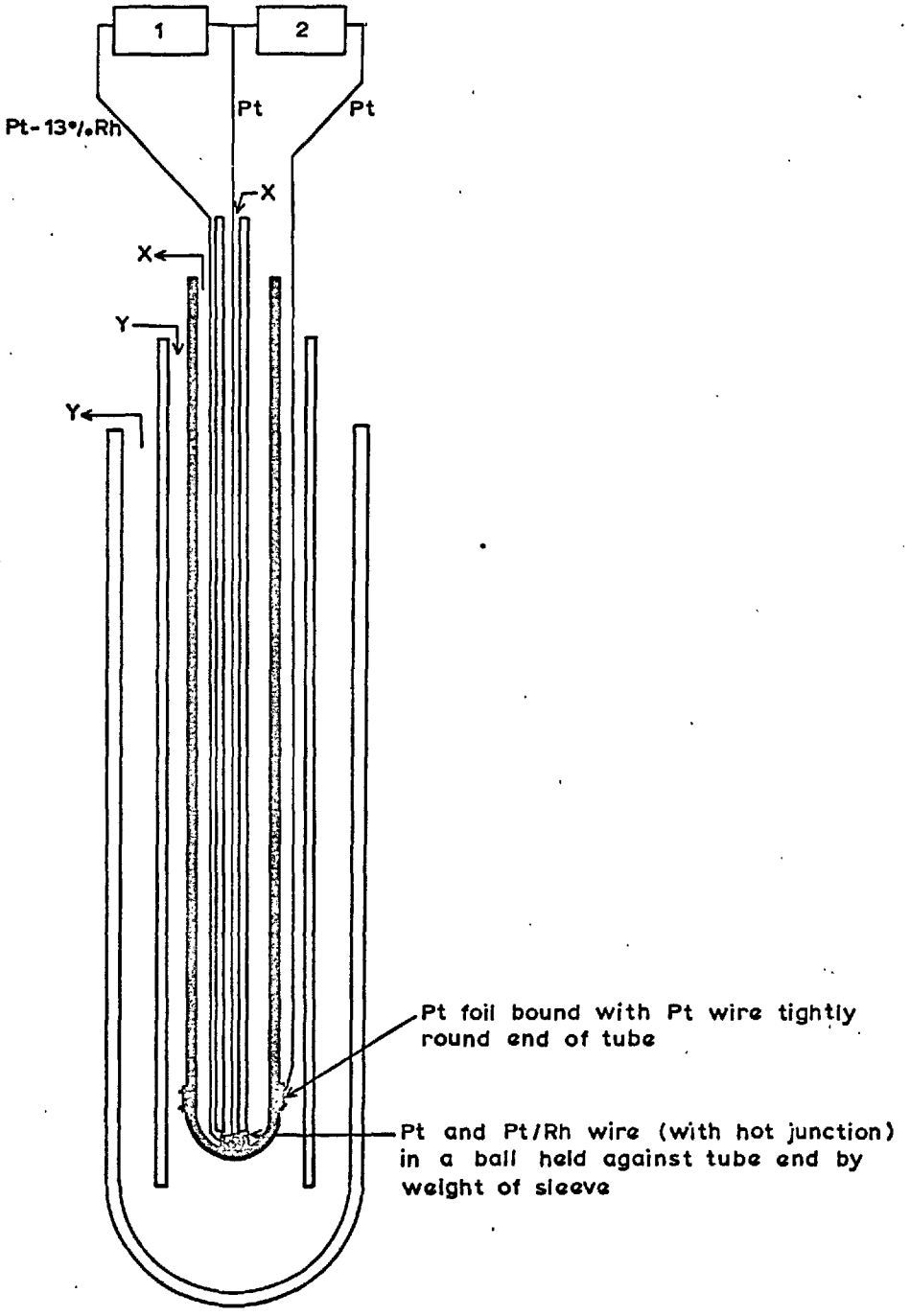

Fig. 4. Diagram of solid electrolyte cell (not to scale)

X Gas under test

Y Standard gas (pure oxygen)

1 Thermocouple potentiometer (with cold junction)

2 Electrometer or high impedance voltmeter

Tube shown in black is ZrO_2/8%CaO; all others are of recrystallized alumina.

on the drop, will keep the temperature of pure iron or nickel at about 1650°. The end of the silica tube through which the gas was supplied was 6-7 mm. above the usual position of the top of a 1.5-2 g. drop.

2. Materials

(a) Gases: The manufacturer's standards of purity for gases supplied in steel cylinders are shown in Table 1. Each gas passed through 'Anhydrone' (magnesium perchlorate) to ensure dryness; other methods of purification are described in connection with the relevant experimental work. Flow-rates were controlled and measured by capillary meters together with "bleed-off" columns filled with dibutyl phthalate. The capillary jets were calibrated for flows up to 2 litres per minute by the soap-film method, where the timed movement of the film sweeps out a known volume. An oil-filled rotary meter was used in calibrating larger jets. The errors, judged by the degree of scatter of the points about a smooth curve, were not greater than ± 3%.

Figure 2 shows schematically how various gas mixtures could be supplied to the reaction vessel. A special four-way valve (Fig. 3) allowed the flow to the reaction vessel to be changed by means of a 60° turn from an inert to a reactive gas without disturbing the pressure and rates of flow of the gases. With the valve connected close to the reaction vessel, the intervening volume of only 8 cm^3 could be swept out (assuming "plug flow") in about 0.5 s. by a gas flow of 1 litre/minute. The pinch-cocks shown in Figure 2 on the two waste outlets were adjusted to equalise the resistance to gas flow in the two lines.

The proportion of oxygen in mixtures with inert gases was checked frequently with a solid-electrolyte cell (constructed by Mr. L.E. Leake), in which a tube of "semi-stabilised" zirconia containing 7.5% lime was kept at 900 ± 5° in a Nichrome wire-wound tube furnace. Figure 4 shows the arrangement of zirconia

and alumina tubes and the electrical connections to the cell. The cell resistance was about 12 kilohms and the potential difference had to be measured by instruments of high impedance. A Vibron Electrometer was used for most of the work but a Keithley Electrometer or a Solartron digital voltmeter were substituted at times. The "zero reading", caused by thermo-electric effects at the cell terminals and by the effects of stray fields on the leads to the electrometer was measured from time to time while pure oxygen was supplied to both inlets of the cell. Generally this value was not greater than 0.5 mV.

Table 1: Purity of Gases: Manufacturer's data on typical analyses.

Gas	Impurities: Volumes per million				
	O_2	N_2	CO_2	CH_4	H_2O
Oxygen*	-	-	1	15-20	10-15
Hydrogen	1-2	50 - 70	1	1	2-3
Helium	1 +	3-4	-	-	1-2
Argon	1	-	1	1	1-2

* Also 0.2% Ar

\+ In 250 ft.^{3} cylinders; up to 10 v.p.m. in 44 ft.^{3} cylinders.

(b) Metals and alloying substances: Table 2 shows the sources and analyses of the elemental substances used. The following compounds were also employed:

Nickel oxide: The black "General Purpose Reagent" (HW) of indefinite composition was heated in air to a dull red-heat yielding the light green compound NiO. Analysis by reduction in

Table 2: Analyses of Solid Materials

Material	Source	Percentages					Parts per million								Other data
		Data Source	C	N	O	S	Data Source	Al	Ca	Cu	Fe	Mg	Mn	Ni	Si	
Nickel rods	JM						B	<1	<1	1-3	7-8	<1	<1		4-5	
shot	HW	M	0.01-0.04				M			<10						(M) 0.01-0.04%Fe
powder	HW	M	0.05-0.1		0.1	0.001	S	3	<1	1	30	10			10	(W) 0.06%C; 0.12%O
sponge	JM	B	0.005				B		<1	<1	2-10	<1			1-3	(W) 0.06%O
Iron powder	KL	M	< 0.22	<0.22	<0.4		S		1	5		<1	1	>100	20	(W) <0.03%C; 0.18%O
Graphite powder	JM						B	0.3	0.03	0.01	0.3	0.02		0.1	0.3	
Sulphur crystals	JM						B	0.5	<1		<1			0.1	<1	
'flowers'	HW	"Meets standards of British Pharmacopoeia for Precip. Sulphur: As < 2.5ppm, 'ash' <0.25%, no heavy metals."														

Abbreviations

JM Johnson, Matthey Chemicals Ltd.

HW Hopkin & Williams Ltd.

KL Koch-Light Laboratories Ltd.

B Manufacturer's analysis of batch

M Manufacturer's data for typical levels

S Sample submitted to JM for analysis

W Writer's analyses (by methods described in text)

hydrogen showed that this contained 21.3% of oxygen (theoretical content = 21.4%).

Ferric oxide: the red oxide (KL) of laboratory reagent grade was heated in air to dull red-heat to ensure dryness and complete oxidation to Fe_2O_3.

3. Preparation of Alloy Samples for Levitation

(a) Cast rods: In the early work, pure nickel rods were induction-melted in magnesia or alumina crucibles and nickel oxide was added to the liquid metal. Sticks were cast by drawing the metal up into silica tubes of 7 mm. bore, with a hypodermic syringe body used as a simple suction device. Portions of the sticks were filed to uniform weight and cleaned in hot 50% HCL, followed by rinsing in water and acetone.

It was difficult to cast sound sticks containing more than about 0.5% of oxygen or smaller amounts of sulphur. The alloys solidified slowly because of their long solidification ranges and nickel-rich liquid ran out of the core.

(b) Pressed pellets: The technique of cold-pressing powders into cylindrical pellets was adapted from the method of making reference electrodes for research on solid-electrolyte cells. Mixtures of metal powder with an oxide, graphite or sulphur were made from the weighed components and suitable portions were pressed in a ¼-inch steel die under a load of 6000-8000 lb. The pellets were strong enough to withstand handling and could be levitated and melted easily.

4. Levitation Technique

A sample was raised into the coil on a small silica cup in a stream of inert gas. About a second after the power was switched on, the sample became levitated. With some coils, a flow of argon, which has a thermal conductivity lower than that of helium, had to be used to permit melting but in most experiments samples could be melted in helium. The liquid drop was then held for a short period (usually one minute) to allow the temperature to

become stable.

Small amounts of the added elements were lost during melting - sulphur, for example, was seen to vaporise briefly just before the sample reached red-heat - and the experimental data for "zero time" represent samples melted, held for the usual time and cast in helium.

5. Temperature Measurement

(a) Instruments: The temperature is conveniently measured by detecting visible and near-visible radiation at a location outside the reaction vessel. Two instruments were available:

Land Radiation Pyrometer (Type QSH 100/5: Land Pyrometer Ltd., Sheffield).

The image of the hot surface is focussed on a silicon-cell detector which is sensitive from the visible range into the near infra-red (effective wavelength = 0.9 micron). The instrument had been adapted to view a disc of only 0.05 inch diameter at 5 inches from the main lens. Current generated by the cell is applied across a 500 ohm resistor and the potential difference can be recorded.

Evershed Optical Pyrometer (Evershed & Vignoles Ltd.)

Disappearing - filament type with manual adjustment Effective wavelength = 0.665 micron. Used only for provisional cross-calibration of the Land Pyrometer with metals whose emissivities were known.

The signal from the Land pyrometer was measured on an AEI recording voltmeter in the earlier work. Temperatures of the decarburisation experiments and some other work were recorded on a Honeywell "Electronik 194" instrument which had a wide selection of voltage ranges and chart speeds and could trace rapid temperature variations in detail.

(b) Emissivity of pure metals: The emissivity of the metal must be known so that the pyrometer signals can be corrected to give the true, "black-body" readings. Wien's Law relates the true and apparent absolute temperatures:-

$$\frac{1}{T} - \frac{1}{T_a} = \frac{\lambda \mathrm{Ln}\varepsilon_\lambda}{c_2}$$

where ε_λ is the emissivity at the wavelength λ ,

c_2 is a constant = 14330 micron - °K. The literature gives the following emissivity values:

Metal	Effective λ, microns	Temp. range °C	ε	Workers	Ref. No.
Fe	0.665	1505-1900	0.43-0.50	Dastur, Gokcen	37
Ni	0.665	1453-1600	0.40	Toop	2
Ni	0.9	1500-1750	0.40	Forster	5

The writer estimated the emissivity of nickel by observing a drop with both pyrometers simultaneously. Calculations based on Toop's figure for the Evershed instrument gave an emissivity of only 0.3 at 0.9 microns. Both pyrometers gave consistent readings at the melting point of nickel. To resolve the difference from Forster's value, measurements were made with crucible melts.

Nickel was induction-melted under argon (with a little hydrogen) in an alumina crucible with a thermocouple sheath entering through the base. The filled crucible was viewed by the pyrometer from above while a thermocouple of Pt/Pt + 13% Rh measured the temperature a few millimetres below the liquid surface. The upper limit of readings was 1750°, just below the melting point of the platinum thermocouple wire.

Metal vapour in the space between the metal surface and the gas supply tube, which also provided a path for the radiation to the pyrometer, absorbed some radiation and caused errors at temperatures above 1650°. The effective emissivity measured with the optical pyrometer below this temperature was constant at $(\varepsilon\tau) = 0.365$ and was assumed to apply up to at least 1750°.

The two instruments were then set up to view a levitated nickel drop simultaneously. The gas stream removes virtually all metal vapour, at least at temperatures lower than 1800°. "Black-body" temperatures were calculated from the optical readings by

applying the effective emissivity value given above.

The effective emissivity of iron at 0.9 micron was also determined by the "two-pyrometer" method and the data of Dastur and Gokcen (37) were applied to correct the optical pyrometer readings.

The transmissivity of the viewing windows, cut from Kodak slide cover-glasses 0.85 mm thick, was calculated from the change in the Land pyrometer signal when a second square of the same glass was interposed in the light path(4a). The mean of about 40 values was 0.898.

The values of the effective and true emissivities at 0.9 micron were taken as:

	$(\varepsilon_\tau)_{0.9}$	$\varepsilon_{0.9}$	Temp. range
Ni	0.288	0.320	M.pt. - 1800°
Fe	0.28→0.35	0.31→0.39	M.pt. → 1740°C

(respectively)

(c) Emissivity of alloys: Toop (2) showed that dissolved oxygen and sulphur changed the emissivities of copper and nickel. To provide data for the 0.9 micron wavelength, nickel-based alloys were tested with up to 0.75% of either solute.

Pressed pellets of nickel with known amounts of sulphur or the oxide were added to nickel melts in a crucible fitted with a thermocouple, to give concentrations in steps up to the maximum. The emissivity changes were small and the effective emissivities for the alloys of highest solute concentration, viewed with the optical pyrometer, were:-

	$\varepsilon_{0.665}$
Ni + 0.50% O	0.38
Ni + 0.76% S	0.35

Viewing levitated alloy drops with the two instruments gave the following values:-

	$(\varepsilon\tau)_{0.9}$	$\varepsilon_{0.9}$
Ni + 0.75% O	0.29_0	0.32_3
Ni + 0.75% S	0.27_7	0.30_8

Both solutes are believed to have roughly equal surface-activities in nickel and the effect of sulphur in decreasing the emissivity value is surprising. All tests were made with the same equipment and under identical conditions and there is no reason to doubt the relative changes in emissivity.

Rist and Chipman (8) found that iron-carbon alloys at the eutectic temperature had the same emissivity as pure iron. Because of the other errors in temperature measurements it was considered that accepting the pure-metal emissivities for all alloys of iron or nickel with carbon would not cause serious inaccuracies.

(d) Errors: The Land pyrometer is capable of measuring temperatures in the range of calibration to within a few degrees but much larger uncertainties in the reported temperatures arise from difficulties in controlling sample temperatures.

Under steady conditions of power setting and inert gas flow, the temperature of a levitated drop varies over periods of several minutes by as much as 20° above and below the average, probably because of small variations in the main power supply. The response to manual adjustments of the power is slow and reduces the extent of variation by not more than a third. In addition, changes in alloy composition (particularly in the oxygen content) can strongly affect susceptibility to the high-frequency field and the heating effect.

Temperatures above 1800°C can be obtained only by extrapolating the calibration curve. It was found that plotting log V against 1/T (where V is the signal from the Land pyrometer, in millivolts) gave a straight line which could be extended more easily. This procedure implies an assumption that the

emissivity remains constant. The emissivity of nickel-oxygen alloys containing much more than 0.75% O has not been measured. The temperatures reported for pure nickel drops exposed to oxygen must therefore be taken as guides to the relative increases in temperature rather than as absolute data.

The accuracy of alignment of the pyrometer head was frequently checked by traversing it on two axes to obtain the maximum signal from a liquid drop; the drop was then quenched in a rapid stream of hydrogen and allowed to remelt in helium so that the signal at the melting point could be observed.

6. Analytical Methods

(a) Oxygen in Nickel: The solid samples were reduced at 1300-1350°, following the method described by Young (39) and others (4,5) for copper samples. Because most of the oxygen separates in cast nickel as dispersed particles of oxide, there are no oxide-rich grain boundaries to offer easy routes for diffusion. Diffusion of oxygen atoms through the solid nickel controls the reduction rate.

To shorten the time needed, samples were rolled to plates 0.4 to 0.5 mm. thick. About six of these could be reduced together in an alumina boat. Reduction times were calculated for 99% depletion by the method for a semi-infinite slab (14), applying a diffusivity value extrapolated from the data of Brown and Alcock (40) but experience showed that about twice these periods should be allowed. The patterns of blisters formed during reduction showed that the oxide inclusions were segregated near the core of the cast sample instead of being uniformly distributed as the method of calculation assumes.

Tests with oxygen-free samples showed that accumulated weight losses due to vaporisation of metal or of traces of oil picked up during rolling, together with weighing errors, were not greater than 10^{-4} g. representing a maximum of ±0.007% O on a 1½g. sample.

Any silica or silicate cements in refractories exposed to hydrogen at high temperatures caused serious weight gains which were believed to be due to the formation of volatile silicon monoxide which was reduced on the metal surface.

(b) Oxygen in Nickel containing Sulphur: Hydrogen removes some of the sulphur as H_2S. The oxygen content of the sample, can, however, be determined if the evolved sulphur is measured and the weight loss from the sample corrected.

The gases from the furnace were bubbled through a 15% solution of zinc acetate (with a small addition of acetic acid). At the end of a run (on a single sample) a measured excess of centinormal iodine solution was added, the solution acidified with HCL and the usual back-titration made with thiosulphate and starch solutions.

Samples were too brittle for rolling and were instead crushed in a percussion mortar and the fragments collected in a weighed alumima boat. Samples with more than about 0.3% S were given a preliminary hydrogen-reduction in the cast state, to remove some of the sulphur and minimise losses of the friable sulphides during crushing.

Reduction periods of 1½ to 2 hours were usually sufficient for crushed samples but several were given additional periods to confirm that all oxygen had been removed. The remaining sulphur (30-60 % of the original content) could then be determined by the combustion method.

The procedure yields oxygen and sulphur contents from a single sample but is time-consuming. The fusion method, described below, would probably be more suitable for these oxygen determinations, but was not developed until a later stage of the research programme.

In the reduction method there is a risk that a little H_2S will be carried over from one analysis to the next. It was

possible that sulphur was deposited in cooler parts of the tube, to be slowly reconverted to H_2S when the sample had been removed. The error was minimised by allowing about 20 minutes of purging time after a sample had been withdrawn from the hot zone. Batches of samples were also analysed in order of increasing sulphur content so that losses and gains due to "carry-over" would tend to be annulled.

(c) Oxygen in Alloys containing Carbon: Samples were too hard to be rolled or crushed to permit reduction in a reasonable time; there was also a risk of losing carbon as hydrocarbon gases. The "carrier-gas/fusion" method was developed from that described by Shanahan (41), since vacuum-fusion equipment was not readily available.

The sample was dropped into a copper-nickel melt in an induction-heated crucible turned from high-grade electrode graphite. Fig. 5 shows the reaction vessel. An argon stream, purified by being passed through soda-asbestos and over copper at 600°, carried the evolved carbon monoxide through a copper oxide furnace at 600°C: the carbon dioxide was absorbed in a Nesbitt bottle containing soda-asbestos with a covering of Anhydrone.

Toop (2) also fused his samples in a carbon crucible but passed the gases through heated iodine pentoxide and titrated the iodine produced. The very slow gas-flow made an hour or more of purging necessary. In the present method 15-17 minutes was sufficient.

In the absence of a sample, the absorption bottle showed a weight gain of 0.1-0.2 mg. per minute, which was not eliminated even when the crucible had been in use for a long time. The gain during a 15-minute analysis might represent as much as 0.04% O in a typical sample but the error was kept much smaller than this by checking the "blank" value frequently and deducting it from the measured weight gains. In order to keep the "blank"

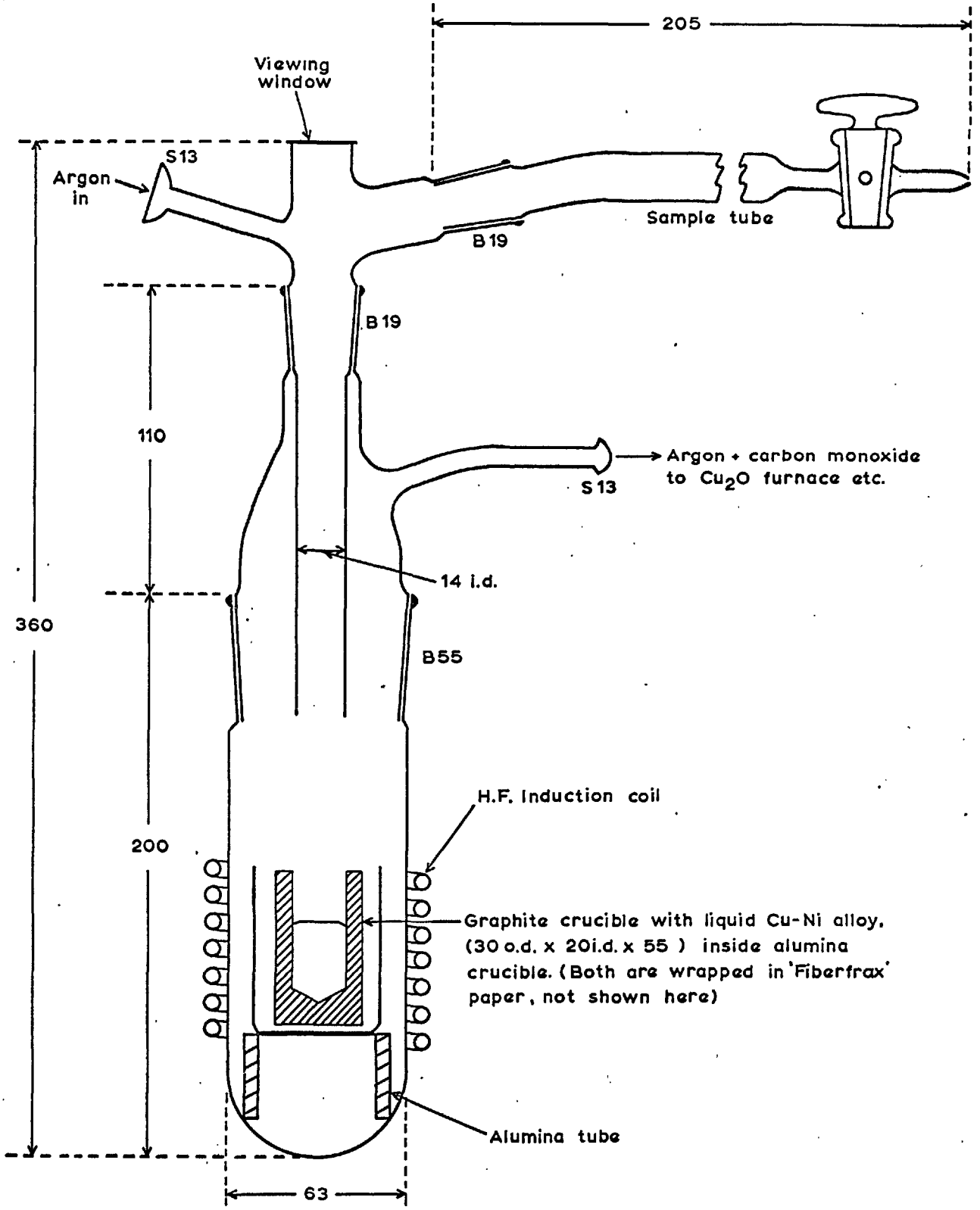

Material: pyrex glass, except as marked

Fig.5. Reaction vessel for analysis of oxygen in metals by the fusion method (All dimensions in millimetres)

value constant or slowly decreasing, it was essential the crucible temperature remained constant.

Fragmented samples were wrapped in copper foil and four such samples could be placed in the side-arm ready for analysis. When iron samples were analysed, a second liquid phase rich in copper began to separate in the crucible but the efficiency of the method was not affected.

Thermodynamic calculations of the equilibria between CO and SO_2, CS_2 or CS show that the carbon monoxide is by far the most stable. There is thus little risk of inaccuracy due to the formation of sulphur compounds from samples containing that element.

(d) Comparison of Analytical Methods for Oxygen: Nickel-oxygen samples were made by melting Ni/NiO pellets in helium and also by exposing nickel drops to flowing helium which contained known concentrations of oxygen (see Section IV: 4).

The cast samples were rolled to discs about 0.7 mm. thick. Each disc was cut into quadrants and diagonally-opposed pairs were treated as single samples, to minimise errors due to segregation of the oxygen. The samples were analysed by the following methods

(i) Hydrogen reduction

(ii) Carrier-gas/fusion

(iii) Vacuum fusion (by courtesy of the Research and Development Department, Swinden Laboratories British Steel Corporation).

The results in Table 3 show no systematic bias in any of the methods. Methods (i) and (iii) agree within 0.01% O. The differences due to the fusion method are up to 0.03% O (on oxygen contents above 0.10%) but appear to be randomly high and low.

(e) Carbon in Iron and Nickel: Samples were ignited in oxygen by the usual method, to produce carbon dioxide which was absorbed on soda-asbestos for weighing.

Table 3: Comparison of Results from 3 Methods of Oxygen Analysis

Sample No.	Seconds in He/O_2*	Oxygen: % Hydrogen Reduction	Carrier gas/ fusion	Vacuum fusion+
620	⊖	0.114	0.118	-
621	⊖	-	0.090	0.118
622	⊖	0.115	-	0.123
623	⊖	0.107	0.103	-
629	15	0.053	0.071	-
630	"	-	0.05	0.055
631	"	0.048	-	0.051
625	"	-	0.125	0.121
627	"	0.119	-	0.129
628	"	0.113	0.106	-
633	45	0.156	0.157	-
626	50	0.193	0.204	-
632	"	-	0.200	0.197
635	"	-	0.191	0.200
634	90	0.352	0.363	-
638	"	0.349	-	0.345
639	"	0.330	0.364	-
636	120	0.460	0.43	-
637	"	0.516	-	0.521

+ British Steel Corp., Swinden Labs.

⊖ Ni/NiO pellets, melted and cast in helium

* Ni shot melted in helium then exposed to $He + O_2$ at 2 litre/minute, $p_{O_2} = 0.008$

The oxygen was purified with anhydrone and soda-asbestos. Iron samples were fluxed with sheet lead or, in later tests, fine turnings of tin and heated to 1200 - 1230° in oxygen flowing at about 1½ litres/minute. When the vigorous reaction had subsided, the flow was reduced to 400-500ml/minute and the apparatus purged for a further 12-15 minutes. For samples that also contained sulphur, two bubblers containing a chromic/sulphuric acid mixture were added to the train of drying agents ahead of the soda-asbestos bottle.

The "blank" analyses of boats containing flux only were lower than those containing pure iron or standard steels. The "blank", which includes all errors in the method, was therefore measured by analysing about 20 samples of standard steels (British Chemical Standards) and allowing for the known carbon content. This gave a figure of 0.0030 ± 0.0016 g., where the uncertainty represents two standard deviations of the data and corresponds to an error of ± 0.03 % C on a 1.5 g. sample. This "blank" and the error are unexpectedly large, although the boats had re-ignited for several hours at 1000-1100°.

Nickel oxide is infusible at practical temperatures and tends to block the combustion of the sample. The furnace was therefore held at 1400-1425° and copper turnings added to the sample as a flux. The sample was preheated in argon for 1½ - 2 minutes to ensure that combustion was rapid and complete when the oxygen was turned on. The purging process continued for 30-40 minutes to collect all the CO_2, some of which is thought to be entrapped by the viscous oxides. The "blank" value of the boats with the copper turnings was 0.0026 ± 0.0013 g. whether or not nickel was present.

(f) Sulphur in Iron and Nickel

Here again the standard combustion method was used, with a temperature of 1300-1330° for iron and 1400-1430° for nickel

samples. Iron samples were fluxed with tin and exposed immediately to the oxygen stream; nickel samples were fluxed with copper and preheated in argon. Gas flows and purging times were the same as in the carbon analyses.

The gases from the furnace pass through a glass wool filter, an empty vessel (of about ½ litre capacity, to dilute the initial surge of SO_2 a little) and a sintered glass bubbler into 200ml. of 2% HCL containing a little KI and a measured volume of N/50 KIO_3 solution. As the combustion and purging proceeded, more KIO_3 was added to maintain a blue colour with added starch solution. Any excess iodine remaining at the end of a run was back-titrated with N/100 $Na_2S_2O_3$ solution.

It is well known that some of the sulphur dioxide is oxidised to the trioxide which does not reduce iodine in the absorbing solution. With a standardised combustion method, the loss is consistent and is usually calculated by analysing standard samples.

Determinations of sulphur in a wide range of standard iron-sulphur samples showed that a smaller fraction of the sulphur was lost from samples of high sulphur content than from those of low sulphur content. The correction curve in Figure 6 for sulphur in iron samples was derived from a logarithmic plotting of the data which gave a more nearly straight line. The range of scatter of the points about the curve represents a possible error of ± 5% in the method.

No analysed nickel-sulphur samples were available. When Cheng and Alcock (42) were measuring sulphur in nickel, they used standard steels for calibration purposes and recovered 84.4 ± 4% of the element. The writer's first analyses of melted nickel-sulphur pellets, whose composition was known within only a small margin of uncertainty, showed that more than 90% of the sulphur was recovered. Pellets were pressed from mixtures of known amounts of nickel powder and sulphur "flowers", wrapped in nickel

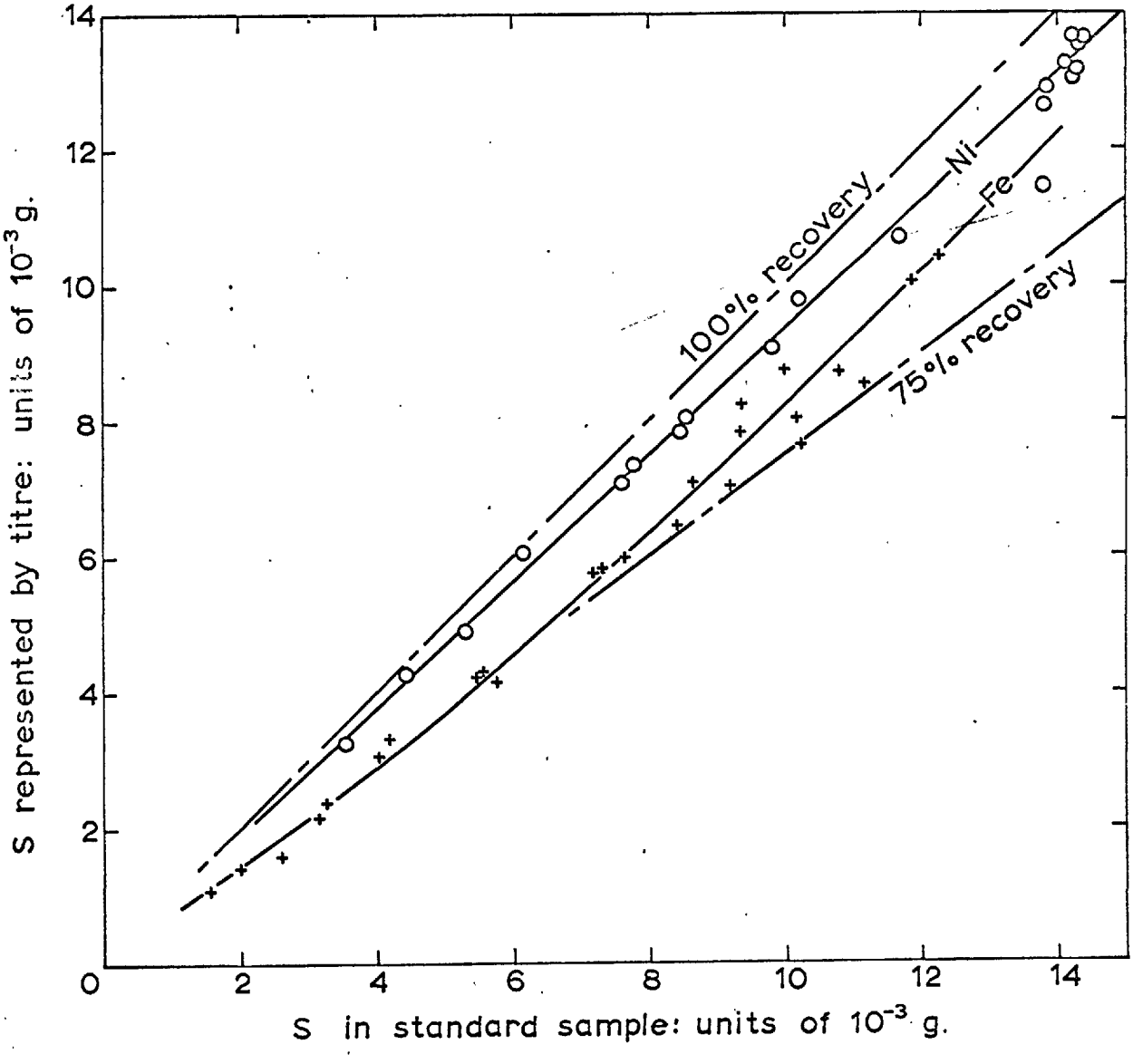

Fig. 6. Calibration curves for Sulphur analysis by combustion.

foil to avoid initial losses by vaporisation and analysed with a flux of copper turnings. The analysis of 21 samples gave a mean recovery of 93.5 ± 3.5 %. The points are plotted in Figure 6 and show that the recovery did not vary with the sulphur content. The improved recovery was not solely due to the higher temperature since steel samples analysed at about 1350° gave recovery values that were not significantly higher than those determined at 1300°.

The average titration "blank" due to sulphur in the refractory boats (with added copper) was 0.25 ml. of the KIO_3 solution corresponding to 0.006%S on a 1.6 g. sample.

IV EXPERIMENTAL WORK

1. Reduction of Nickel-Oxygen Alloys by Hydrogen

(a) Alloys containing less than 1% Oxygen: Samples cut from cast rods of the alloys were levitated as described in Section III:4. After the required time of exposure to hydrogen, each sample was cast into a copper cup by switching off the power supply.

The reaction rate was expected to be controlled by the transport of oxygen in the metal, as explained in Section II:5. Distin calculated the ~~diffusion~~ mass transfer coefficient of carbon in iron, $k_{m(C,Fe)}$ to be 0.032 cm/s. and the figure of the $k_{m(O,Ni)}$= 0.03 cm/s. that was postulated would mean that the oxygen content of a 1½ g. drop should be halved every three seconds. Instead, tests with flow-rates up to 2½ litres/minute showed that 0.8%O could be removed in as little as two seconds (Figure 7a).

Cast-rod samples and pressed pellets were exposed to hydrogen flows of 5 and 8 l/min. but the tests gave rather scattered results owing to the difficulty of controlling and recording the short reaction times accurately with a stop-watch.

In Figure 7 the lines have been drawn as guides to the trends of the data and are not accurate estimates of reaction rates. Nevertheless, the data indicated that the reaction was in all cases much more rapid than that postulated above and that the deoxidation rate increased with the rate of gas flow. Curves showing the oxygen content being halved in uniform increments of time could not be fitted to the data (except perhaps at very low oxygen concentrations). This reasoning implied that the rate was controlled by the counter-diffusion of hydrogen and water vapour in the gas phase and that ~~diffusion~~ transport in the metal phase was much faster than expected.

Because dissolved oxygen is surface-active in liquid nickel (45), it was suggested that rapid local changes in surface tension were caused while the oxygen atoms were being removed by the hydrogen. The resulting interfacial turbulence might then set up eddies which could greatly enhance the rate of transport of oxygen atoms to the surface.

So that any turbulence could be observed, the reduction of a drop was filmed with a "Fastax" camera at 1000 frames per second. The sample contained about 1%O and a few milligrammes of fine zirconia powder were added so that the floating particles could serve as "markers".

The film showed that the particles became strongly agitated as soon as the hydrogen flow was turned on. Surprisingly, the drop also "boiled" as Distin's iron-carbon drops had done and droplets of metal were ejected. Some frames showing this reaction are reproduced in Figure 8. Part of the metal remained solid during the reaction but this was probably caused by the increased heat loss due to the more strongly radiating zirconia, added to the usual cooling effect of the hydrogen. The "boil" was still in progress at the end of the film, 3.5 seconds from the first signs of "spitting".

The "boil", which had not been observed in any other reduction experiment, was evidently caused by heterogeneous nucleation. Because the project was concerned with the homogeneous phenomenon, no further experiments were made with refractory particles but interfacial turbulence was investigated in additional experiments.

(b) Effects of sulphur: Sulphur is also surface-active in transition metals (45,46) but is less rapidly removed because the equilibrium partial pressure of H_2S, which controls the diffusion gradient in the gas, is very low. Small amounts

Table 4: Reduction of Nickel/Oxygen Drops in flowing Hydrogen.

H_2: 8 litres/min.		H_2: 10 litres/min.	
Time (sec)	% O	Time (sec)	% O
0	5.79	0	5.28
0.	5.83	0	5.35
2.0	3.97	0	5.07
2.25	3.51	2.0	2.95
3.5	2.95	2.25	2.90
3.75	1.54	2.5	2.64
5.25	1.00	3.25	1.97
6.25	0.13	3.5	1.12
8.25	0.012	3.5	1.11
9.0	0.007	4.25	1.55
		4.25	1.00
		4.75	0.69
		5.0	0.58
		5.0	0.35
		5.25	0.027
		5.75	0.005
		6.25	0.000
		7.0	0.009
		7.75	0.001

of sulphur were introduced to keep the surface tension at a lower value which would be unaffected by the depletion of oxygen. This addition was expected to suppress any interfacial turbulence.

The hydrogen was passed over heated copper sulphide; an analysis of the gas made by bubbling a known volume through zinc acetate solution gave $P_{H_2S} = 8.5 \times 10^{-4}$ atm. The equilibrium sulphur content of a nickel drop held at 1500° in this mixture would be about 0.3%. In further tests, nickel sulphide was added to the Ni/NiO mixture to give a nominal sulphur content of 0.1%; these samples were also reduced in the H_2/H_2S mixture.

Figure 7c shows no evidence of any change in the reduction rates. The residual sulphur content of the cast samples was below 0,015%: probably sulphur had been lost by reactions with the dissolved oxygen immediately the samples melted.

Because this approach no longer appeared promising, other ways of studying gas/metal reactions were explored, as later chapters will describe. At a much later stage in the research it became possible to return to the problem of rapid reduction rates, with an improved experimental method.

(c) Alloys containing more than 5% Oxygen: Uniform rods could not be cast when the Nickel contained more than about 0.5% oxygen. Pellets containing more than 0.9% often fell out of the coil as they melted. Later studies of the rate of oxidation of pure liquid nickel showed that 5 to 6 % O could be dissolved reproducibly in drops that remained levitated. (see Section IV: 4b). It then became possible to study longer reduction reactions.

Samples of nickel shot (believed to originate in the Mond Carbonyl process) were filed down to uniform weight. The levitated drops were exposed to the following sequence

of gases:

(i) He, 2½ l/min., for 1 min from time of melting.

(ii) O_2/He (as in step vi), 2-4 sec. to oxidise carbon.

(iii) He, about 30 sec.

(iv) H_2, 3-4 l/min, about 10 sec. to remove oxygen.

(v) He, about 1 min. to remove H_2 and allow temperature to become stable.

(vi) O_2/He, p_{O_2} = 0.20 atm., 3 l/min., 25 sec. exactly.

(vii) He, 30 sec.

(viii) H_2, for measured period of 1 to 9 sec.:-

First series: 8 l/min.

Second series: 10 l/min.

Samples were then cast into the copper cup.

Experimental results are shown in Table 4 and Figure 9. The data have been replotted with logarithmic ordinates in Fig. 10 to test for possible slow transport in the metal at lower levels of oxygen content. The straight lines in Figure 9 were first constructed to fit the data as well as possible. These lines were replotted in Figure 10 to give the convex upper curves and the dotted straight lines were added as tangents to fit the remaining data. The dotted lines were transferred back to Figure 9 to give the lower curves.

(d) Errors: (i) Timing: It was difficult to observe the time accurately on a stopwatch while operating the apparatus when reaction times were less than two seconds. The times recorded are unlikely to be more accurate than ± ¼ second.

It was also impossible to ensure that the sample was exposed to pure hydrogen for precisely the time intended. A short but significant time of 0.2-0.4 sec. is needed to purge helium from the small volume between the change-over valve and the end of the 'jet' tube. The reaction may also

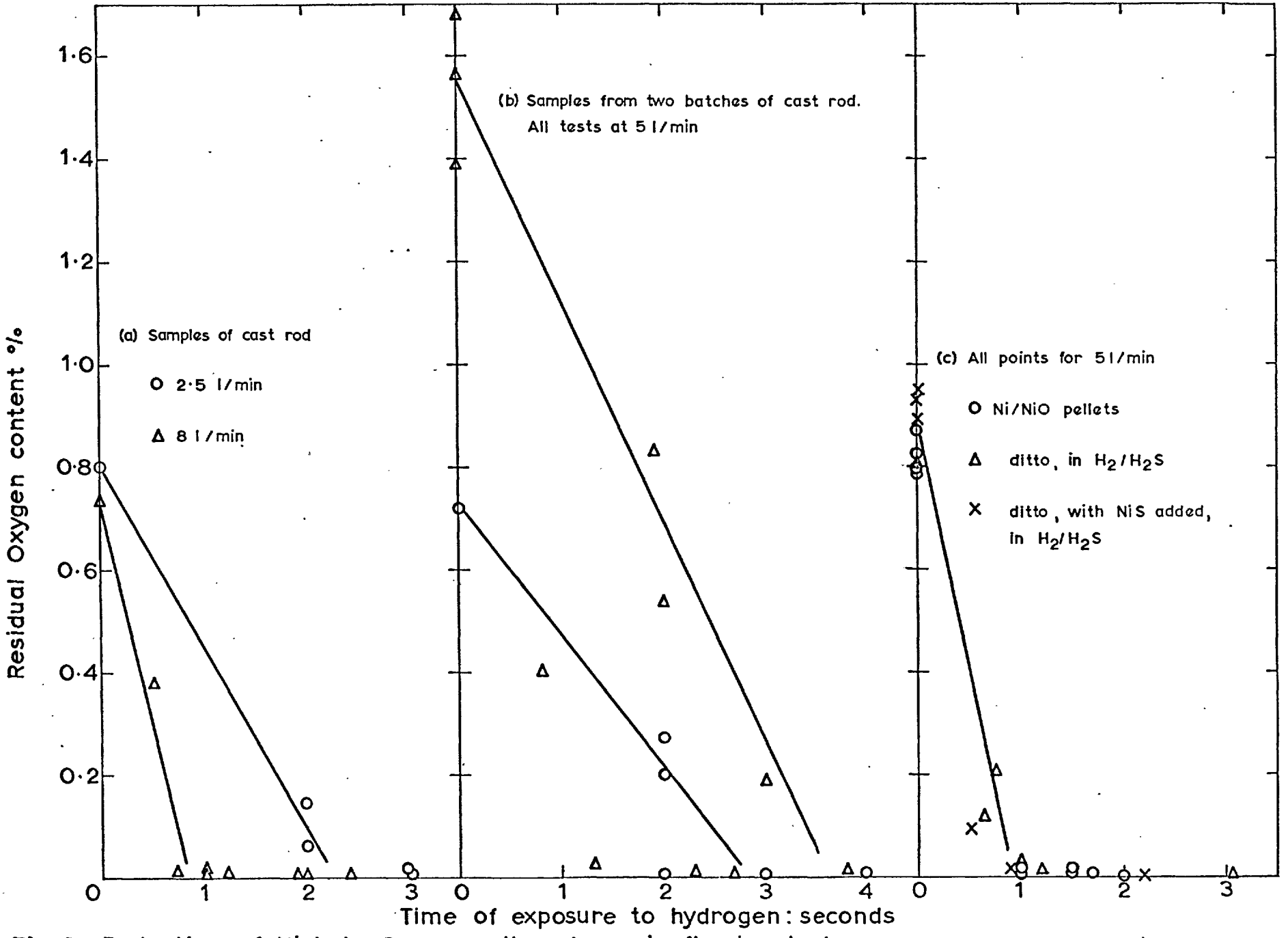

Fig. 7. Reduction of Nickel - Oxygen alloy drops in flowing hydrogen.

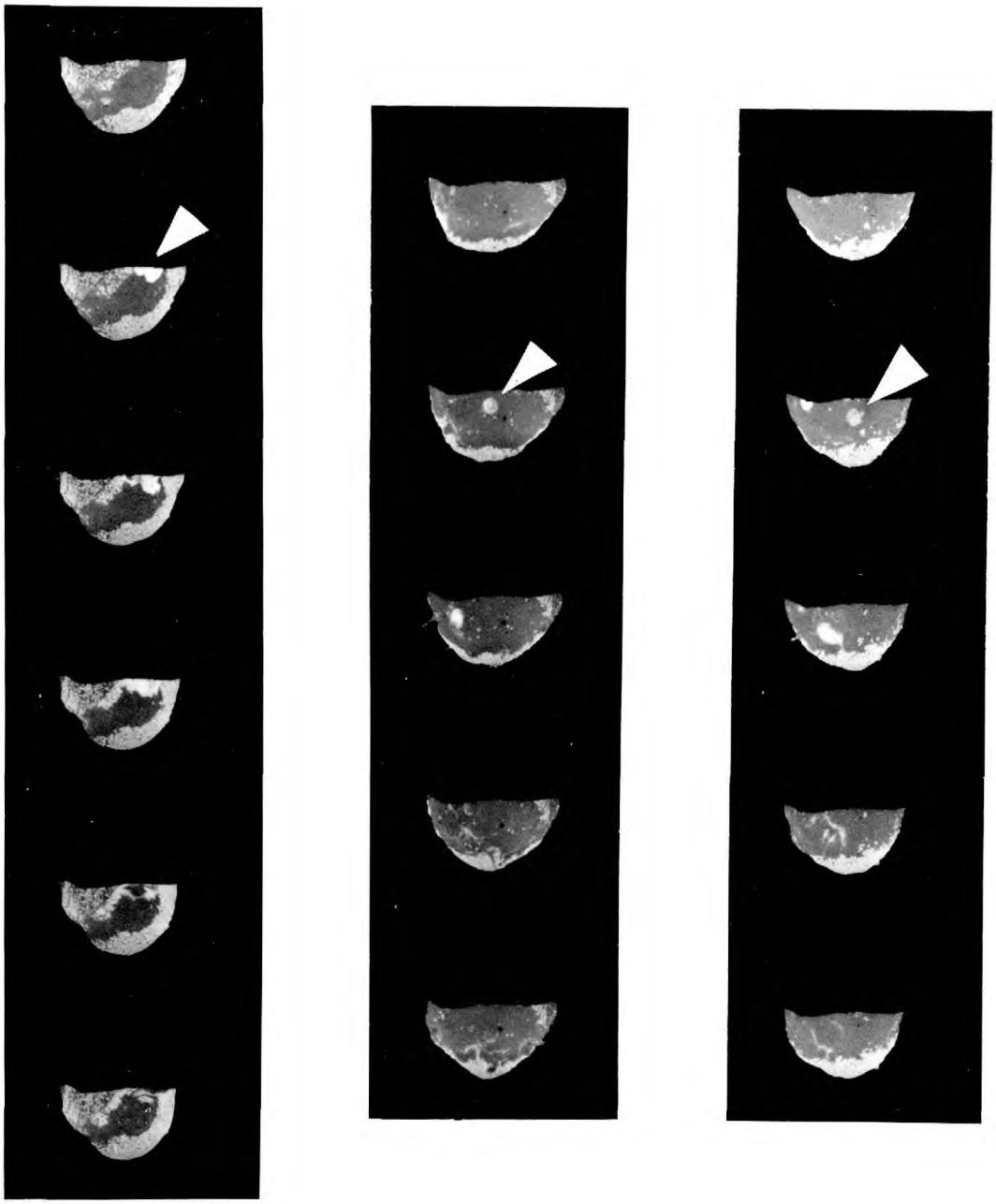

a b c

Figure 8: Reduction of a Nickel-Oxygen Drop by Hydrogen

(Film taken at 1000 frames/second)

Three sequences showing the gentle 'boiling' action. Note the bright spots which appear to be associated with bubble bursts

(Note: Surface is partly covered with particles of zirconia)

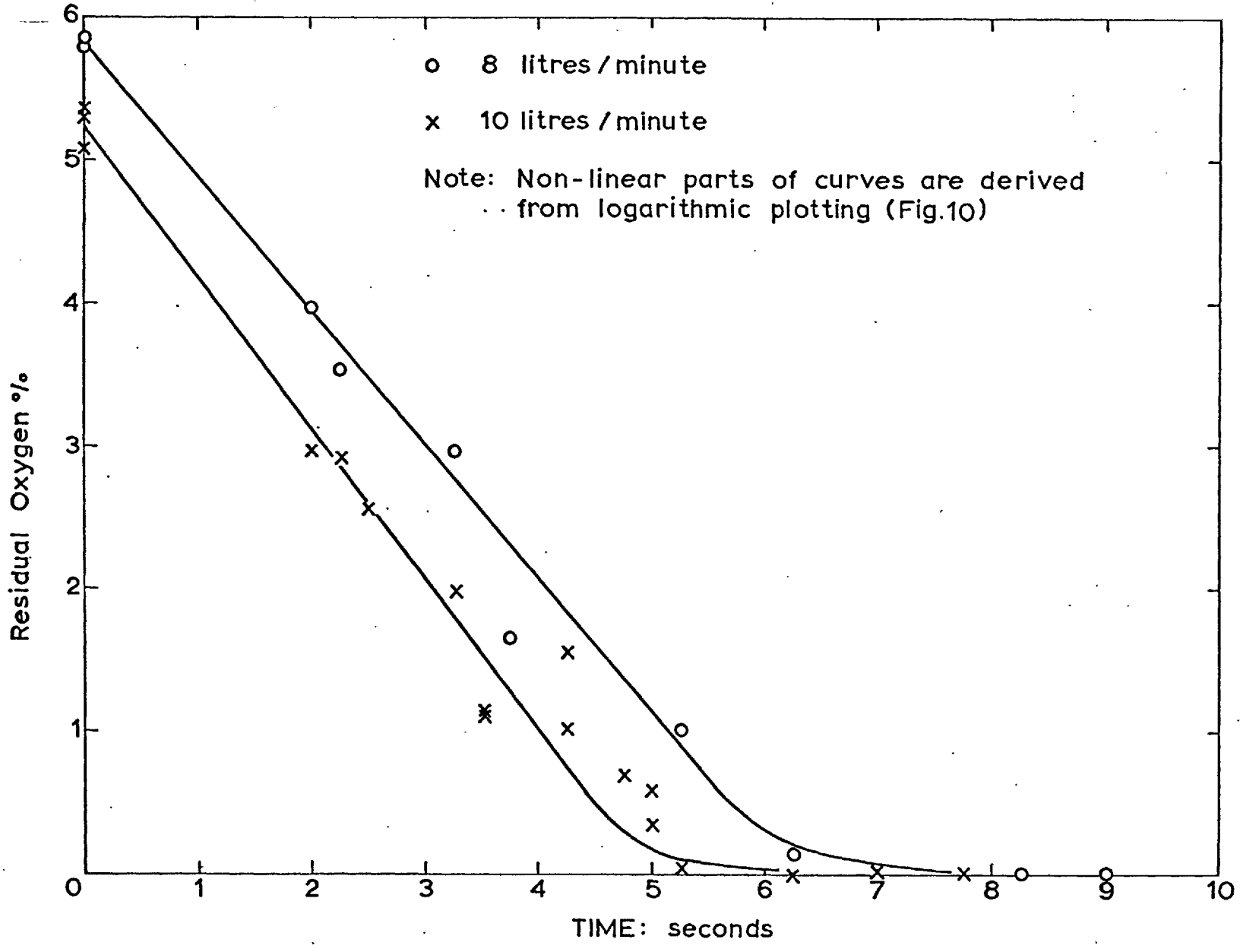

Fig. 9. Reduction of Nickel - Oxygen drops in flowing Hydrogen.

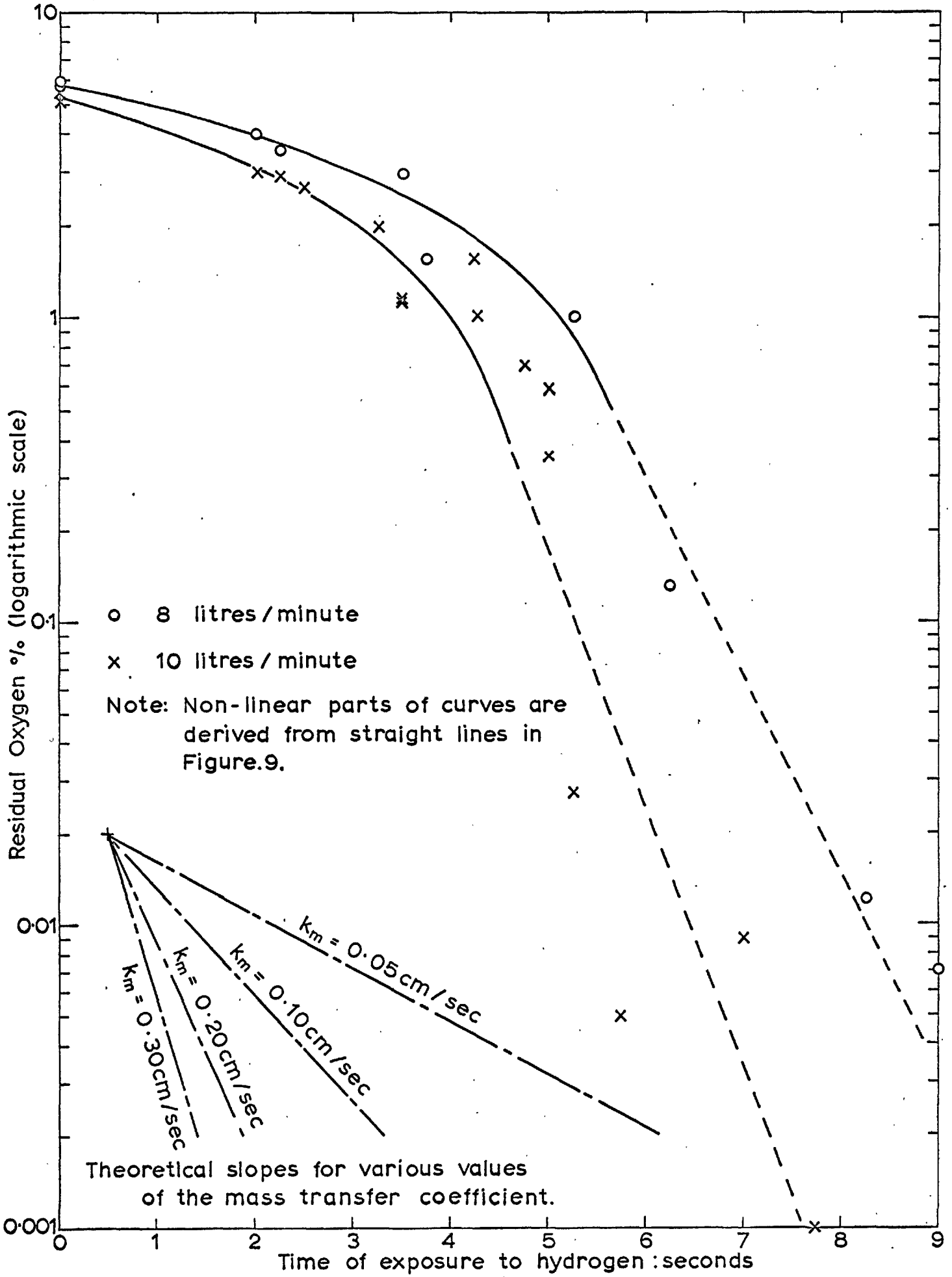

Fig. 10. Reduction of Nickel-Oxygen drops in flowing Hydrogen

have continued briefly during the ¼-½ second while the metal flowed to fill the copper cup and began to solidify. These errors in the reaction time should be about the same for all samples in a given series of tests. They have the effect of transposing all the points, except that for 'zero-time', in the same direction on the time scale by a small amount but they can probably be neglected in view of the larger errors in observing the time interval.

(ii) Oxygen losses: Some oxygen may be lost as the cast metal solidifies. Samples cast before all oxygen had reacted became 'inflated' when cast, probably because water vapour was formed and expelled. Those cast after longer exposures and containing only hydrogen were less inflated.

Nickel at 1500° dissolves 0.0036% H (38). If this amount of hydrogen were present and reacted with dissolved oxygen during casting, about 0.03%O might be lost. This is not very important for oxygen levels down to perhaps 0.2% but could cause serious errors (if indeed the hydrogen content reached saturation) at levels below 0.1%.

2. Reduction of Iron-Oxygen Alloys by Hydrogen

Two short series of reduction tests were made to determine whether the transport of oxygen atoms was as rapid in liquid iron as in liquid nickel.

The ferric oxide addition to the iron powder for pelletising was calculated to give an oxygen content of 0.4% oxygen, some of this being intended to oxidise carbon present in the iron powder. The iron powder itself was later found to contain 0.18%O. This raised the oxygen content of the liquid metal to about 0.5% and FeO covered the lower part of the drop surface before reduction. The pyrometer was focussed on the bare metal of the upper part of each drop.

The drops were exposed to hydrogen flowing at 2½ or 5 litres/minute. Results are shown in Table 5 and Figure 11.

Here again the difficulty of obtaining accurate exposure times was encountered. Starting and finishing temperatures were in the range of 1700-1725°; in some reactions transient peaks to about 1755° were recorded.

The positions of the points for the 5 litres/minute hydrogen flow (Figure 11a) suggest curvature of the line to the right. We know that at least part of the curve must be linear, since the rate of reduction of the oxide coating is almost certainly controlled by gaseous ~~diffusion~~ mass transfer. The straight portion was therefore plotted to intercept the first point and the data for this line transferred to logarithmic ordinates (Fig. 11b). The straight line in the latter diagram was then constructed, on a hypothesis of first-order kinetics with respect to oxygen, to be a tangent to this curve and to intercept the points furthest to the right. In this way, a conservative estimate of the ~~diffusion~~ mass transfer coefficient 'k_m' for oxygen was indicated.

Table 5: Reduction of Iron-Oxygen Alloy drops in flowing Hydrogen Sample weight = 1.79 ±0.01 g.

H_2 at 2½ litre/min		H_2 at 5 litre/min	
Seconds	%O	Seconds	%O
0	0.48	0	*
0	0.52	¾	0.27
0	0.52	1	0.09
1½	0.39	1½	0.15
2	0.30	2	0.067
2½	0.25		
3½	0.13	3	0.044

* Same powder mixture used for both series of tests.

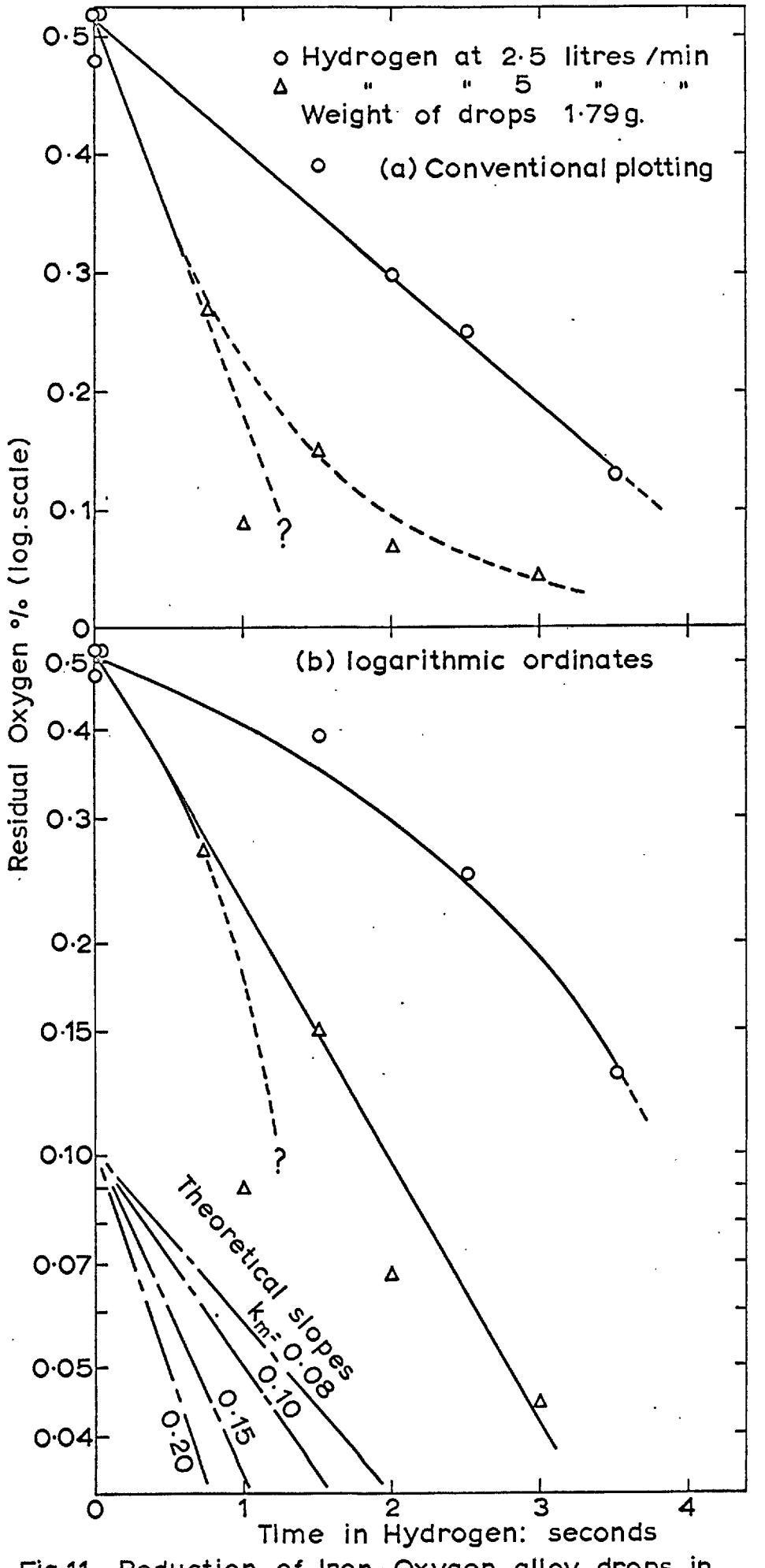

Fig.11. Reduction of Iron-Oxygen alloy drops in flowing Hydrogen.

3. Oxidation of Nickel-Sulphur Alloys

(a) Choice of System: The early work on the reduction of nickel-oxygen alloys in hydrogen indicated that the surface activity of the oxygen might affect reaction rates. Kinetics were quite different from those expected by analogy with the rates of oxidation of carbon in iron and it may be significant that carbon has little or no effect upon the surface tension of iron (45,46) and nickel (47).

Sulphur is also strongly surface-active in these metals (45,46) but reactions in which it is absorbed by a metal from H_2S (5) or is removed by reduction with hydrogen (1,5,48) are controlled by a slow gaseous ~~diffusion~~ transport step.

The oxidation of a metal/sulphur alloy offered a reaction between two elements, both of which are strongly surface active. Nickel was chosen because of its high capacity for dissolving oxygen. The reacting oxygen was diluted with helium to provide fairly long reaction times with moderate gas flows and to avoid the steep temperature rises that occur in pure oxygen.

Nickel powder or 'sponge' was mixed with sulphur 'flowers' (or crushed pure crystals in the later experiments) and pelletised as usual. After the reaction in the helium-oxygen mixture, each cast sample was analysed for both oxygen and sulphur by the methods described in Section III: 6, parts (b) and (f).

(b) Results: Numerical data are given in Table 6. The first two series of experiments (I & II) yielded sulphur-depletion curves of unusual form (Figure 12 a & c) and other conditions of gas composition and flow-rate were then studied. When attempts were made to obtain additional points for existing sets of data, it proved difficult to reproduce test conditions precisely after an interval of several days (e.g. Series VI

Table 6: Oxidation of Nickel-Sulphur Drops Weight for all tests: 1.60 ± 0.02 g.

L: flow of helium/oxygen mixture, litr./min. Oxygen and Sulphur listed as wt.%

T: temperature range, °C.

'Time' = Seconds of exposure to helium/oxygen mixture.

No.	I		II			III			IV		V	
p_{O_2}	0.008		0.020			0.008			0.008		0.008	
L	1		1			1			4		1	
T	1700±20		1700±20			1700±20			1600±25		1685±20	
Time	O	S	Time	O	S	Time	O	S	Time	S	Time	S
0	0.045	0.45	(Samples as in Series I)			(Samples as in Series I)			0	0.59	(Samples as in Series IV)	
0	-	0.46							0	0.57		
0	0.033	0.44	20	0.10	0.44	90	0.28	0.28	0	0.58	30	0.57
0	0.023	0.47	40	0.42	0.34	146	0.36	0.100	20	0.54	45	0.54
10	0.016	0.44	60	0.53	0.21	150	0.30	0.134	22	0.52	60	0.48
10	0.002	0.46	90	0.50	0.095	180	0.44	0.051	32	0.46	90	0.39
20	0.028	0.44	120	0.73	0.052	190	0.41	0.031	40	0.41	120	0.27
40	0.16	0.43	180	1.28	0.026	210	0.54	0.023	60	0.29	150	0.22
63	0.20	0.38				240	0.66	0.011	81	0.11	180	0.14
92	0.21	0.31							100	0.041	210	0.056
120	0.36	0.25							120	0.042		
210	0.36	0.053							150	0.028		
									180	0.004		

Table 6 contd.

No.	VI		VII		VIII		IX	
p_{O_2}	0.008		0.020		0.008		0.025	
L	1		1		1		2.5	
T	1740±20		1750±20		1760±20		1725-1850	
Time	O	S	Time	O	S	Time	O	S	Time	O	S
0	0.032	0.68	(Samples as in			(Samples as in			0	0.030	0.72
0	0.020	0.64	Series VI)			Series VI)			0	0.032	0.72
0	0.013	0.66	10	0.045	0.60	30	0.088	0.66	20	0.28	0.58
10	0.066	0.66	20	0.096	0.65	55	0.096	0.64	20	0.28	0.56
20	0.078	0.65	30	0.15	0.61	75	0.139	0.60	30	0.36	0.44
30	0.103	0.61	40	0.17	0.60	95	0.17	0.56	30	0.34	0.46
40	0.12	0.64	55	0.18	0.56	120	0.16	0.52	40	0.51	0.31
55	-	0.55	75	0.22	0.45	165	0.17	0.42	50	0.71	0.21
80	0.27	0.45	95	0.27	0.37	265	0.30	0.21	60	0.60	0.12
120	0.21	0.42	110	0.33	0.33	280	0.24	0.17	60	0.61	0.11
140	0.17	0.44	130	0.38	0.22	300	0.29	0.12	70	0.71	0.098
160	0.18	0.37	150	0.34	0.20	346	0.31	0.084	85	0.98	0.037
200	0.23	0.31	170	0.40	0.14	380	0.37	0.051	95	1.16	0.026
230	0.21	0.24	200	0.49	0.078				110	1.41	0.017
250	0.25	0.19							120	1.60	0.017
270	0.28	0.12							140	1.90	0.011
290	0.25	0.14							165	2.37	0.019
315	0.30	0.093									
361	0.36	0.063									

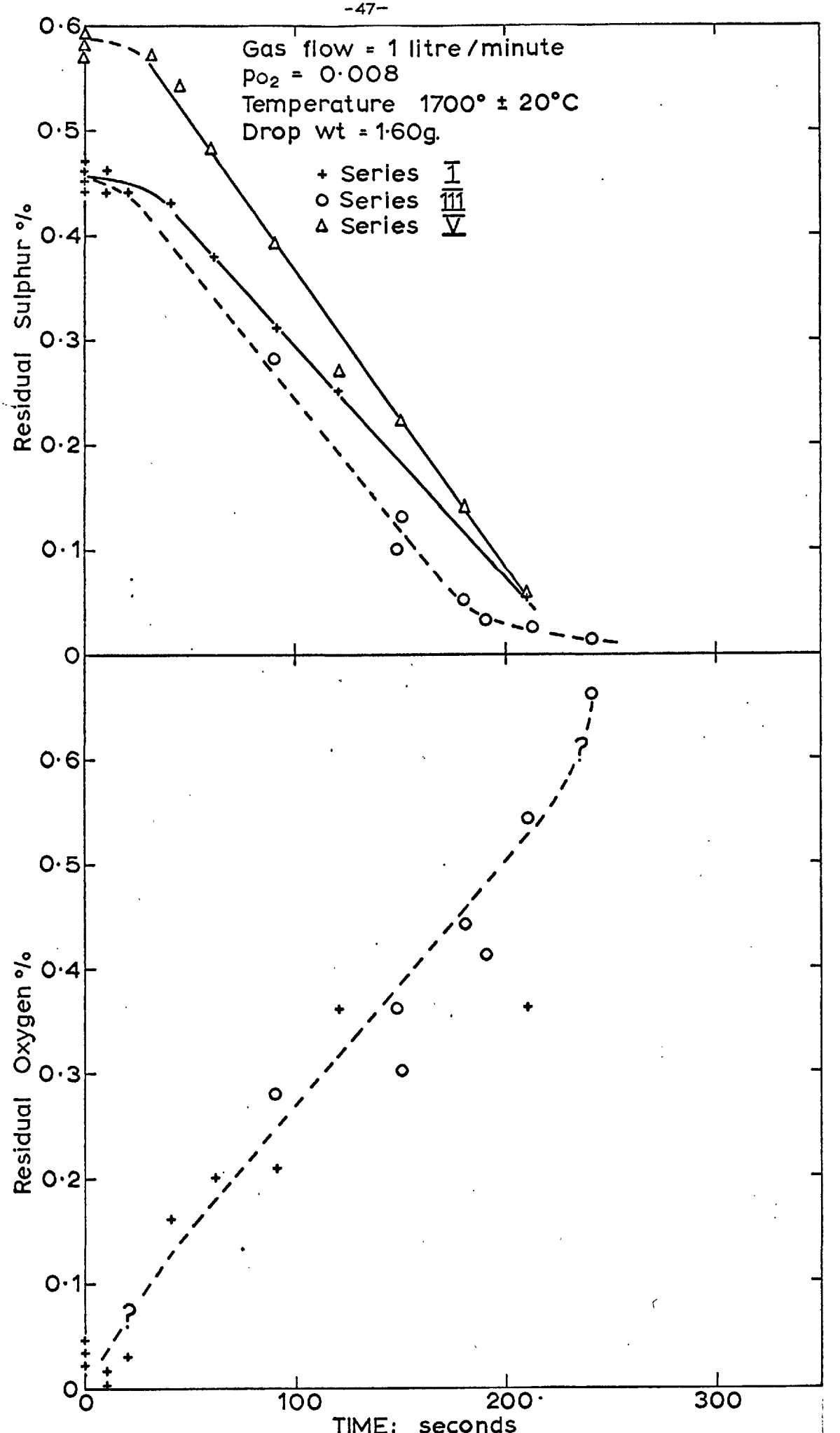

Fig. 12a. Oxidation of Nickel-Sulphur drops by Helium-Oxygen mixtures.

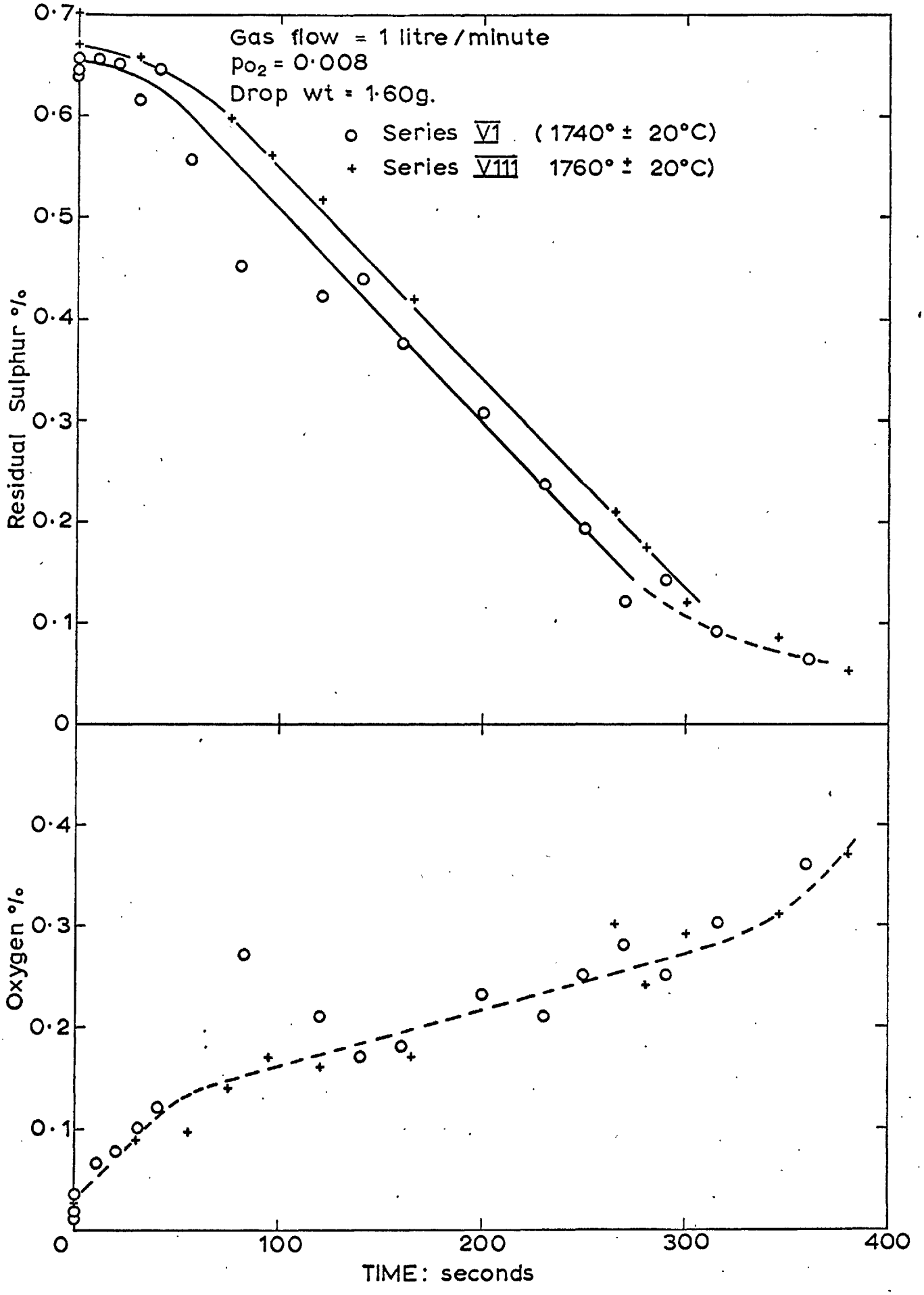

Fig.12b. Oxidation of Nickel-Sulphur drops by Helium-Oxygen mixtures.

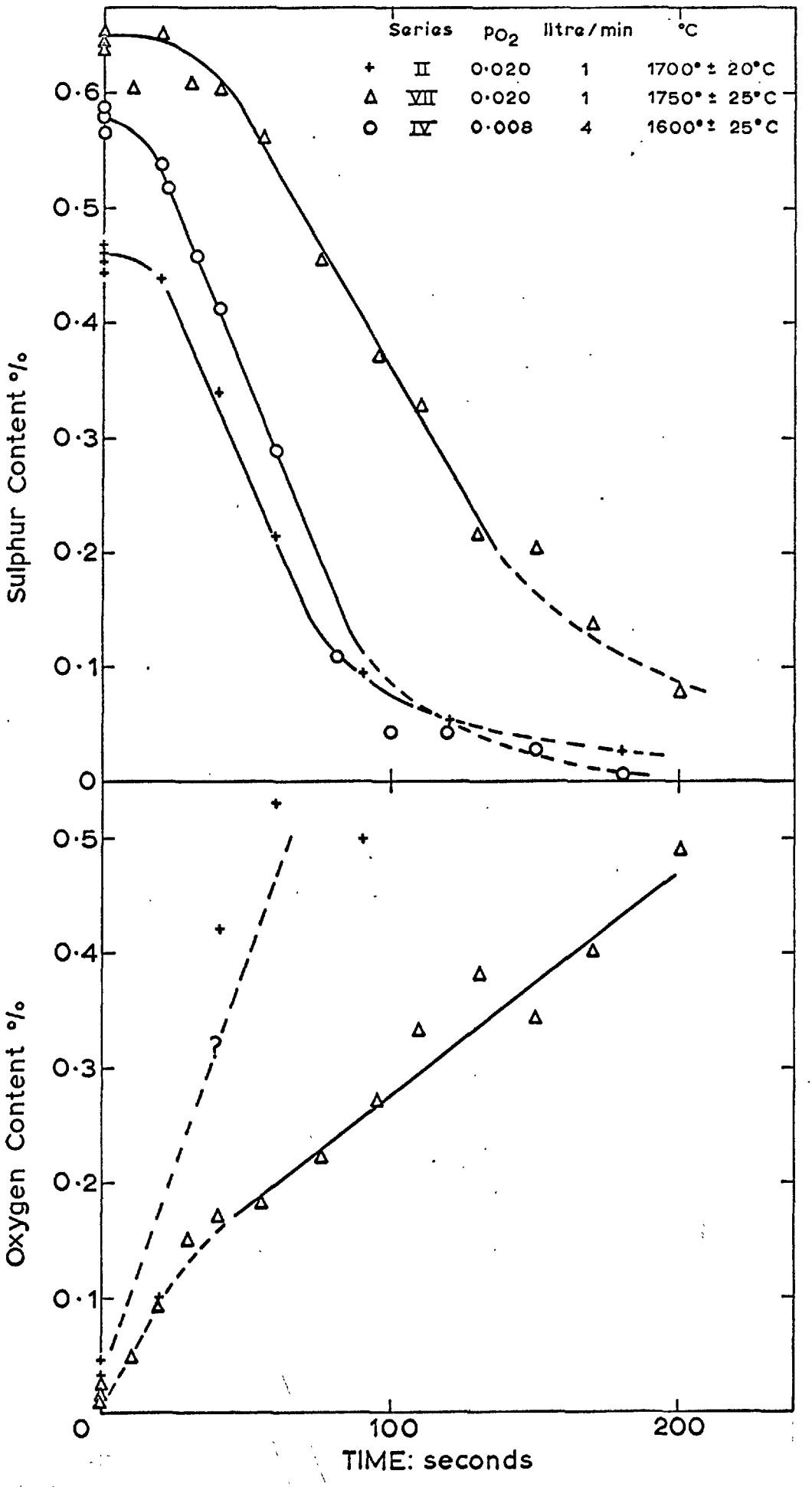

Fig.12c. Oxidation of Nickel-Sulphur drops in Helium-Oxygen mixtures

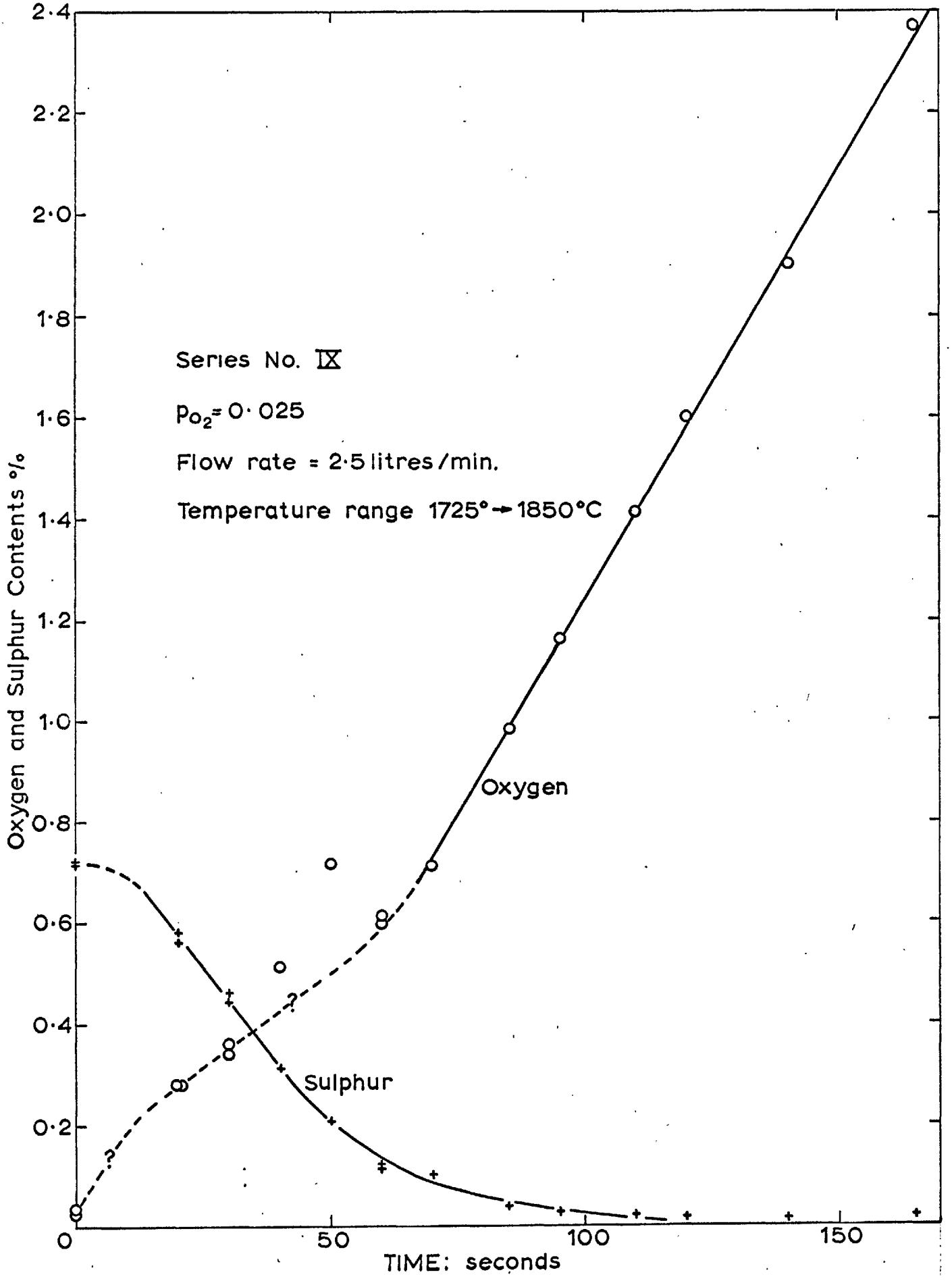

Fig. 12d. Oxidation of Nickel-Sulphur drops in a Helium-Oxygen mixture.

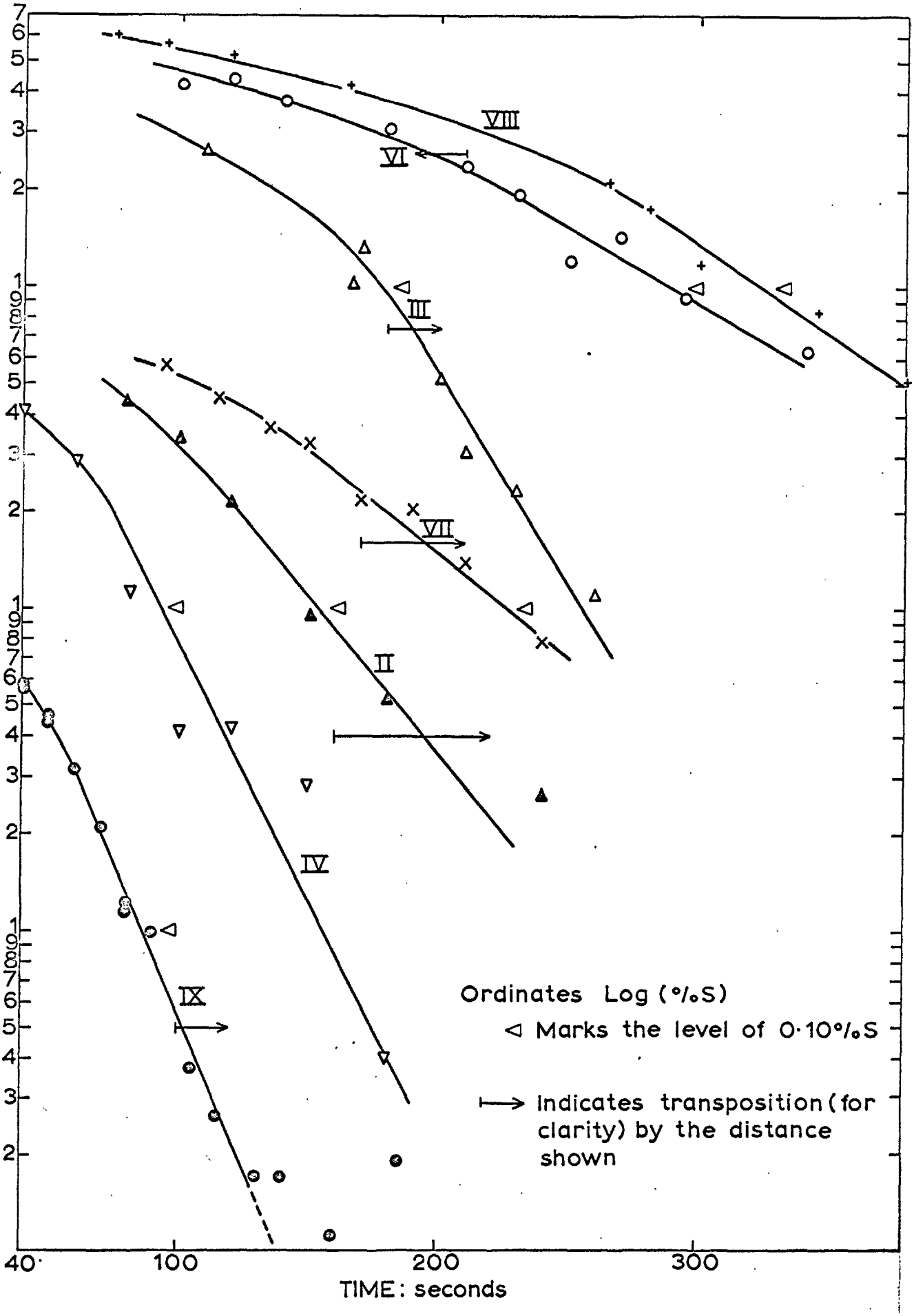

Fig.13. Oxidation of Nickel-Sulphur drops (logarithmic plotting)

& VIII, Fig 12 b).

Data for the lower part of each curve of sulphur content are shown replotted on logarithmic ordinates in Figure 13 to test the hypothesis that the reaction kinetics had changed from zero-order to first-order with respect to the sulphur. The straight lines drawn through these points were then replotted to give the lower non-linear parts of the curves in Figures 12 a,b,c& d.

(c) Temperature and Observations: In many of the experiments the metal temperatures rose by 30-40 degrees during the first few seconds of exposure to the oxidising gas stream, then settled down to a level close to the original one. In Series II and V, several samples emitted a spray of fine droplets at the initial exposure but the phenomenon was not always seen and could not be reproduced later for filming.

Towards the end of the longer exposures, the temperature rose slowly as much as 100 degrees above the steady level. The rise began at a moment close to the end of the period of uniform depletion of the sulphur. At about the same time, the small 'slag' particles present on the drop surface appeared to increase slightly in size.

These particles normally appear as very small bright gyrating spots and are present on all metal drops (except after reduction in hydrogen), in spite of the high purity of the materials used. The word 'slag' is used for want of a better description, since the very small black spot that was also seen on many cast specimens appeared glassy but has not been analysed. It is possible that the particles are formed from traces of silicon, perhaps in combination with the oxide of the bulk metal or of other trace impurities.

(d) Note on the Oxidation of Iron-Sulphur Alloys: A few samples made from iron powder with crushed sulphur crystals

were exposed to oxygen-helium mixtures under conditions similar to those of Series IV and IX described above. After 20-22 seconds or 13-14 seconds, in the respective series, bright streaks moved rapidly down the sides of the drop and a coating of iron oxide formed at the base of the drop. As the oxidation continued, the area of the oxide coating slowly increased. Other data are shown in Table 7.

Table 7: Oxidation of Iron-Sulphur Alloy Drops in Oxygen-Helium Mixtures.

(i) p_{O_2} = 0.008 atm. Flow-rate = 4 l/min.

Seconds	%S	%O
0	0.735	-
0	0.762	-
50	0.759	-
55	-	0.55
120	0.732	-
135	-	1.15

(ii) p_{O_2} = 0.025 atm. Flow-rate = 2½ l/min.

Seconds	%S	%O
0	(As before)	
30	0.746	-
40	-	0.87
70	0.742	-
120	0.735	-

In another sample that was levitated and cast in helium only, 0.18%C was measured.

Temperature range: (i) 1650-1700 °C

(ii) 1680-1790°C

Weight of samples (all experiments) = 1.6 g.

4. Oxidation of Liquid Nickel.

(a) Low Oxygen Partial Pressures: The oxidation of the pure metal was studied under conditions of gas composition and flow similar to those for the desulphurising experiments, so that the rates of absorption of oxygen in the presence and absence of sulphur could be compared.

Samples of nickel shot were filed to uniform weight and were levitated and melted in flowing helium. A stream of hydrogen was admitted for a few seconds to ensure that the metal contained no oxygen. After a further minute in helium, the drop was exposed to the oxygen-helium stream. The reaction was terminated by switching back to pure helium and quickly casting the sample.

Results are shown in Table 8 and Figure 14.

(b) High Oxygen Partial Pressures: Tests for Oxide Formation:

If oxygen can be supplied to the metal drop more rapidly than the eddy and molecular diffusion processes in the liquid can transport the dissolved element into the interior of the drop, the metal oxide should form on the surface although the average concentration of oxygen in the drop is below the saturation level. From this average or 'bulk' concentration it should be possible to estimate the limiting gradient for mass transfer and the mass transfer coefficient for oxygen.

Levitated drops of nickel were exposed in succession to increasing concentrations and flow-rates of oxygen, diluted with helium. Table 9 shows the oxygen contents attained and the temperature range of each experiment. Observations concerning oxides are described more fully in sub-section(d) below.

The difficulties of measuring temperatures above 2000^{0} have already been discussed (Section III: 5d); furthermore the data for the emissivity at high oxygen contents are

Table 8: Oxidation of Ni Drops by Oxygen-Helium Mixtures (low oxygen concentrations).

L = Total Flow-rate in litres/minute (inert gases stated).

T = Temperature range, °C.

Time = Seconds of exposure to O_2/He mixture.

No.	I		II		III		IV		V		VI	
p_{O_2}	0.008		0.008		0.008		0.008		0.020		0.040	
L	1He		3He		3He+ 2Ar		5He+3Ar		1He		1He	
T	1690-1760		1640-1720		1680-1760		1630-1720		1700-1800		1700-1820	
	Time	%O	Time	%O	Time	%O	Time	%O	Time	%O	Time	%O
	30	0.083	60	0.30	10	0.094	40	0.34	20	0.131	15.	0.28
	45	0.117	60	0.31	20	0.192	65	0.59	30	0.195	20	0.38
	50	0.184	80	0.38	20	0.170	90	0.82	40	0.30	25	0.44
	75	0.24	120	0.58	30	0.25	100	0.88	60	0.44	30	0.60
	90	0.29	158	0.75	40	0.32	115	1.03	80	0.63	40	0.82
	105	0.33	201	0.94	50	0.48	120	1.07	90	0.75	50	1.04
	120	0.39			50	0.45			100	0.78	60	1.16
	140	0.46			60	0.50			120	0.92	75	1.55
	160	0.51			60	0.55			140	1.06		
	210	0.62			80	0.70			160	1.26		
					90	0.78						
					90	0.81						
					100	0.92						
					120	1.14						
					140	1.31						

Wt. of drops: Series I: 1.84 ± 0.02 g.
All others: 1.60 ± 0.02 g.

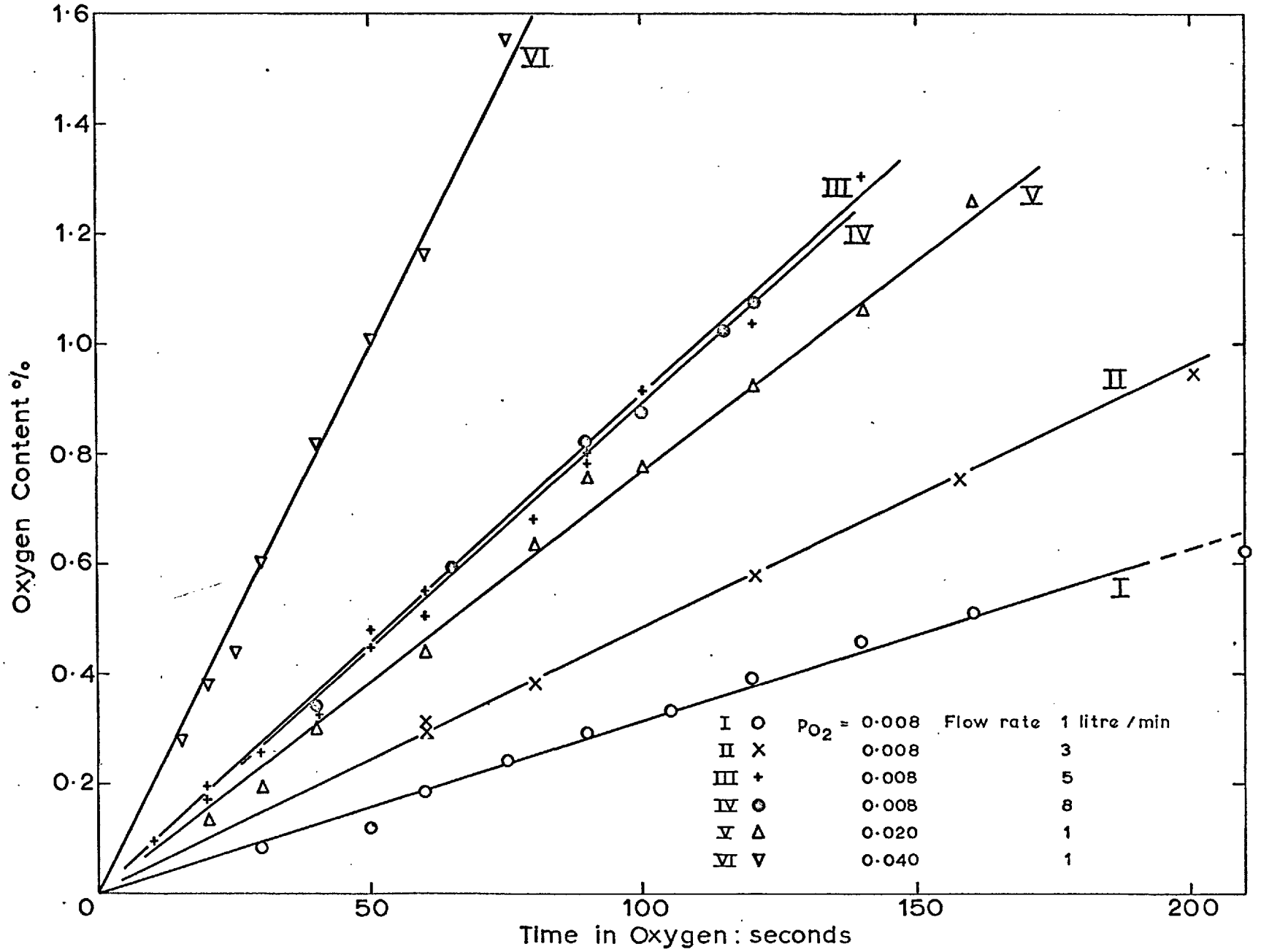

Fig. 14. Oxidation of Nickel drops by Helium Oxygen mixtures. (low oxygen partial pressures)

Table 9: Oxidation of Liquid Nickel

(with high concentrations of oxygen in the gas stream).

Weight of drops = 2.00 ± 0.02g.

No.	i	ii	iii	iv	v	vi	vii
p_{O_2}:atm	0.08	0.12	0.20	0.20	0.40	0.60	1.00
Gas flow: l/min	3	3	3	5	5	5	5
Sec. in O_2/He	90	60	45	35	15	6	4*
Temp.°C, start	1715	1710	1715	1700	1730	1730	1730
final	2025	2050	2125	2150	2250	2275	>2275
%O	6.52	6.78	9.30	9.66	10.9	9.11	8.61

* Approximate: Sample fell from coil while power was still on.

lacking. The calibration curve for nickel containing $\frac{1}{2}$ - $\frac{3}{4}$ %O has therefore been extrapolated so that a comparison of relative temperature levels can be made.

(c) High Oxygen Partial Pressures: Rates of Oxygen Absorption:

Two series of samples were exposed for various times to gas streams containing 30 and 60 % of oxygen, to show the form of the absorption curves.

Analyses and temperatures are shown in Table 10 and Figure 15. The temperature curves represent averages of the traces from each series; the temperatures of the individual experiments varied in the range of $\pm$ 20° from the values shown.

(d) Oxides and 'slag' spots: The data in Table 9 show that oxygen concentrations up to 10% were achieved in periods shorter than 20 seconds but no phase identifiable as nickel oxide was seen to form. In the final test with pure oxygen flowing at 5 litres/minute, the general brightness and strong fuming due to the steeply-rising temperature made observation difficult but there was no clear evidence of oxide formation. Each of the temperature traces showed a steep but smooth rise to temperature levels above 2200°. The formation of an oxide coating would have caused a sudden increase in light emission and in the apparent temperature: none of the records showed this feature.

The small bright spots that appeared on nickel-sulphur samples were again observed when nickel was being oxidised at low oxygen partial pressures. They usually became more prominent, although not very large, near the end of an experiment. These spots were particularly noticeable during the first experiments made under the conditions of Series II and IV and the final oxygen contents of the samples (not recorded here) were very erratic and generally below the

expected levels. When the experiments were repeated, the drops were first treated in turn with hydrogen, then oxygen to remove traces of carbon and hydrogen again for thorough deoxidation. During this short period of oxidation, the temperature was allowed to rise to about 1750° so that any silica present might volatilise at least partly. (4). Little or no 'slag' was observed in the following periods of controlled oxidation and the results, as Figure 14 shows, conformed closely to smooth curves.

The difficulty was not experienced in the other series of experiments in which nickel shot from the same batch was used and it is thought that the higher temperatures in those series, resulting from the lower rates of gas flow, may have volatilised silica more rapidly.

Three films of oxidation at high oxygen concentrations were taken at 1000 frames per second with the "Fastax" camera:-

1. Pure oxygen at 3 l/min.
2. O_2/He: p_{O_2} = 0.6 atm., 5 l/min.
3. As 2, but pre-treated as described above with H_2, O_2/He and again H_2.

Each film showed that a faint coating began to form almost immediately the oxygen stream encountered the drop (Fig. 16). This coating was only slightly more luminous than the bare metal and did not appear to thicken or to increase in brightness during the 3-4 seconds of film exposure.

Table 10: Oxidation of Liquid Nickel (high oxygen concentrations): Data on rates of absorption.

Gas mixture flowed at 5 litres/minute.

p_{O_2} = 0.30 atm. w = 1.70 ± 0.02g.				p_{O_2} = 0.60 atm. w = 2.0 ± 0.05g.			
Time in O_2 Sec.	Temp. °C. Start	Max.	%O	Time in O_2 Sec.	Temp. °C. Start	Max.	%O
3	1710	-	1.52	1.2	1735	1860	2.04
5¼	1710	1860	2.44	2.1	1735	1970	3.81
7	1690	1900	3.28	2.5	1725	2000	4.66
8¼	1765	2125	4.39	2.9	1735	2030	4.41
12¼	1685	2070	6.61	4.0	1750	2150	6.55
16¼	1705	2150	8.46	6.0	1700	2210	8.32
18¼	1685	2110	9.68	6.1	1745	2275	9.21

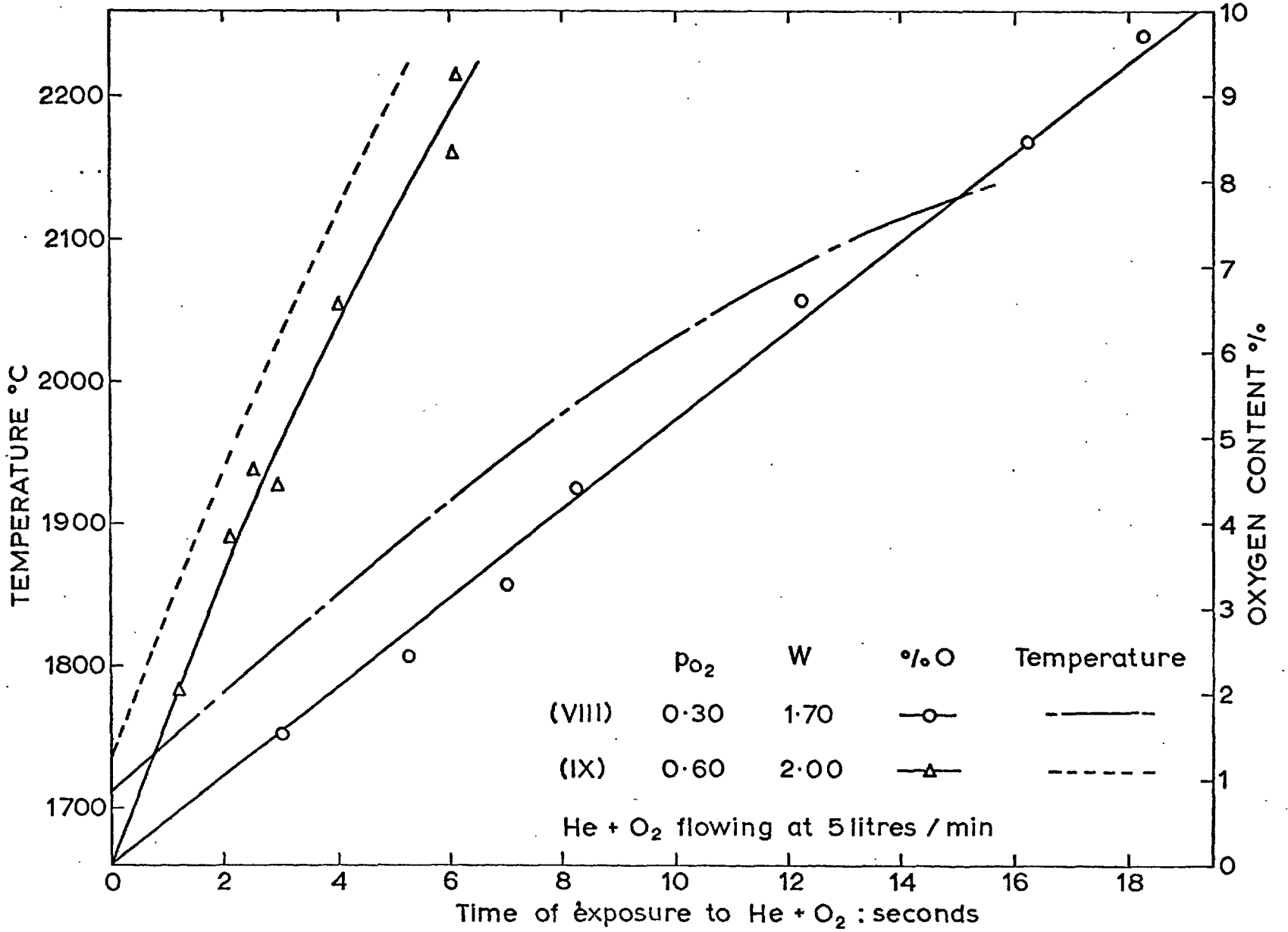

Fig. 15. Absorption of oxygen by liquid Nickel drops.

Fig. 16: ERRATUM

For "Films No. 2 - 4" read "Films No. 1 - 3"

a

b

c

Figure 16: Oxidation of pure Nickel Drops

Frames from Films No. 2-4, showing development of 'silica ' coatings in the first few milliseconds of contact with oxygen.

a: Film No. 1.

b: Film No. 2.

c: Film No. 3.

5. Loss of Oxygen from Nickel-Oxygen alloys in Inert Gases

In experiments on the reduction of nickel-oxygen alloys, measurable amounts of oxygen were lost when drops were held in helium only. Because of the general interest in heterogeneous reactions involving oxygen, three series of experiments were made in which Ni/NiO pellets were melted in helium and kept levitated in helium or helium-argon mixtures.

"Zero-time" was set at 45 seconds from the moment the temperature of a newly-melted sample passed the 1500° mark. As the oxygen content of a drop became depleted, its temperature tended to decrease (owing to the increased conductivity of the metal) and the power supply was adjusted from time to time to keep the temperature steady. In the experiments with the highest rate of gas flow, argon was mixed with the helium to avoid cooling the drops excessively.

Experimental results are shown in Table 11 and Figure 17.

Table 11: Loss of Oxygen from Nickel-Oxygen Alloy Drops in Inert Gas Streams.

N.B. Time in minutes.

Series	I	II	III
Gas Flow (l/min)	1He	2He	3He + 2 Ar
Drop wt. (g.)	1.42±0.01	1.40±0.01	1.42+0.01
Temp. °C.	1760±20	1760±30	1750±20

Time	%O	Time	%O	Time	%O
0	0.772	0	0.717	0	(As in
0	0.737	0	0.715		Series I)
0	0.735	0	0.708	2½	0.705
3	0.668	0	0.721	5	0.655
7	0.612	0	0.727	10	0.574
12	0.524	3	0.658	17	0.504
18	0.477	5	0.658	17	0.510
18	0.423	7	0.591	26	0.429
25	0.401	10	0.588	35¼	0.345
36	0.315	15	0.518		
		15	0.493		
		20	0.465		
		26	0.424		
		31	0.349		
		33	0.397		
		40	0.357		

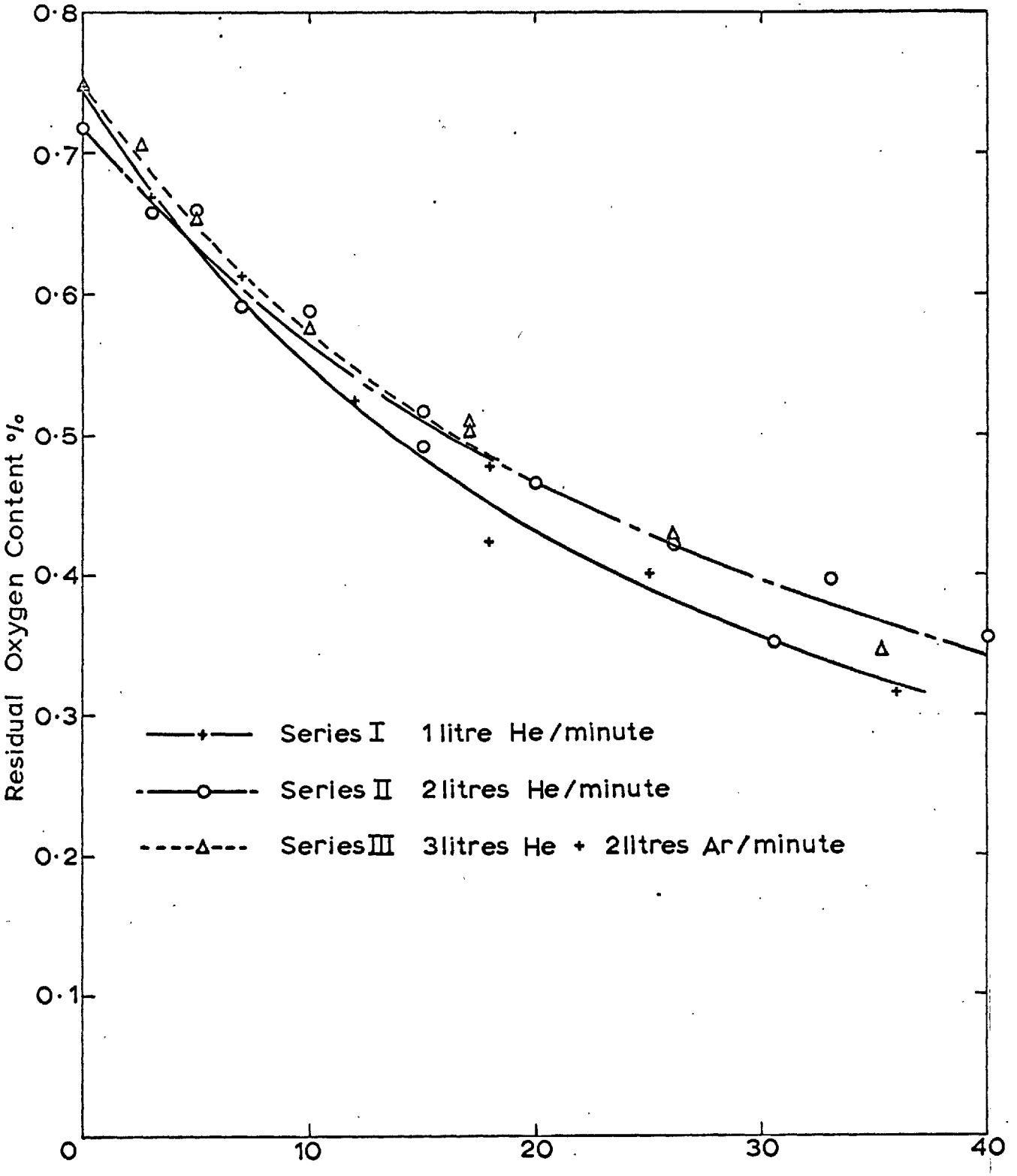

Fig. 17. Loss of oxygen from Nickel-Oxygen alloy drops in flowing inert gases.

6. Oxidation of Nickel-Carbon Alloys

(a) Introduction: Decarburisation studies were made with nickel alloys to test whether the period of initial slow reactions, observed with the nickel-sulphur alloys, could also be detected here. About 2.8%C can be dissolved in nickel at 1700°C (50). Compared with iron, nickel has a high capacity for dissolving oxygen (49,50) and it was possible that this might lead to high supersaturations of CO.

The principle of diluting the oxygen with helium was retained to give longer reaction times and smaller temperature rises.

(b) Method: Pellets made from nickel 'sponge' and pure flake graphite were levitated and melted in helium. The oxygen-helium mixture was turned on one minute after all the graphite had dissolved. Samples from Series I and IIa were analysed for carbon only, to show the general form of the decarburisation kinetics.

Distin found that small quantities of CO were released as the cast samples solidified and that the oxygen content of this gas had to be measured and added to the oxygen content of the solid metal. His method of casting the sample in a separate vessel and determining the CO gas released in that vessel was modified in some details.

Nickel drops broke up when cast into alumina powder and a simple split steel mould was used instead, with a sleeve or 'funnel' of copper foil to catch splashes of liquid metal. The principle of converting the CO to CO_2 and absorbing this gas for weighing was taken from the fusion method of analysing for oxygen (Section III: 6c). Figures 18 & 19 show the arrangement and details of the casting column.

The plug valve was permanently attached to the outlet from the levitation cell but the column could be swung aside so

that pellets could be raised into the coil. While the drop was being held for the first minute in helium, the column was flushed out with argon. Just before the sample was due to be cast, the outlet tap of the column was closed, allowing a slight pressure of argon to build up. The plug valve was opened and closed quickly, shutting off the power by means of the micro-switch. The gases in the column were then flushed out for 8-9 minutes by argon at 400 ml/min. to the copper oxide furnace and soda-asbestos bottle, as in the method for oxygen analysis by fusion. The 'Blank' for this method with only argon flowing through the apparatus was 0.0001g. CO_2 or less.

(c) Results: These are shown in Table 12 and Figures 20 a-e. The times of the boil were noted visually and later checked by measuring the deviations from the smooth curve on the temperature records. The relation between the deviations and the progress of the boil was found with the aid of high-speed filming and will be described later. Generally the times for the start of the boil measured on the temperature records were about one second less than the visual estimates. These starting times varied fairly widely in each series:-

I	(No boil observed)
II	75-84, average 79½ seconds
III	33¼-39, average 35½
IV	15-16¾, average 16
V	8¼-10, average 9

Plotting the oxygen contents on the normal time base gave scattered points for the later samples. These contents appeared to be related instead to the time from the start of the boil and plotting on this base gave more consistent curves. Figs. 20b - e include these curves whose time bases start at the average times for the start of the boil.

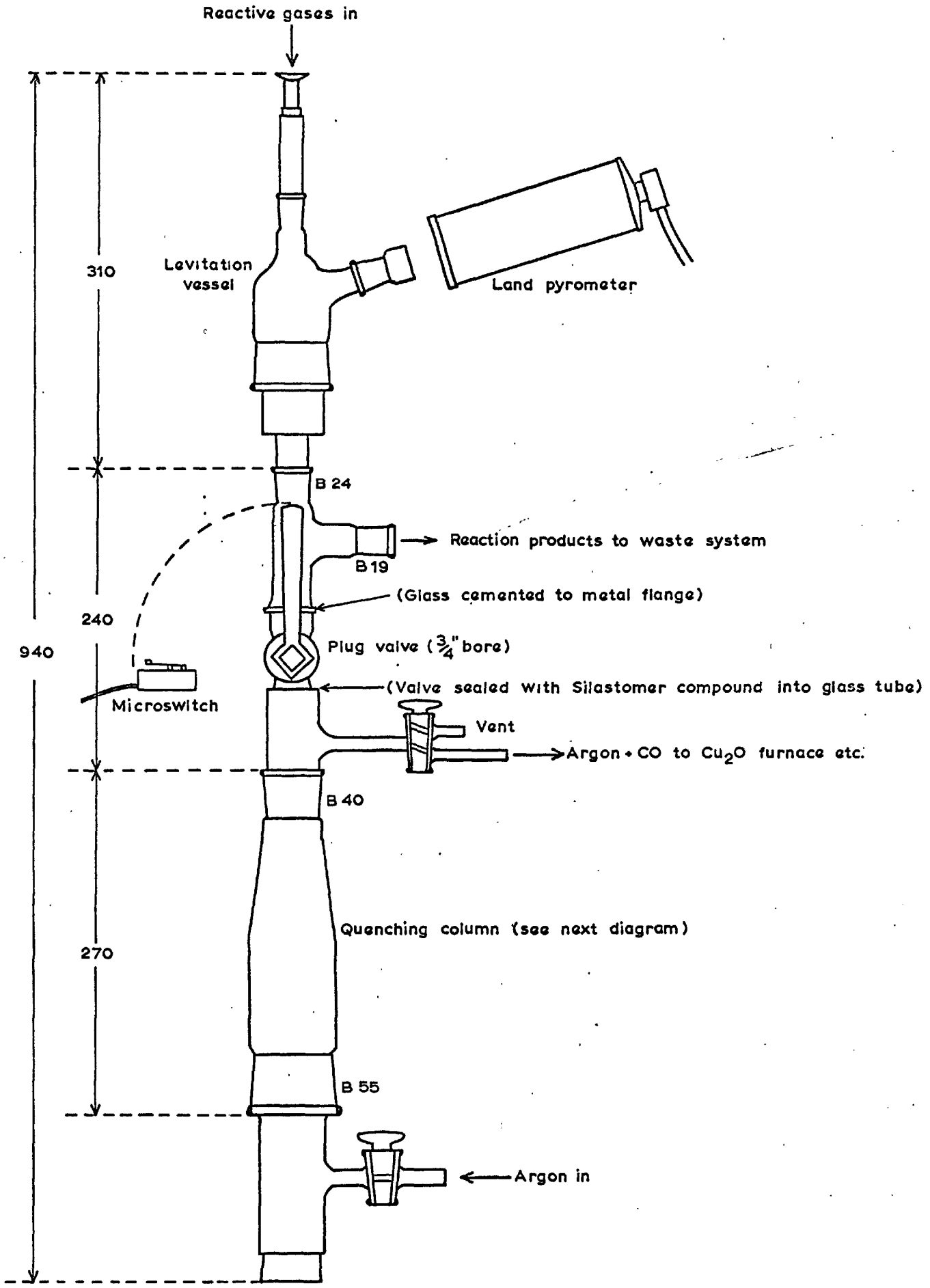

Fig.18. Arrangement of Quenching Column used in decarburization experiments
Scale: One quarter size (All dimensions in millimetres)

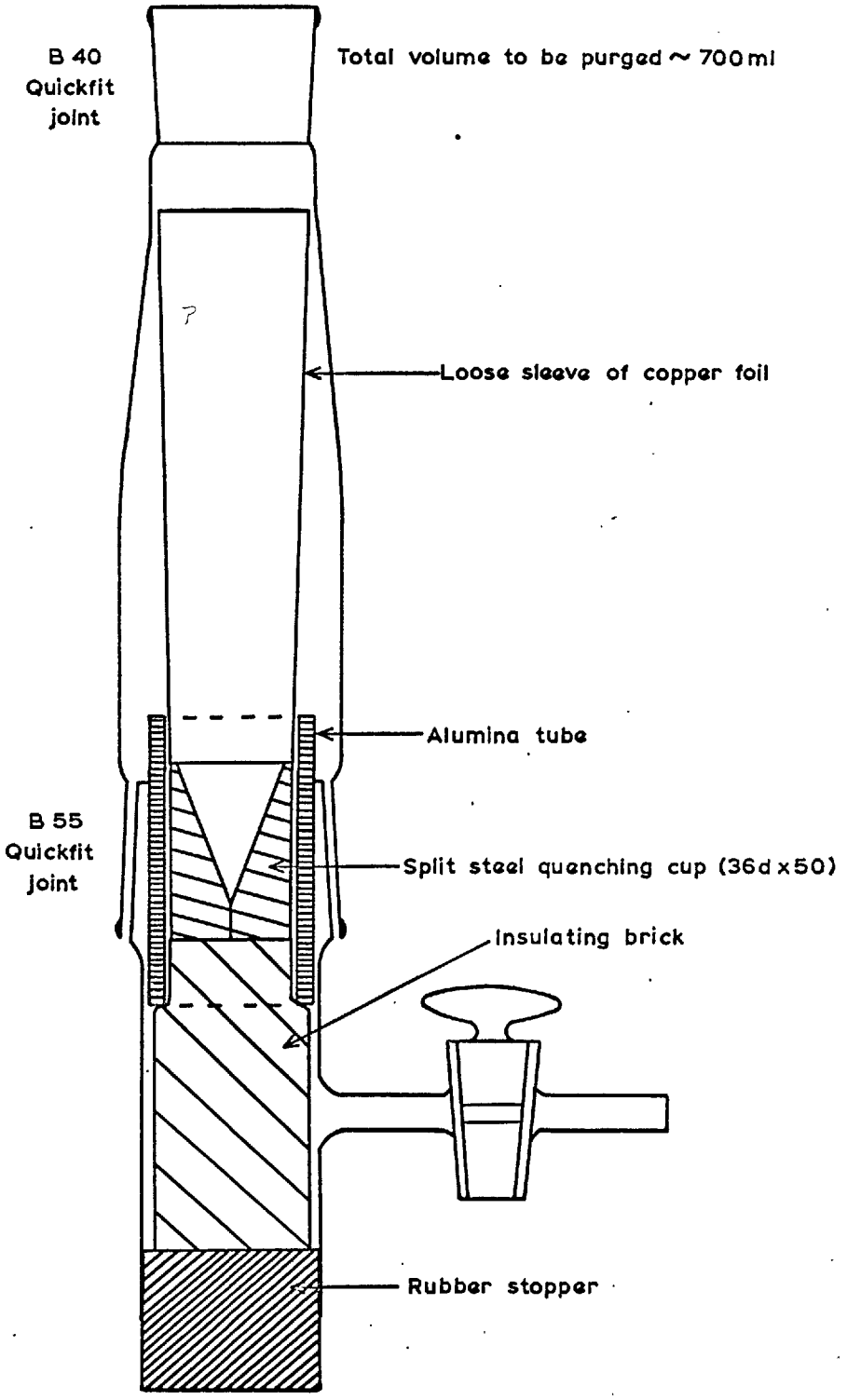

Fig.19. Details of Quenching Column used in decarburization experiments.
Scale: Half size.

Table 12: Oxidation of Nickel-Carbon alloy drops by flowing Oxygen-Helium mixture. (See also page 70b)

Note: All times are given in seconds. "Time of Boil" was measured on temperature record. e End of reaction (sample cast) Ev'd = evolved. (i.e. oxyger evolved in the form of CO from solidifying sample)
Brackets indicate approximate figures.

Series No.	I		II				
p_{O_2} atm.	0.02		0.06				
Gas flow litr/min	2		2				
Initial %C	2.38*		2.38*				
	Time total	%C	Time Total	Boil	%C	% O Ev'd	% O Total
	10	2.29	IIa				
	13	2.30	20	-	1.82	-	-
	20	2.22	40	-	1.29	-	-
	30	2.15	60	-	0.55	-	-
	60	1.83	70	-	0.41	-	-
	120	1.41	75	-	0.24	-	-
	150	1.08	85	(80)	0.02	-	-
	180	0.77	IIb				
	240	0.29	30	-	-	<.003	0.010
	300	0.03	45	-	0.94	0.004	-
			69½	-	-	0.016	0.026
			74½	-	0.29	-	-
			77	-	-	0.012	0.037
			79½	-	0.27	0.007	-
			80	76½/79	-	0.003	0.13
			83	-	-	0.007	0.017
			84	80/83	-	0.020	0.12
			85½	79/82½	-	0.00	0.19
			86	-	-	0.00	0.02
			86	78½/82	-	<.003	0.28
			88	81/84	-	0.032	0.27
			92	81/86	-	0.023	0.31
			97	84/88	-	0.032	0.40
			100	79½/82½	-	0.016	0.69
			109	75/79	-	0.00	1.00

* Average of 4 analyses: 2.34, 2.39, 2.41, 2.39

Average times of 'CO Boil': I: none observed II: 79½-82¾ sec.
III: 35½ - 37¼ sec. IV: 16-17½ sec. V: 9-10¼ sec.

Table 12 contd:

Series no.	III					IV					V				
p_{O_2} atm.	0.12					0.25					0.25				
Gas flow: litr/min	2					2					4				
Initial %C	2.08 ‡					2.08 ‡					2.08 ‡				
	Time Total	Boil	%C	%O Ev'd	Total	Time Total	Boil	%C	%O Ev'd	Total	Time Total	Boil	%C	%O Ev'd	Total
	11½	-	1.53	0.002	-	7½	-	1.22	0.007	-	4	-	1.27	-	-
	19¼	-	-	0.007	0.023	11	-	-	0.00	0.021	5	-	-	0.00	0.002
	20	-	1.08	0.006	-	11¾	-	0.75	0.00	-	6¼	-	0.91	-	-
	20	-	-	0.011	0.028	13¾	-	-	0.00	0.022	7	-	-	0.00	0.026
	29½	-	-	0.005	0.017	14	-	0.50	0.00	-	7¾	-	0.41	0.00	-
	30	-	0.5+	0.007	-	16¼	-	-	0.006	0.027	8	-	-	0.00	0.025
	35	-	0.-	0.003	0.022	17¾	15½/17	0.06	-	-	9	-	-	0.005	0.032
	35	-	0.16	0.010	-	18¼	16¾/17¾	-	0.00	0.27	9¾	9/e	0.18	-	-
	36¾	35¼/36¼	-	0.023	0.22	19½	16½/18¼	0.01	0.016	-	10¼	8¾/e	-	0.00	0.09
	38	37/e	-	0.016	0.037	20	16¼/17½	-	0.002	0.76	10½	9¾/e	0.043	-	-
	39	33/36½	0.02	0.009	-	24	15¾/17¼	-	0.002	2.06	11	10/e	0.008	-	-
	40	35/38	-	0.002	0.32	26	15/17¼	-	0.012	2.56	11	9¼/10¾	-	0.008	0.33
	40½	35/37	0.004	0.007	-						11½	8¼/9¾	0.018	ND	-
	42	36/39½	0.002	0.003	-						12¼	8¾/10¼	0.008	-	-
	45-	39/(42)	-	0.00	0.56						13	9/10¼	-	0.002	1.31
	45+	36/(38)	-	0.007	0.80						15¼	8½/10¼	0.002	-	-
	50½	36/(39)	-	0.00	1.22										
	50½	33¾/36½	-	0.012	1.49										
	54½	-	-	-	1.62										

‡ Average of 6 analyses 1.99, 2.03, 2.10, 2.17, 2.08, 2.08

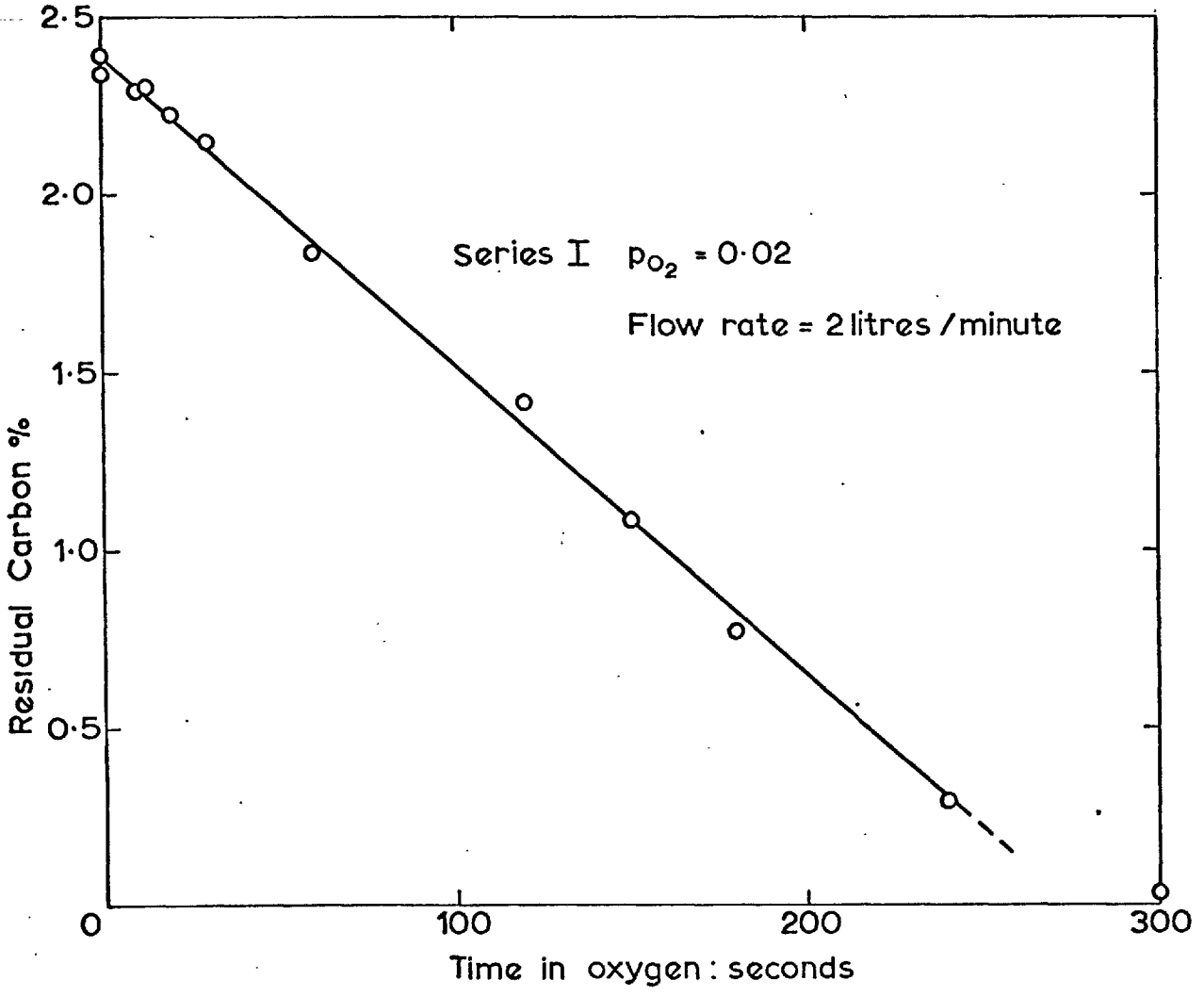

Fig. 20a. Oxidation of Nickel-Carbon alloy drops in flowing Helium - Oxygen mixtures.

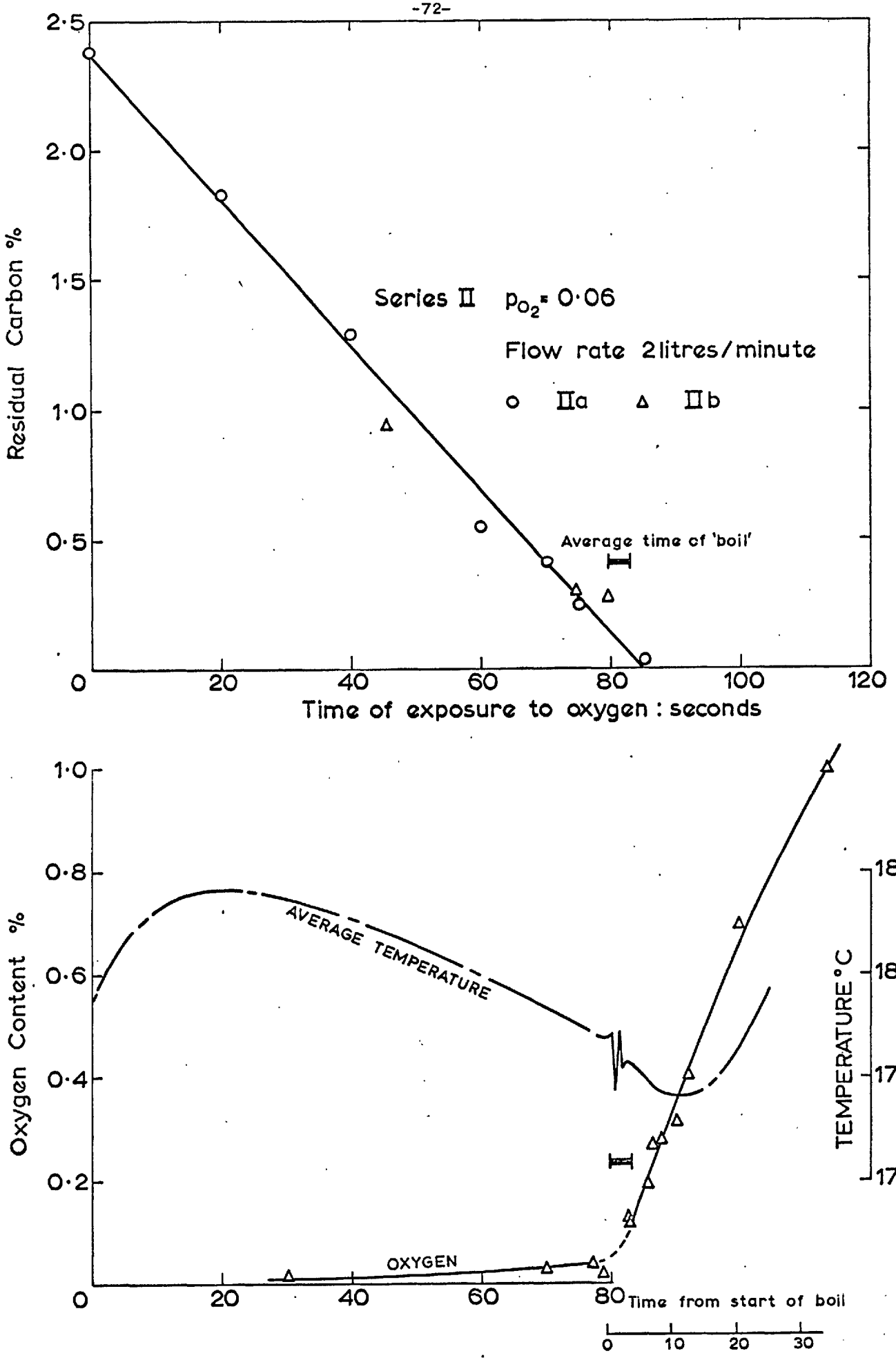

Fig. 20b. Oxidation of Nickel-Carbon alloy drops in flowing Oxygen-Helium mixtures.

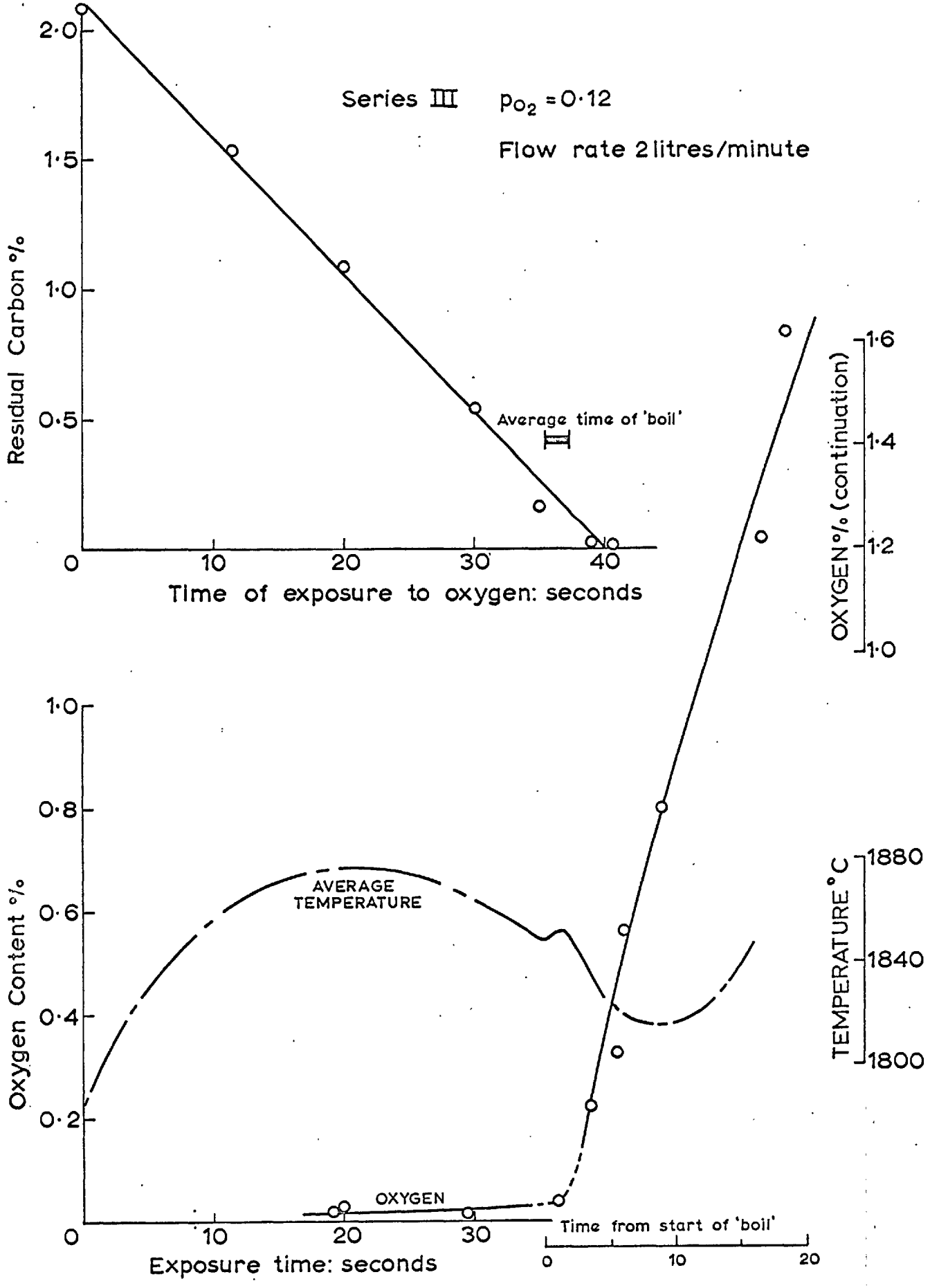

Fig. 20c. Oxidation of Nickel-Carbon alloy drops in flowing Oxygen-Helium mixtures.

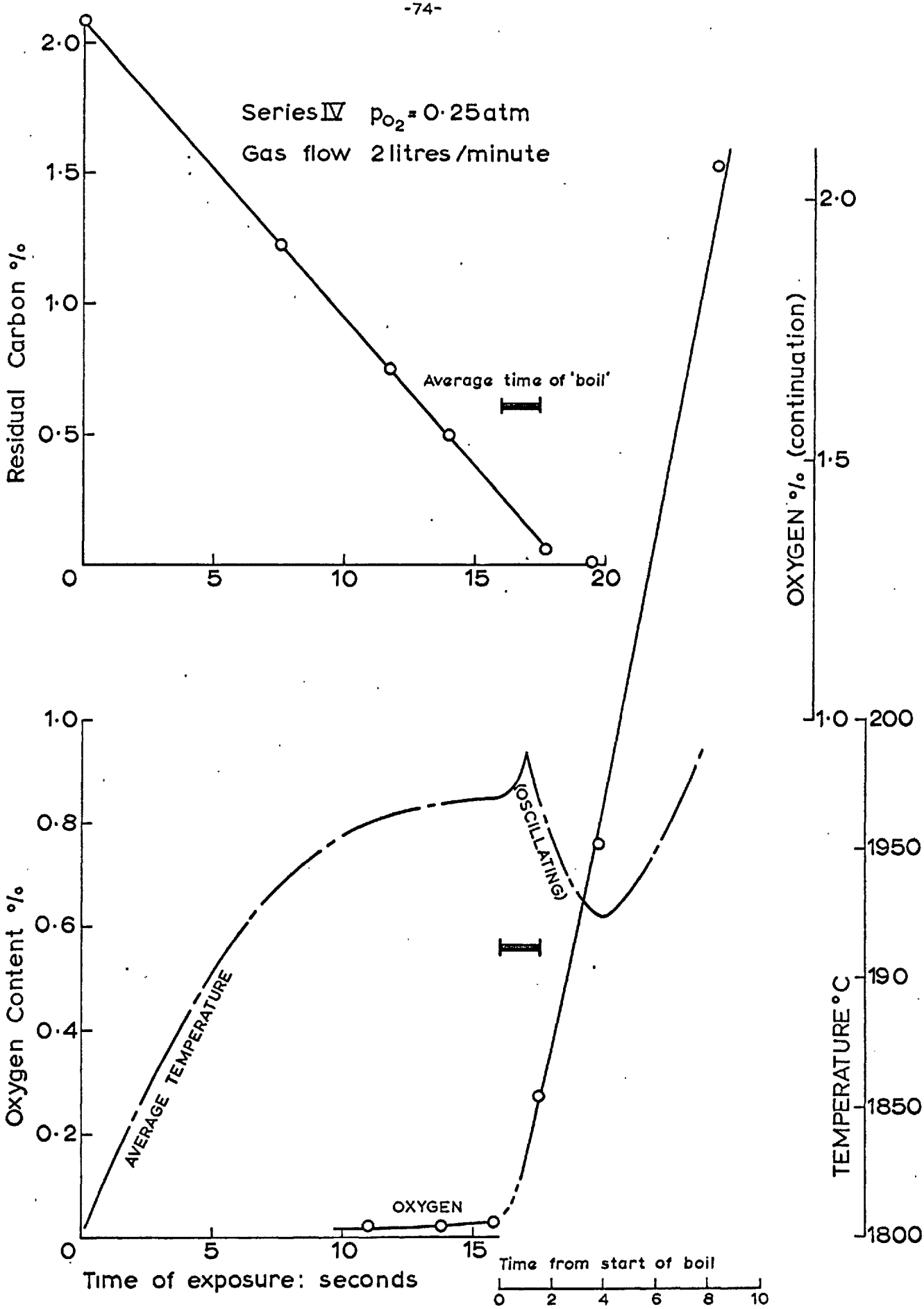

Fig. 20d. Oxidation of Nickel-Carbon alloy drops in a flowing Oxygen-Helium mixture.

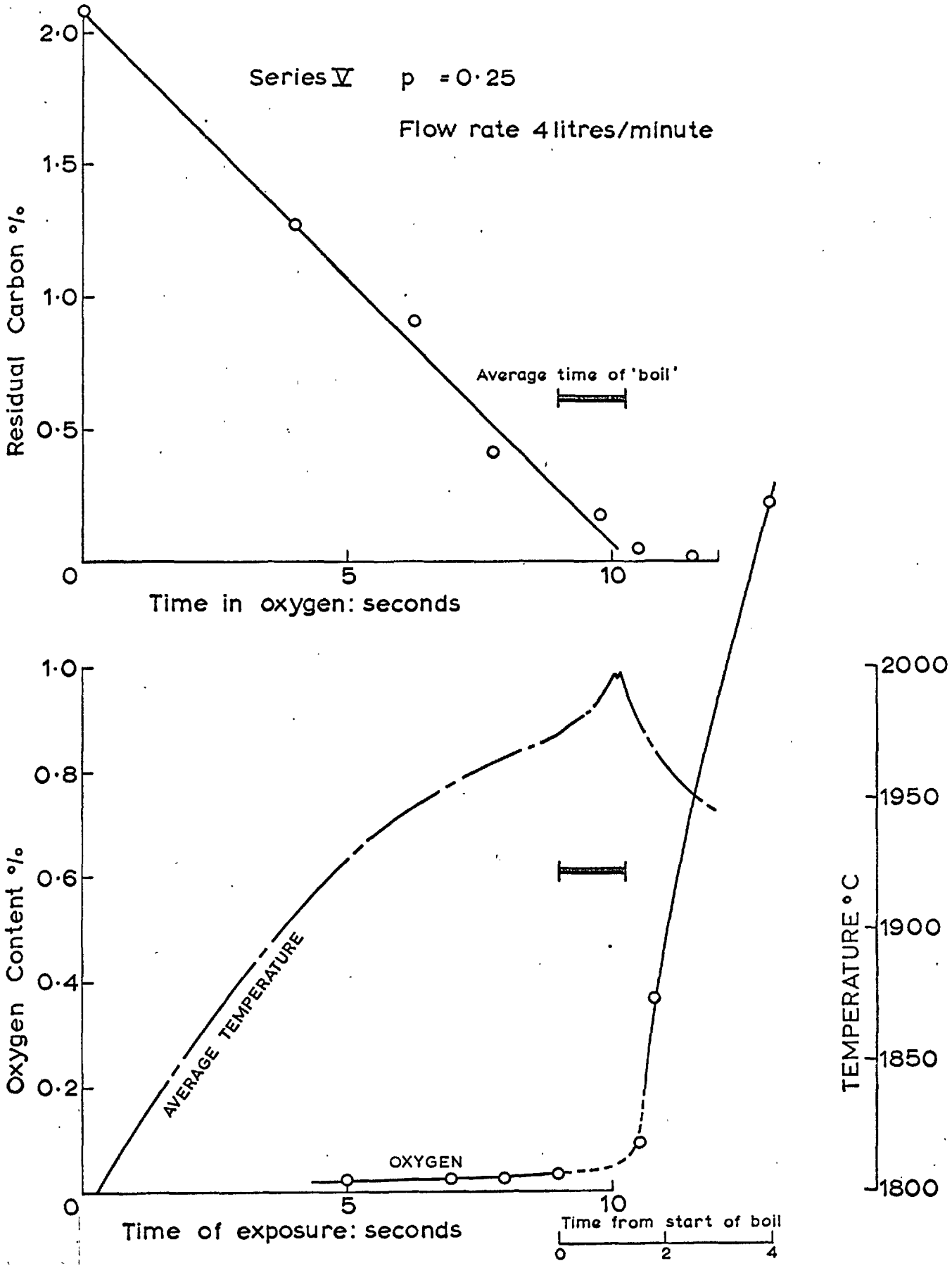

Fig. 20e. Oxidation of Nickel-Carbon alloy drops in flowing Oxygen-Helium mixtures.

The ends of the small black bar in each Figure show the arithmetic mean times of the start and end of the boil. The measured oxygen content just before the boil was in the range 0.03 - 0.04% in each series of experiments.

The temperature traces were transformed from a scale of millivolts to one of degrees and the average of the resulting curves is shown. The original curves were up to 20° above or below these averages but the pattern of steady temperature rise and the deviations during the boil were closely similar for all experiments in any one series. The deviations due to the boil have been plotted to coincide with the 'average time of boil' as marked, to show the typical pattern of changes.

Immediately after the peak of each boil reaction the drop began to oscillate in the coil and the temperature trace fell. After it had reached its minimum, the trace rose again fairly steeply as the oxygen content of the drop increased. The minimum apparent temperature occurred several seconds after the carbon had all been removed and the oxygen content had risen well above its former low level. No oxide coating was seen to form during any of these experiments, even when the average oxygen content of a drop was well above the 1% level.

(d) High-Speed Films: Cine films were taken of the boil reaction, with the 'Fastax' camera mounted close to the window normally used for pyrometric viewing. The radiation from the drops gave ample illumination and the lens was stopped down to f/22. The camera was switched on ½ to 1 second before the boil was due to begin.

Film No.	p_{O_2} (atm.)	Flow (l/min.)	Frames/sec.	ASA film speed
4	0.25	4	1000	64
5	0.25	4	4000	250
6	1.0	1.5	1000	64

During film No. 4, a temperature record was made with the pyrometer viewing the top of the drop (through the alternative gas jet: see Fig. 1). Events on the film could be related through the 0.01-second timing marks to the temperature trace. Taking the maximum activity as coinciding with the peak temperature, the comparison showed that the initial slight rise in the drop temperature occurred during the first gentle 'spitting' of the drop. The peak, 1-1½ seconds later, was the part of the action most easily seen by the naked eye. This explains why visualestimates of the time of 'boil' are usually a second or more larger than those made by measuring the temperature traces.

Less than 0.1sec. before the first spitting became visible, ripples could be seen on the profile of the drop. Measurements on a film analyser showed that these may have been moving at about 40 cm/sec. In addition to the spitting and increasingly violent ejection of droplets that Distin has described, the films all showed bright spots of light appearing as each bubble burst (Figures 22 & 23). These usually began as almost circular spots, and broke up giving patterns reminiscent of ripples spreading on water although they were more uneven and did not form full circles. On film taken at 4000 frames per second, markings from a single spot could be followed for as many as 16 frames from the first appearance of the spot, that is, for a time of 0.004 sec. At the peak of the action the drop was distended to about 1½ times its normal diameter. The reaction subsided fairly rapidly leaving the drop appearing as it was before the boil.

Detailed sequences of the events during each film are shown in diagrammatic form in Figure 21. The onset of fine "spitting" has been taken as a convenient zero mark for each sequence.

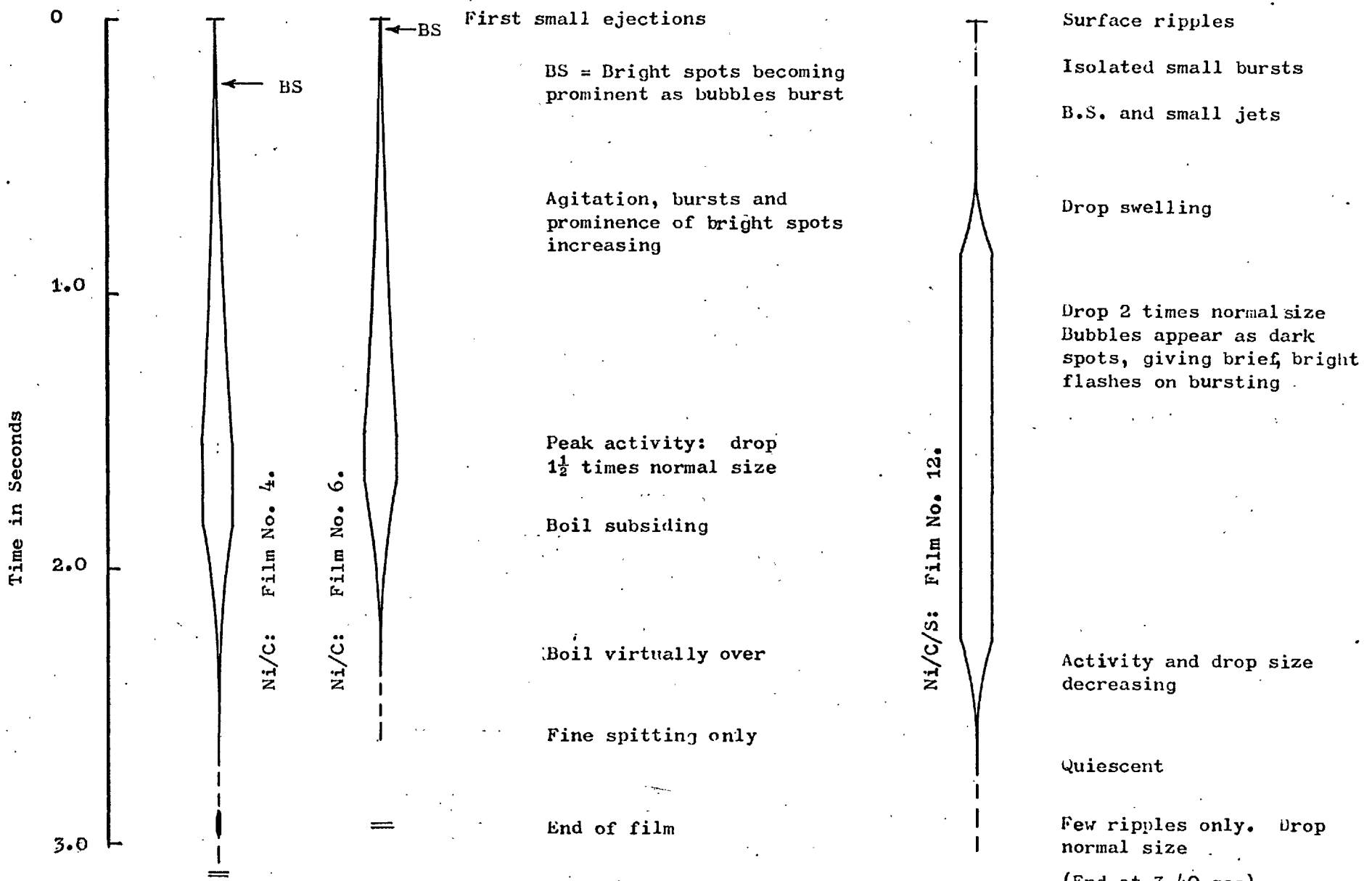

Figure 21: High-Speed Films: Details of Boil Reactions in Nickel Alloys

Figure 22

Stages of the CO boil in a Nickel-Carbon Alloy Drop exposed to O_2/He mixture flowing at 2 litres/minute.

p_{O_2} = 0.25 atm. (See also Figure 21)

a. Ripples on surface of drop (slightly irregular profile) a few milliseconds before the boil began)

b. Typical small ejection seen in the early stages of the boil.

c. About 0.75 sec. after 'b': 'bright spots' appearing together with small ejections.

d. About 1.2 sec. after 'b': peak activity of boil. Note increased diameter of drop, compared with 'c', and development and break-up of a 'bright spot'

e. About 1.35 sec. after 'b': boil subsiding. Note that ejection occurs at site of 'bright spot'.

Note that the "bright spots" are more brilliant in the original films than they appear to be here. Some contrast is unavoidably lost in photographic reproduction.

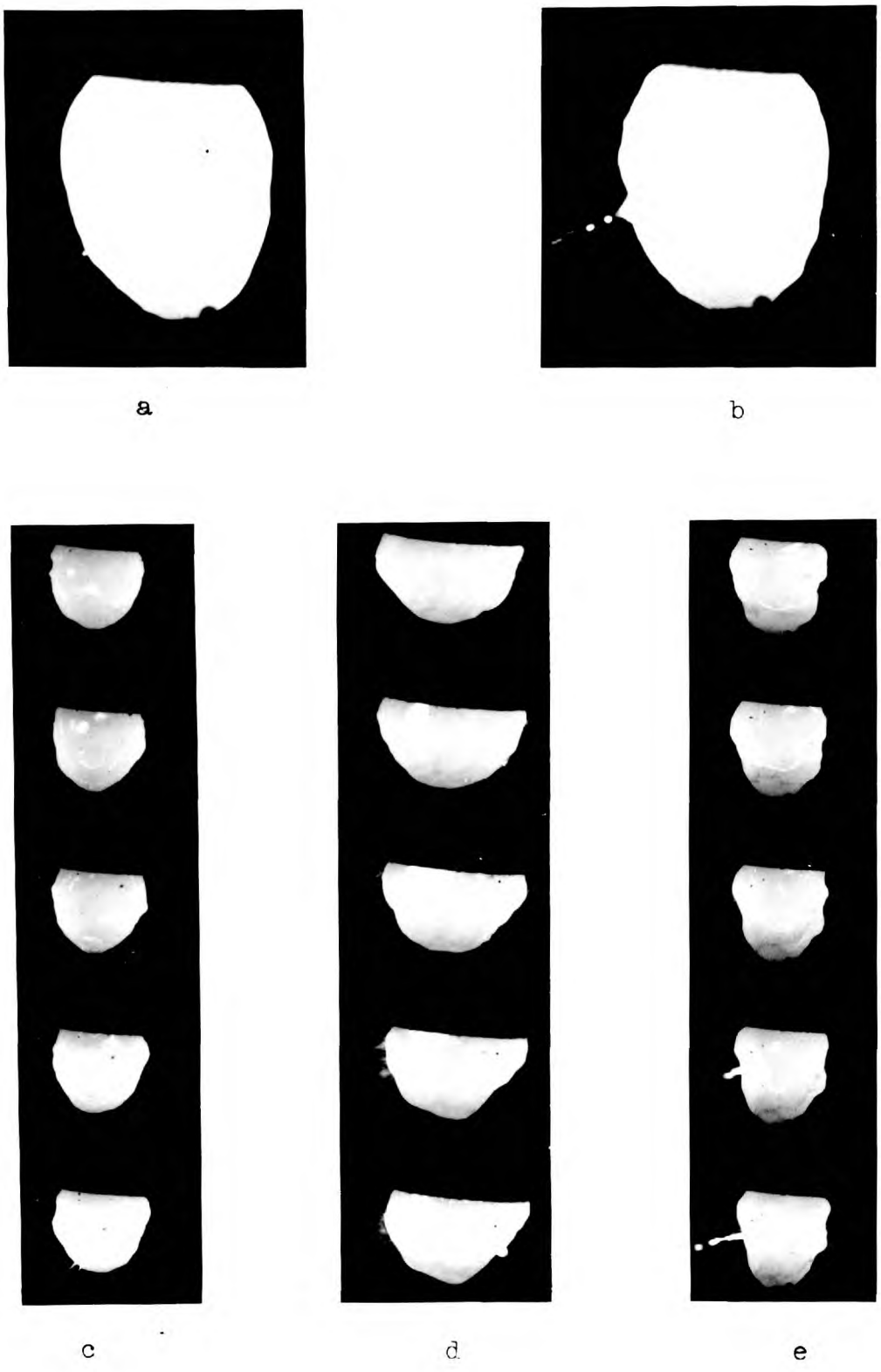

Figure 22: 'CO Boil' in Nickel-Carbon Alloy Drops

(Film No. 4; taken at 1000 frames/second)

Figure 23

$a_1 - a_2$: $p_{O_2} = 0.25$ atm
Gas flowing at 2 litres/min.
Sequence at peak of boil activity showing formation and dispersion of a 'bright spot'.

b: Pure oxygen flowing at 1½ litres/min. Showing agitation and 'bright spots' at peak of boil activity.

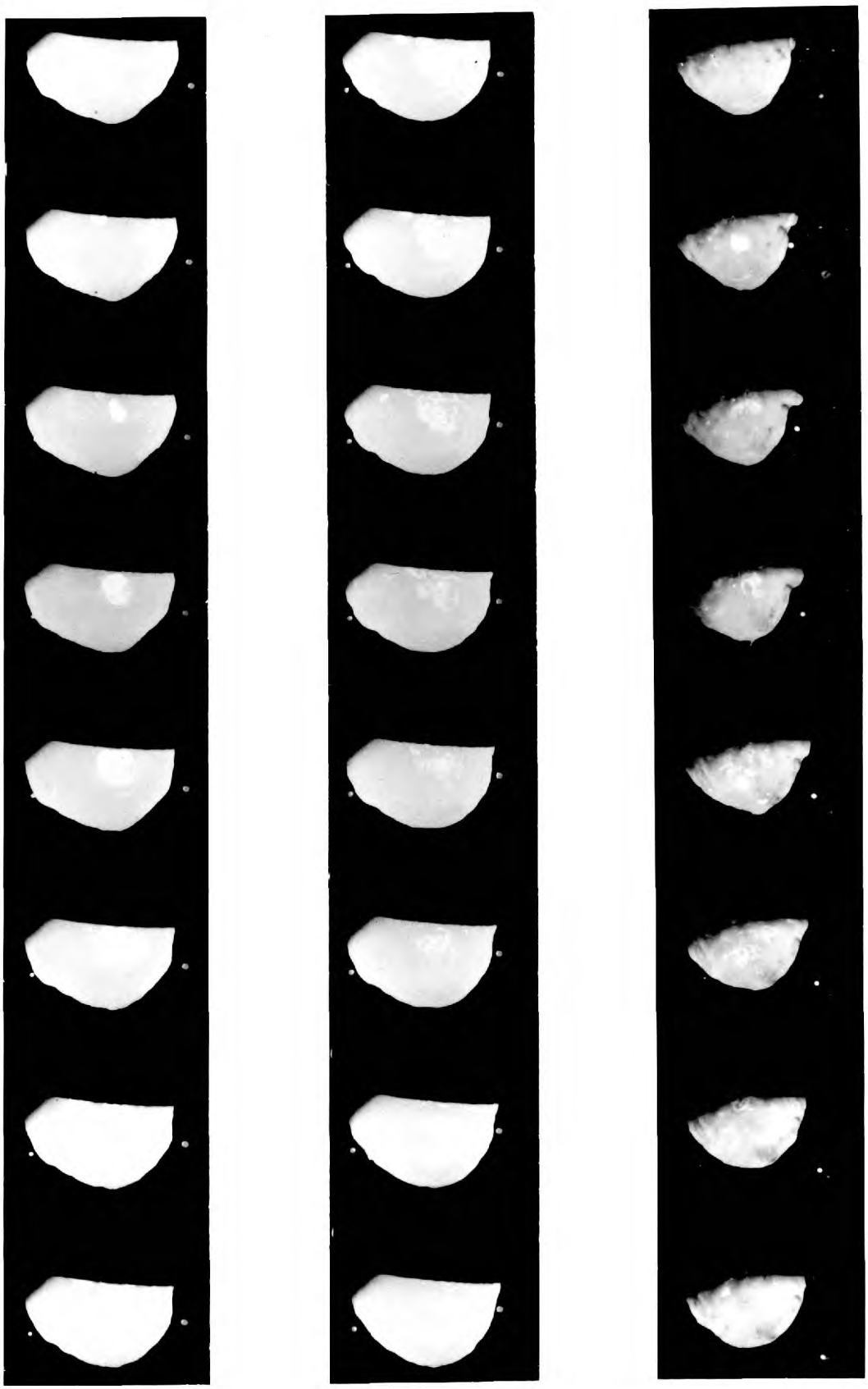

a_1 a_2 b

Figure 23: The 'CO Boil' in Nickel-Carbon Alloy Drops

a_1 - a_2: Film No. 5: 4000 frames/sec.

b Film No. 6: 1000 frames/sec.

7. Oxidation of Iron-Carbon Alloy Drops:

(a) General: The experiments were made for direct comparison with those on the nickel-carbon alloys and particularly to show when iron oxide began to form in relation to the time of the boil. Oxygen-helium mixtures were again used and the apparatus and experimental method were similar to those already described.

(b) Results: Table 13 and Figures 24 a-c present the numerical data. The ranges of the starting times of boils, measured on the temperature records, were:

I	$37\frac{1}{2}$ - 40,	average $39\frac{1}{4}$ seconds.
II	16 - $18\frac{3}{4}$,	average $17\frac{1}{2}$ seconds.
III	$10\frac{1}{4}$ - $12\frac{1}{4}$,	average 11 seconds.

Here again the average time of the start of the boil has been used to establish a time base for oxygen contents and temperatures after that event.

The boil occurred as two or three rapid agitations of the drop in succession, instead of the more uniform increase and decrease that was observed for the nickel-carbon drops. The end of the boil was difficult to identify on the temperature records. In Series I many samples gave the rising curve consistent with increasing oxygen content, with no clear break. In Series II and III the trace oscillated strongly when the boil was over and passed through a minimum before rising again. The brighter oxide phase appeared on drops that were held beyond the time of the boil but was not seen before or at the start of that event. The average oxygen content just before the boil began was 0.05-0.06% in each Series.

(c) High-Speed Films: Four films were taken of boil reactions:

No.	p_{O_2}	l/min.	Frames/sec	ASA film speed
8 & 9	0,25	2	1000	64
10	"	4	"	"
11	"	"	4000	250

Diaphragm setting = f/22.

Diagrams showing the detailed sequences of events are presented in Fig. 25. Frames from the films are reproduced in Figs. 26 and 27.

About 0.05 - 0.10 sec. before the first "spitting" of a drop occurred, there was a small but noticeable increase in the amount of fume being produced and small ripples appeared on the profile of the drop. The boil usually began with a very strong ripple which distorted the drop and led to the ejection of fairly large droplets. The bubble bursts, ripples and ejections continued for a short period and subsided very quickly. This sequence was repeated with almost equal vigour three or four times, with intervening periods of almost complete inactivity.

In films No. 8 and 9, with the lower rates of gas flow, iron oxide did not begin to appear until at least half a second after the last boil activity. A small bright cap appeared at the top of the drop and extended "streamers" of oxide down the sides which broke up and redissolved nearer to the base. In films No. 10 and11, some bubble bursts continued as the oxide began to appear. The bursts occurred at random in both the clear and the oxide-covered parts of the surface and there were no obvious signs that the surface was providing nuclei for the bursts.

In general the oxide patches had sharply defined edges but the bright spots and ripples associated with bubble bursts had less well defined and slightly rougher edges,although

Table 13: Oxidation of Iron-Carbon Alloy Drops by flowing Oxygen-Helium mixtures

ND: Not determined

e: end of reaction (when sample was cast)

Ev'd: Oxygen evolved as CO from solidfying sample

Brackets indicate approximate or uncertain figures.

Average time of 'CO boil': I: $39\frac{1}{4}$ - ? (End uncertain)

II: $17\frac{1}{4}$ - 20

III: 11 - ($12\frac{3}{4}$) (End uncertain)

Series No.	I				II				III			
p_{O_2} atm.	0.12				0.25				0.25			
Gas flow: litres/min	2				2				4			
Weight g.	1.56 ± 0.02				1.59 ± 0.02				1.59 ± 0.02			
Initial % C.	2.42, 2.44				2.39, 2.44				2.39, 2.44			
Time			%C	%O	Time		%C	%O	Time		%C	%O
Total	Boil			Ev'd	Total	Boil			Ev'd	Total	Boil			Ev'd	Total
$14\frac{1}{2}$	-		1.56	0.007	-	$5\frac{3}{4}$	-	1.72	0.007	-	5	-	1.52	0.00	-
$24\frac{1}{2}$	-		0.99	0.002	-	10	-	-	0.00	0.031	$6\frac{1}{4}$	-	1.28	ND	-
30	-		-	0.002	0.041	12	-	1.04	0.027	-	$7\frac{1}{4}$	-	-	0.004	0.037
$35\frac{1}{2}$	-		0.35	0.00	-	$13\frac{3}{4}$	-	0.76	0.007	-	8	-	0.88	0.18	-
36	-		-	0.008	0.047	14	-	-	0.004	0.031	$9\frac{1}{2}$	-	-	0.00	0.037
40	-		0.17	0.007	-	16	-	0.54	0.002	-	10	-	0.49	0.014	-
40	(38/e)		-	0.024	0.088	$16\frac{3}{4}$	-	-	0.006	0.051	$10\frac{1}{2}$	$10\frac{1}{4}$/e	-	0.014	0.048
$41\frac{1}{2}$	(39/e)		-	0.029	0.20	$17\frac{1}{4}$	-	-	0.006	0.065	$11\frac{1}{4}$	$10\frac{3}{4}$/e	-	0.019	0.062
44	(40/e)		-	0.005	0.41	$18\frac{1}{2}$	$17\frac{1}{4}$/e	0.27	0.016	-	$11\frac{1}{4}$	$10\frac{1}{2}$/e	0.33	0.012	-
45	(39/e)		0.01	0.006	-	$18\frac{1}{2}$	16/e	-	0.021	0.091	12	11/e	0.10	0.009	-
45	39/43		-	0.006	0.41	$19\frac{1}{2}$	$16\frac{1}{2}$/$19\frac{1}{4}$	-	0.016	0.115	$12\frac{1}{2}$	$11\frac{1}{4}$/e	-	0,00	0.28
$46\frac{1}{2}$	$37\frac{1}{2}$/43		-	0.011	0.62	$19\frac{3}{4}$	$17\frac{1}{4}$/$19\frac{1}{2}$	0.04	0.037	-	$13\frac{1}{4}$	$10\frac{3}{4}$/$12\frac{1}{2}$	0.075	0.019	-
$47\frac{1}{4}$	40/(43)		0.01	0.011	-	$20\frac{1}{2}$	17/20	-	0.037	0.13	$13\frac{1}{2}$	$10\frac{1}{4}$/(12)	-	0.011	0.41
$47\frac{3}{4}$	(39)/$44\frac{1}{2}$		-	0.005	0.73	21	$17\frac{1}{2}$/$20\frac{1}{2}$	0.03	0.017	-	$14\frac{3}{4}$	$12\frac{1}{4}$/$13\frac{3}{4}$	-	ND	0.71
50	38/(41)		-	0.008	1.01	22	$18\frac{3}{4}$/$20\frac{1}{2}$	-	0.005	0.38	16	$11\frac{1}{4}$/$12\frac{3}{4}$	-	0.004	1.18
						26	$17\frac{1}{2}$/$19\frac{1}{2}$	0.00	ND	-					

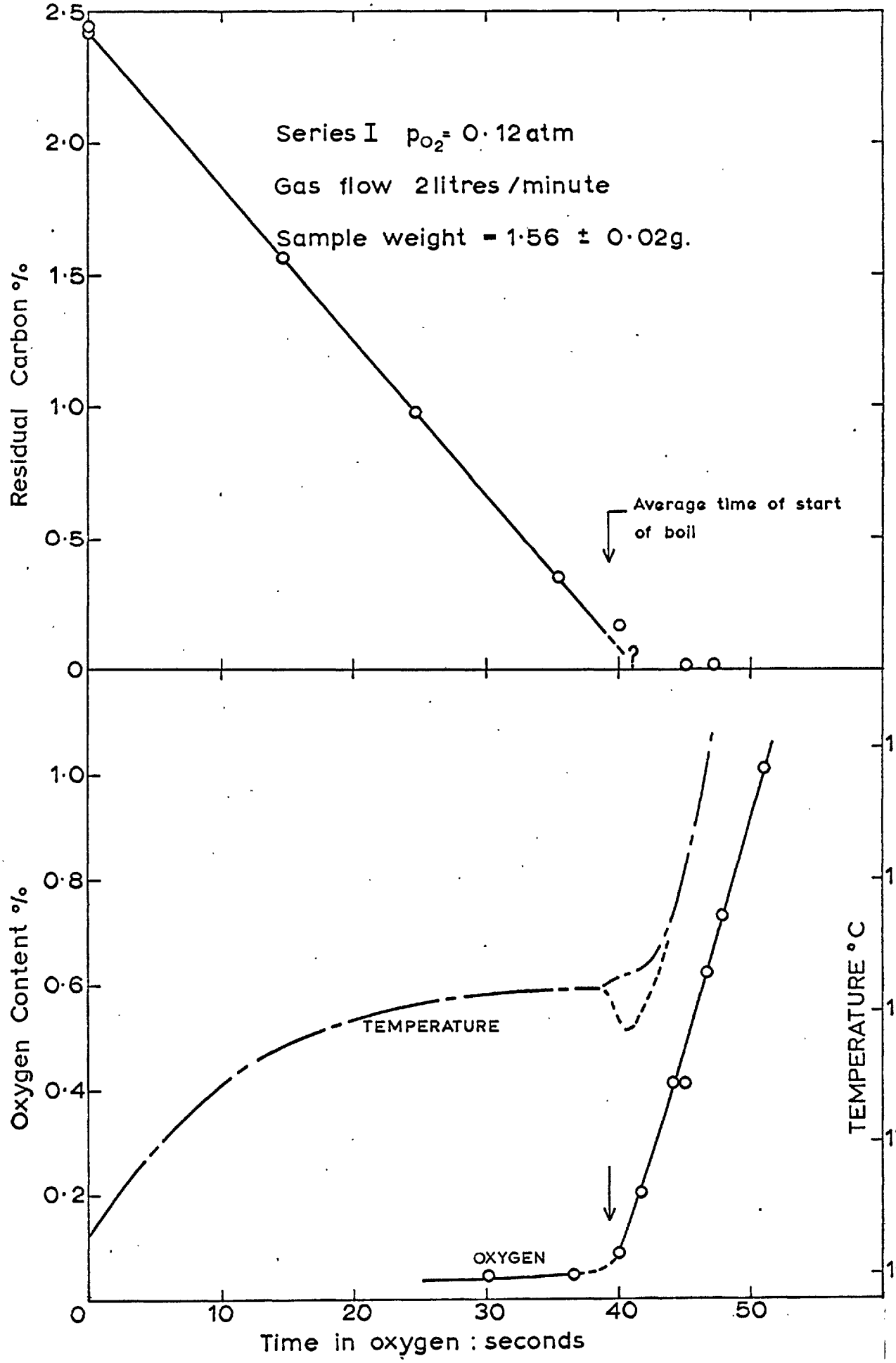

Fig. 24a. Oxidation of Iron-Carbon alloy drops by a flowing Oxygen - Helium mixture.

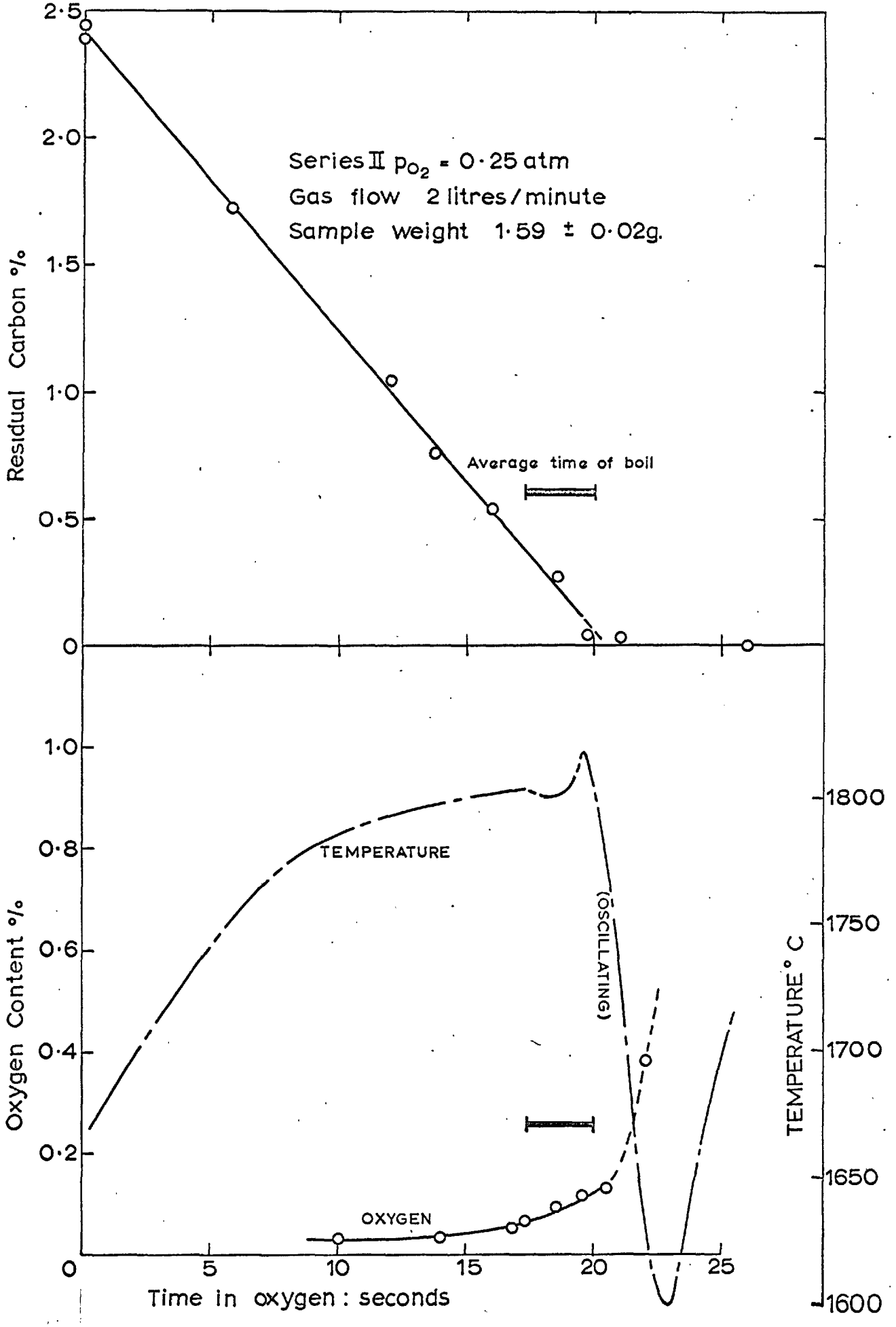

Fig.24b. Oxidation of Iron-Carbon alloy drops in a flowing Oxygen-Helium mixture.

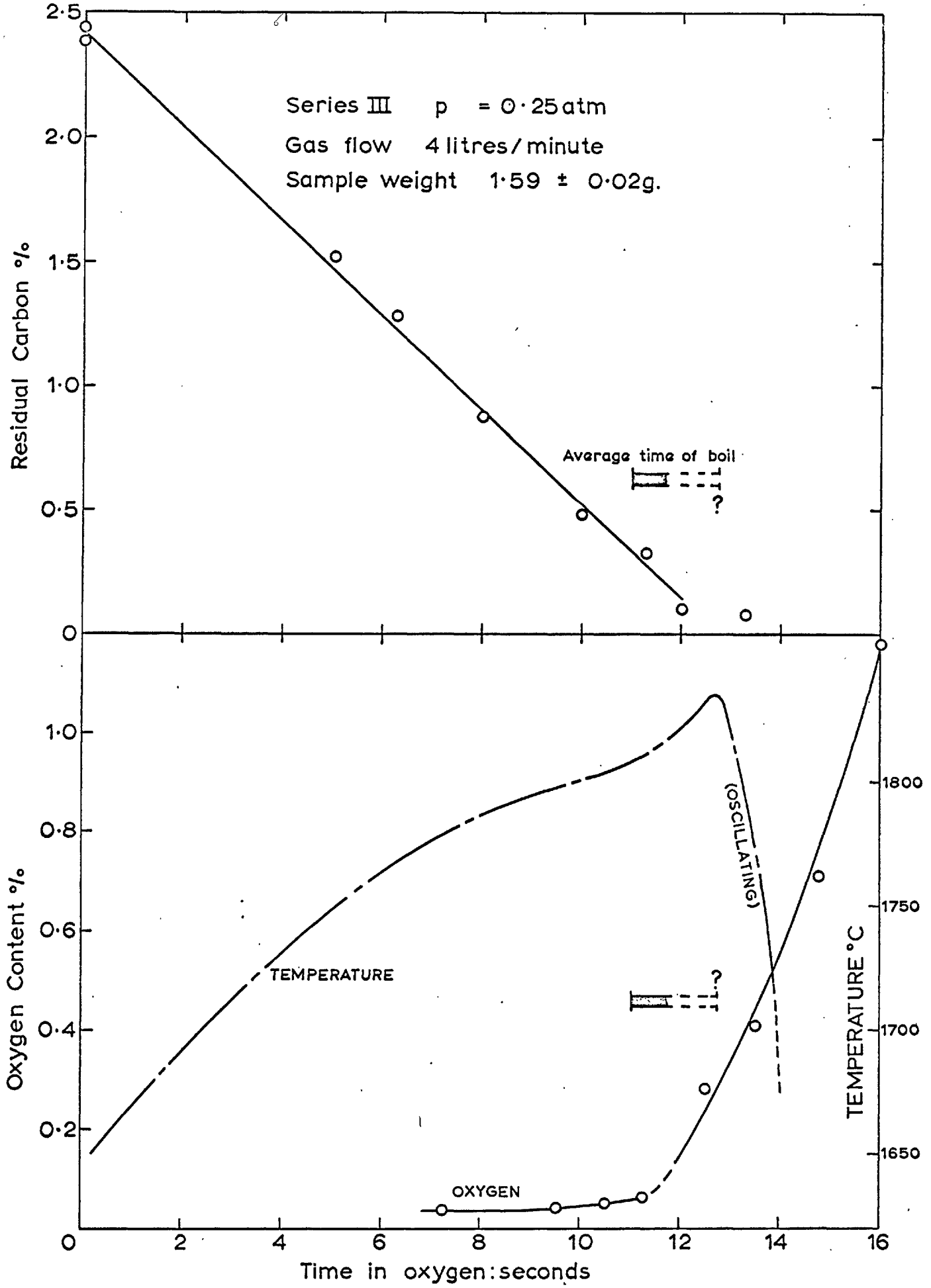

Fig. 24c. Oxidation of Iron-Carbon alloy drops in a flowing Oxygen-Helium mixture.

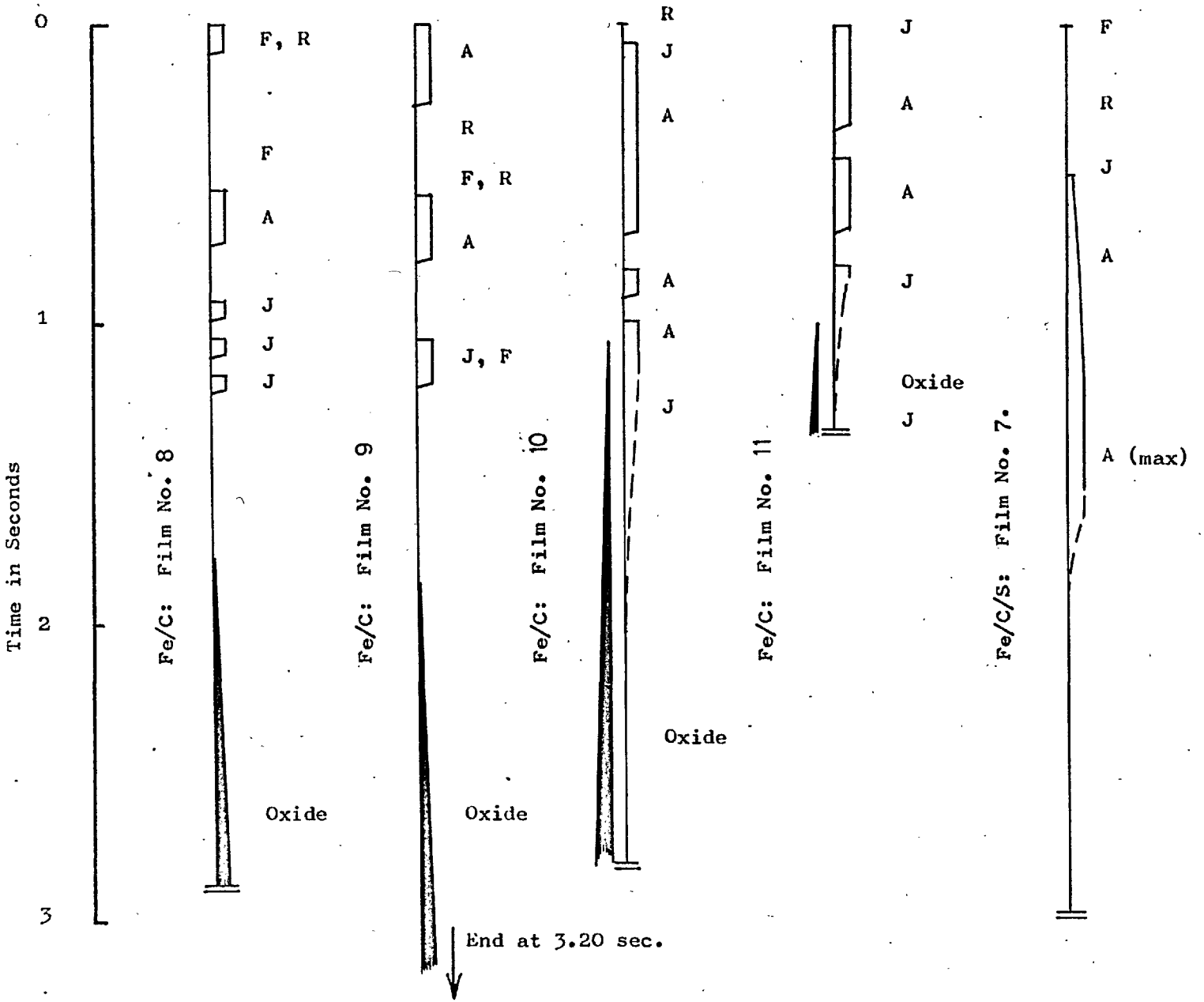

Fig. 25: High-Speed Films: Details of Boil Reactions in Iron Alloys

Figure 26

Stages of the CO boil in an Iron-Carbon Alloy Drop exposed to O_2/He mixture flowing at 2 litres/min. p_{O_2} = 0.25 atm. (See also Figure 25).

---

a. Ripples on drop surface (note rough profile on left) a few milliseconds before the boil began.

b_{1-3} Sequence during first period of agitation, showing development of a 'bright spot' followed by agitation nearly dividing drop into two,

c. Large 'bright spot' following shortly after sequence b.

d. About 1.2 sec. from start of boil; activity subsiding, but one large jet forms.

e. Early stage of iron oxide formation, about 2.2 sec. from start of boil. Note that more fume appears to be produced where oxide is present.

f. Later stage of formation of oxide coating, about 3.1 sec. from start of boil.

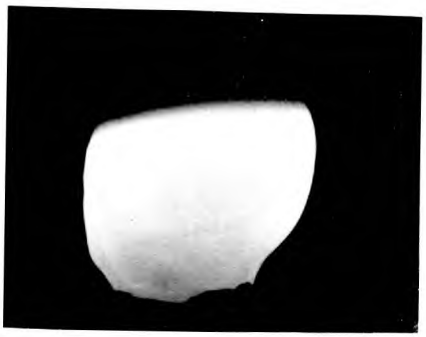

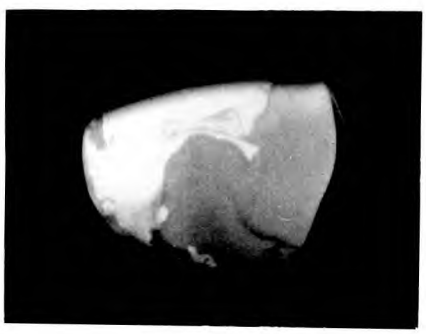

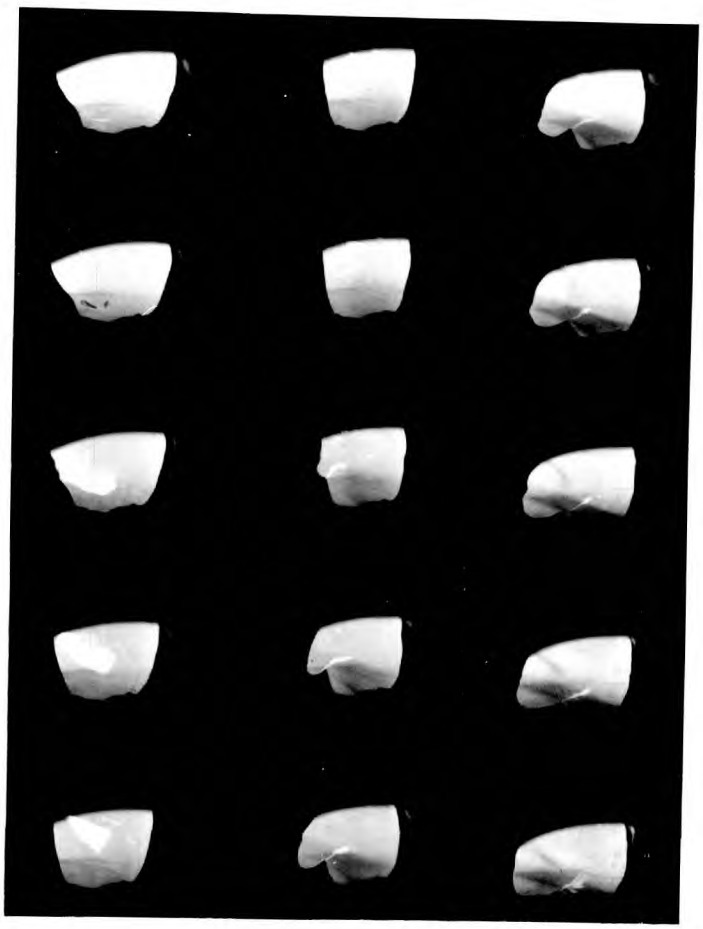

a b 1 - 3

e

f c d

Figure 26: The 'CO Boil' in an Iron-Carbon Alloy Drop.
(Film No.8 taken at 1000 frames/second)

Figure 27

a. Iron-Carbon Alloy Drop in O_2/He flowing at 4 litres/min: p_{O_2} = 0.25 atm. (1000 frames/sec). About 0.4 sec. from start of boil = 'bright spot' leading to jet of droplets.

b. Same film: about 1.65 sec. from start of boil. Oxide network on upper part of image (partly cut off by viewing port). 'Bright spot' also appears, apparently unconnected with oxide, and leads to formation of a jet.

c_1-c_3 Conditions as in a & b but filmed at 4000 frames/sec. Sequence showing formation and dispersion of a 'bright spot' at peak of boil activity (about 0.95 sec. from start of boil).

a

b

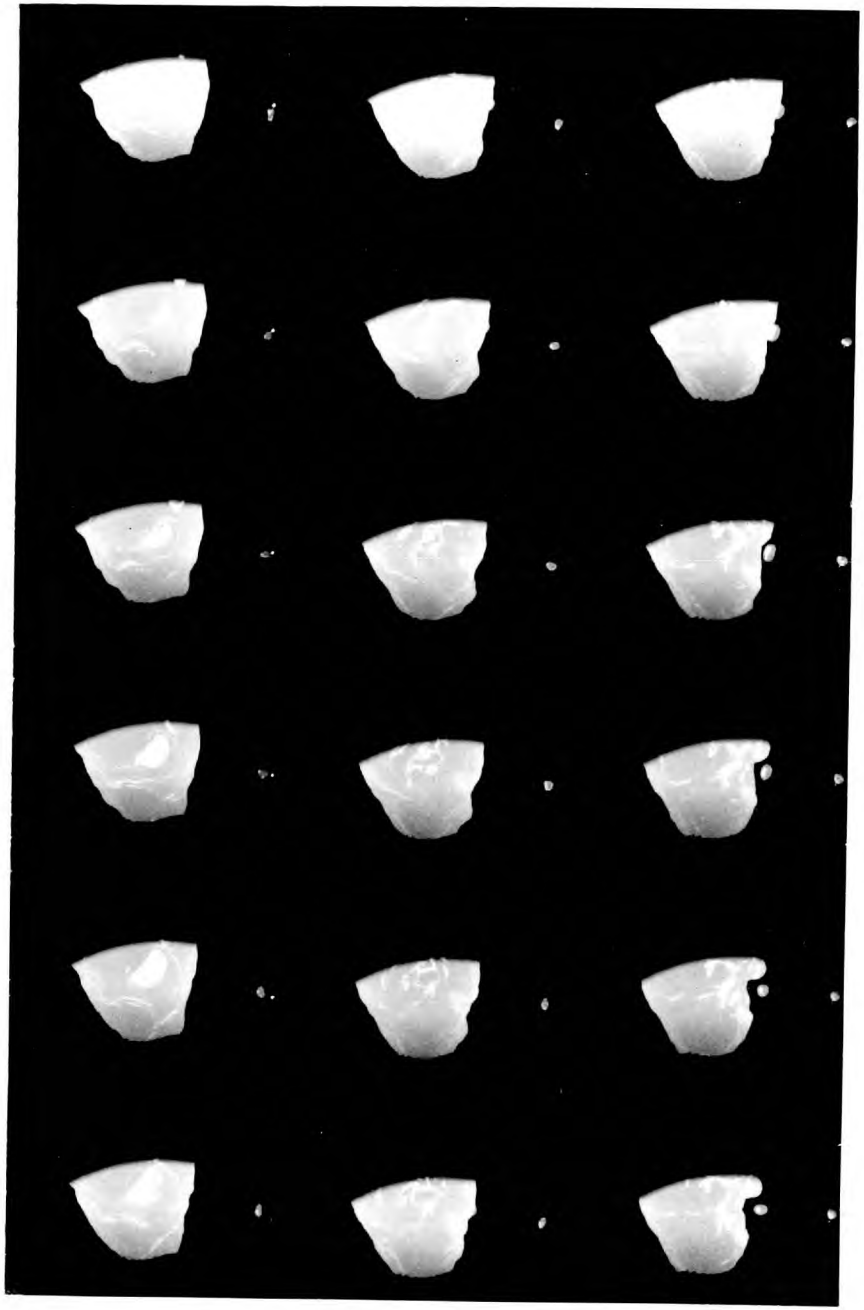

Figure 27: 'CO Boil' in Iron-Carbon Alloy Drops
a & b = Film No. 10.
c = Film No. 11.

$c_1 - c_3$

the luminosity of both phenomena was roughly the same.

8. Oxidation of Alloys containing Carbon and Sulphur

(a) General: Sulphur was added to show whether any of the behaviour of the nickel-sulphur alloys would be repeated and particularly whether the oxygen content would show an early increase. It was also possible that the decarburisation rate might be changed.

Samples were made up as before but 0.7-0.75% S was added in the form of crushed crystals. The oxidising gas in all experiments was an oxygen-helium mixture with p_{O_2} = 0.25 atm., flowing at 2 l/minute.

(b) Nickel alloys: The 26 experiments of Series A were made for carbon and sulphur analyses only and were cast into the copper cup. Later the seven experiments of Series B were made with samples from the same powder mixture; the four of these intended for oxygen analysis were cast into the argon-filled column. Experiments of Series C were made to provide additional data on oxygen contents just before the boil. Results are shown in Table 14 and Figure 28.

Lines representing carbon depletion in nickel-carbon and iron-carbon drops under similar conditions have been entered in Fig. 28 for comparison. It appears that carbon depletion was a little slower when sulphur was present and that there was a slight change of rate after about 6 seconds. Although a horizontal straight line should perhaps be drawn through the sulphur data up to the 20-second mark, the trends are consistent enough to indicate a slight minimum in the curve at about 6-8 seconds. The slow increase in the sulphur content, after that moment can be explained as a 'concentrating' effect due to the loss of carbon and metal

vapour. The weights of the cast samples when multiplied by their sulphur contents give a reasonably constant figure.

Temperatures and the later oxygen analyses have been plotted as described in Section IV: 6 & 7.

The boil differed strikingly in its appearance from that of the nickel-carbon boils. The drop became distended to a seemingly smooth sphere considerably larger than the original diameter and remained this way for a second or longer. There was a spray of very fine droplets during this time but none of the strong agitation or ejection of large droplets observed before in nickel-carbon or iron-carbon boils.

In a high-speed film taken of the boil reaction at 1000 frames/sec (**Fig.29**) a 'froth' of bubbles appeared as the drop began to swell. These bubbles were less bright than the rest of the metal and held their form for several frames before bursting. At the moment a bubble burst a bright flash of light was seen similar to those reported for Ni/C and Fe/C alloys but lasting for only one frame (0.001 seconds). As the action progressed, the bubbles merged and became larger. The convex profiles of the bubbles could be seen at the edges of the drop image. At the peak of the boil activity, the diameter of the drop was almost twice its original size. The general appearance was reminiscent of frothing in a rather viscous fluid but there is nothing in the composition of the raw materials to indicate that a slag could form. When the boil subsided, the appearance of the drop was again that of a smooth and clean metal surface. The diagram representing the sequence is included in Figure 21.

(c) Iron Alloys: Samples of both Fe/C/S and Fe/C alloys were decarburised in random order during the same series of

Table 14: Oxidation of Nickel-Carbon-Sulphur alloy drops in a flowing Oxygen-Helium mixture

p_{O_2} = 0.25 atm.,
Gas flow = 2 litres/minute
Sample wt.= 1.60 ± 0.02g.

S E R I E S 'A'

Time: seconds Total exposure	%C	%S	Time:seconds Total exposure	Start of boil	%C	%S
0	2.45	-	$10\frac{1}{2}$	-	-	0.479
0	2.47	-	$12\frac{3}{4}$	-	1.26	-
0	-	0.459	$13\frac{1}{4}$	-	-	0.478
0	-	0.502	$16\frac{1}{2}$	-	0.99	-
0	-	0.472	17	-	-	0.494
$1\frac{3}{4}$	-	0.484	$19\frac{1}{2}$	-	0.61	-
$1\frac{3}{4}$	2.30	-	$20\frac{1}{4}$	20	-	0.500
$3\frac{1}{4}$	2.16	-	$20\frac{1}{2}$	-	0.50	-
$5\frac{3}{4}$	-	0.470	22	$21\frac{1}{4}$	0.36	-
$5\frac{3}{4}$	1.96	-	$22\frac{1}{4}$	$(20\frac{3}{4})$	-	0.337
$7\frac{3}{4}$	1.77	-	$22\frac{1}{2}$	(18)	-	0.420
8	-	0.472	24	$21\frac{1}{2}$	0.15	-
10	1.50	-	-	-	-	-

S E R I E S 'B'

Time:sec. Total exposure	Start of Boil	%S	% Oxygen Evolved	Total
$7\frac{1}{4}$	-	-	0.011	0.036
11	-	-	0.005	0.037
13	-	-	0.011	0.08
14	-	-	0.000	0.030
16	-	-	0.000	0.023
$16\frac{1}{2}$	-	-	0.002	0.043
$17\frac{3}{4}$	-	-	0.005	0.022
20	18	-	0.002	0.28
$21\frac{3}{4}$	18	-	0.016	0.47
$22\frac{3}{4}$	$18\frac{1}{2}$	-	0.016	0.68
$23\frac{1}{2}$	$18\frac{1}{2}$	-	0.000	1.00
$23\frac{1}{2}$	$18\frac{1}{4}$	0.400	-	-
24	19	-	0.006	0.74
27	19	0.257	-	-
$30\frac{1}{4}$	$17\frac{1}{4}$	0.093	-	-

Average time of start of boil: Series A $20\frac{1}{2}$ seconds. Series B $18\frac{1}{4}$ second..

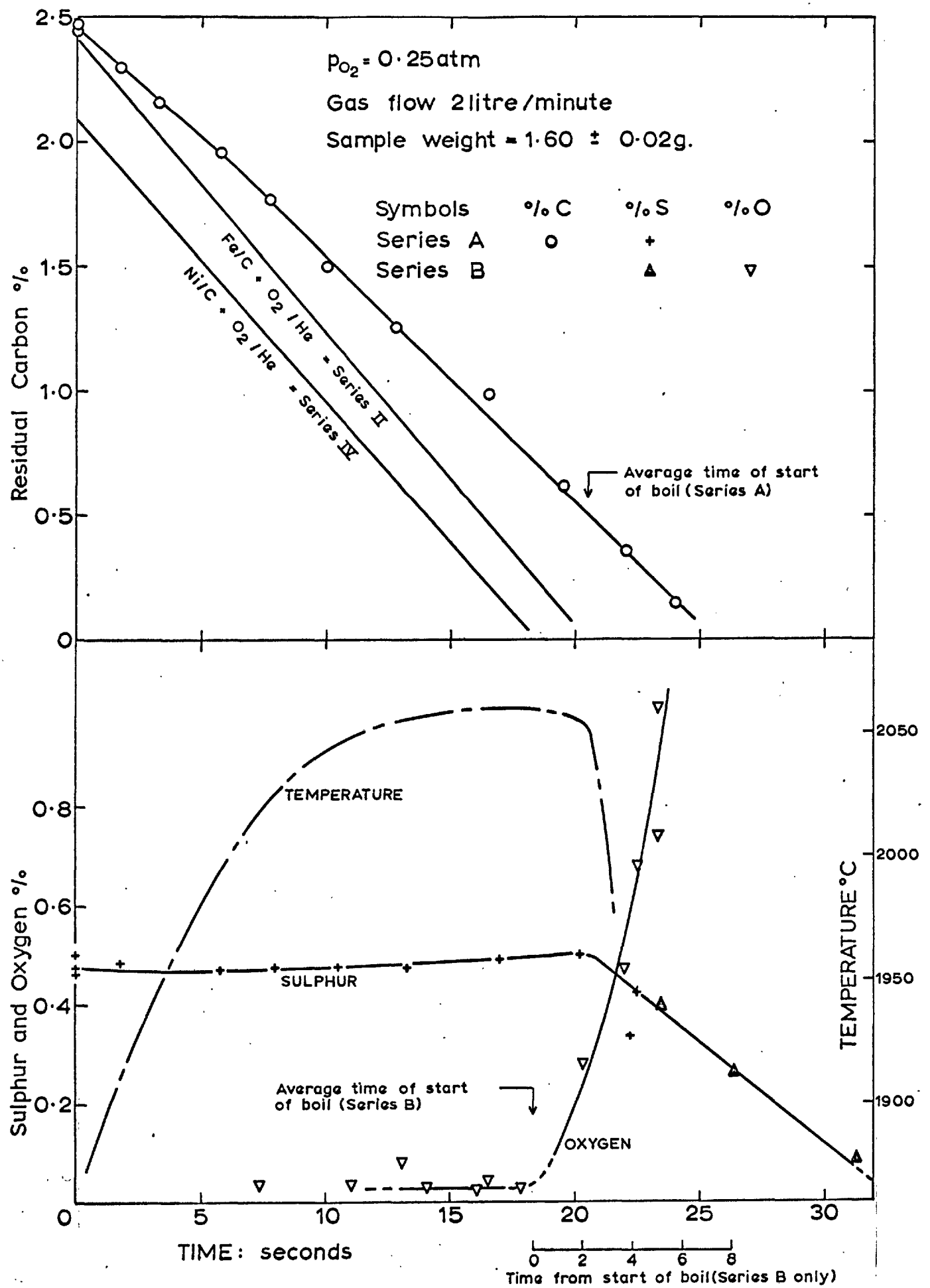

Fig. 28. Oxidation of Nickel - Carbon - Sulphur alloy drops in a flowing Oxygen - Helium mixture.

Figure 29

Nickel-Carbon-Sulphur Alloy Drop in O_2/He flowing at 2 litres/min., p_{O_2} = 0.25 atm. (Sulphur = 0.5% approx.).

a. Drop swelling and bubbles appearing, about 0.65 sec. from start of boil.

b. About 0.75 sec from start of boil.

c. Peak activity about 1.25 sec. from start of boil: large 'bright spots' as bubbles burst.

d. Sequence about 0.2 sec. after 'c' showing bursting of large dark bubble. Note that bright 'ripples' quickly vanish.

e. Boil subsiding, few bubbles present; about 2.3 sec. from start.

f. Drop at about normal size, 2.55 sec from start.

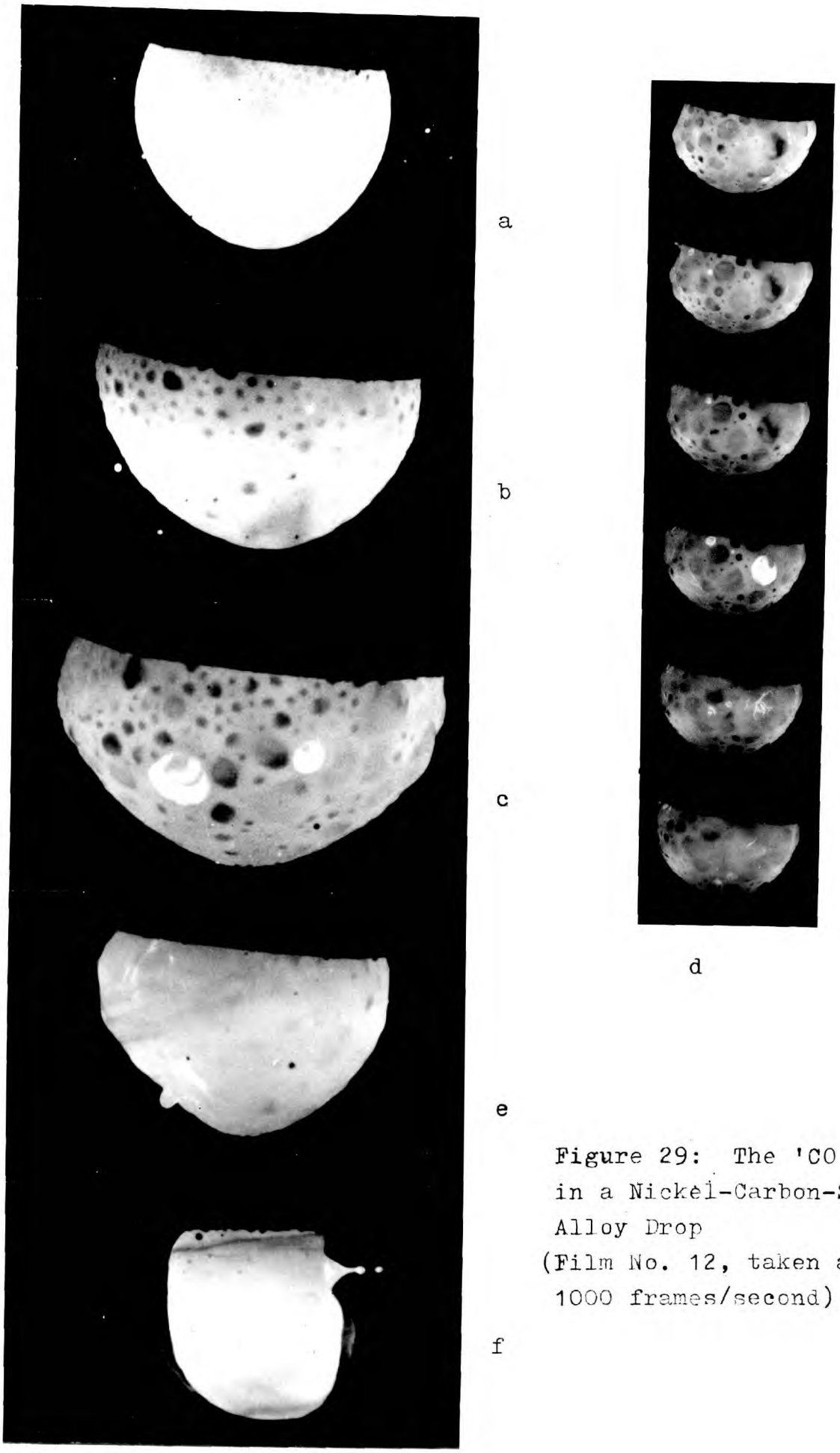

Figure 29: The 'CO Boil' in a Nickel-Carbon-Sulphur Alloy Drop
(Film No. 12, taken at 1000 frames/second)

experiments, so that an exact comparison of the reaction rates could be made. The experimental method was as already described.

Table 15 and Figure 30 show the results. Here again the points for the samples that contained sulphur show that there was a slight change in decarburisation rate at about 6 seconds and that the sulphur content probably went through a slight minimum at about the same moment.

The appearance of the boil was similar to that of the iron-carbon alloys; the drops did not swell up in the same way as the nickel-carbon-sulphur alloys had done. A high-speed film (No. 7) showed that the maximum diameter of the drop was about 1.6 times its original size but the shape was distorted instead of being spherical and the action was shorter than that with the nickel alloy. The diagram showing the sequence of events in the film is included in Fig. 25, and frames are reproduced in Fig. 31.

No oxide was recorded on the film but it is probable that the film ended just before oxide began to appear and that the moment of first appearance of the oxide was not significantly later than in experiments with iron-carbon drops. Direct observation of drops containing sulphur showed that the boil occurred after 21-22 seconds of oxidation and that there was an accumulation of oxide at the base of the drop at 25 seconds.

9. Additional Data on Decarburisation Reactions

(a) Extent of Oxidation of CO to CO_2: No flame of burning CO was seen in any of the experiments but measurements were made to determine how much secondary oxidation had occurred.

With the apparatus shown in Fig. 34 the gases could be collected during a decarburisation experiment without

Table 15: Oxidation of Iron-Carbon and Iron-Carbon-Sulphur Alloy Drops in an Oxygen-Helium Mixture

p_{O_2} = 0.25 atm., Gas Flow = 2 litres/minute

All times in seconds: "Total" refers to time in O_2/He

Fe/C			Fe/C/S								
Time			Time			Time			Time		% Oxygen
Total	Boil Start	%C	Total	Boil Start	%C	Total	Boil Start	%S	Total	Boil Start	Evold. All
0	-	2.41	0	-	2.60	0	-	0.745	0	-	0.00 0.033
0	-	2.37	0	-	2.59	0	-	0.73	0	-	- 0.042
$2\frac{1}{2}$	-	2.07	0	-	2.54	0	-	0.74	5	-	0.005 0.029
5	-	1.72	$1\frac{1}{2}$	-	2.40	4	-	0.71	$14\frac{3}{4}$	-	0.002 0.083
$5\frac{1}{2}$	-	1.62	$2\frac{1}{2}$	-	2.30	13	-	0.68	$17\frac{3}{4}$	-	0.009 0.062
10	-	1.16	$3\frac{3}{4}$	-	2.21	$21\frac{1}{4}$	-	0.71	$20\frac{1}{2}$	(20)	0.009 0.081
$14\frac{1}{2}$	-	0.50	$4\frac{3}{4}$	-	2.07	23	20	0.71	$21\frac{1}{4}$	-	0.017 0.063
17	?	0.14	7	-	1.87	$24\frac{1}{2}$	20	0.68	$22\frac{1}{2}$	?	0.007 0.056
18	16	0.01	$15\frac{1}{2}$	-	0.84	$26\frac{1}{2}$	(20)	0.73	$24\frac{1}{4}$	$22\frac{1}{2}$	0.025 0.27
$18\frac{1}{2}$	($18\frac{1}{4}$)	0.07	$19\frac{3}{4}$	($18\frac{1}{4}$)	0.30	29	$18\frac{3}{4}$	0.765	$25\frac{1}{2}$	$21\frac{1}{2}$	0.007 0.97
$20\frac{3}{4}$	$16\frac{1}{2}$	0.03	$23\frac{3}{4}$	21	0.22				$27\frac{3}{4}$	$21\frac{1}{2}$	0.002 1.13
$21\frac{3}{4}$	18	0.01	$24\frac{1}{2}$	($20\frac{1}{2}$)	0.15				$29\frac{1}{2}$	(20)	0.00 1.87
			$25\frac{1}{4}$	20	0.15				$31\frac{1}{2}$	$21\frac{3}{4}$	0.007 2.11
			$25\frac{3}{4}$	20	0.16						
			$26\frac{3}{4}$	$20\frac{1}{4}$	0.14						

Average time of start of boil: Fe/C drops $17\frac{1}{4}$ seconds

Fe/C/S drops $20\frac{1}{2}$ seconds

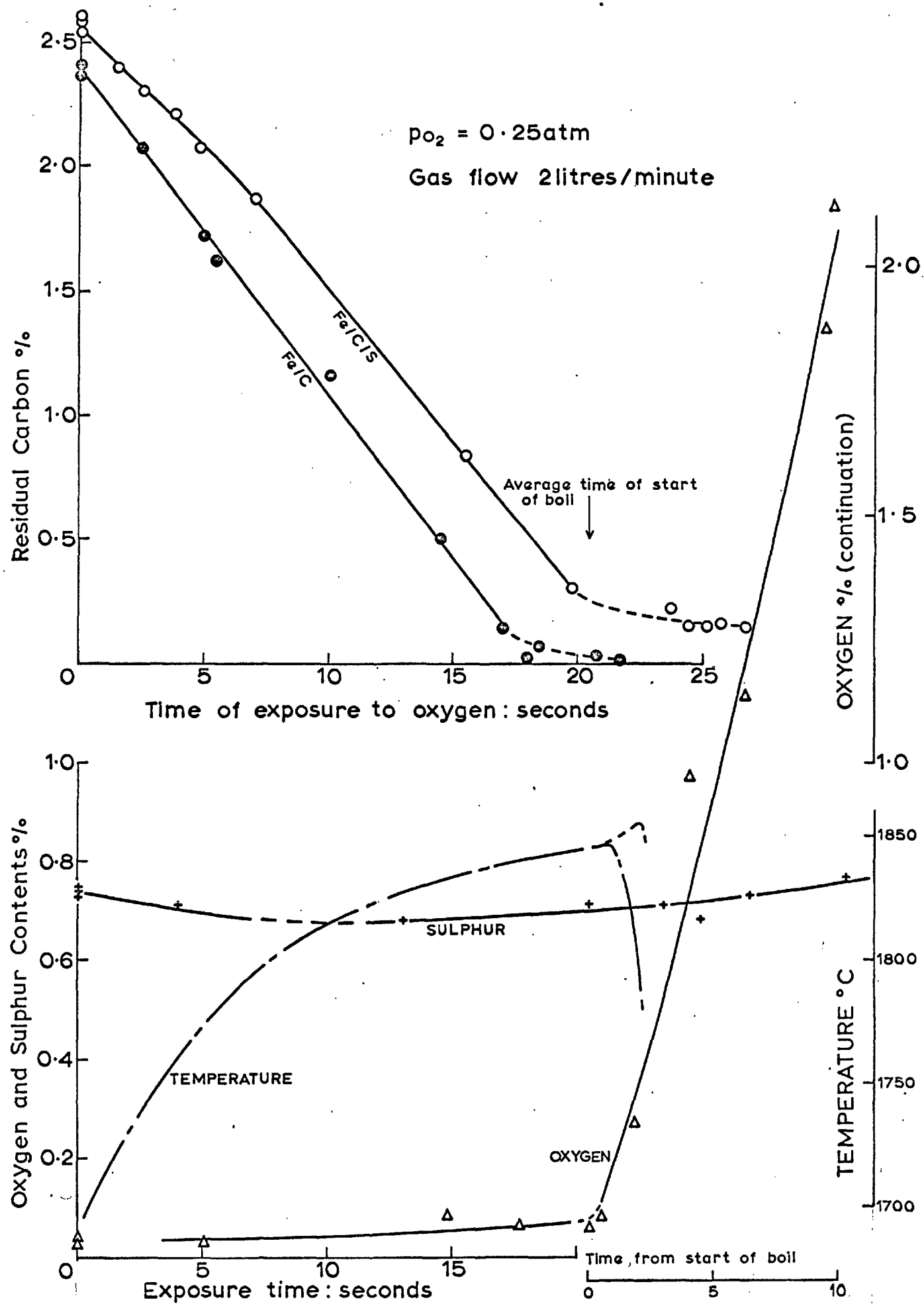

Fig.30. Oxidation of Iron-Carbon and Iron-Carbon-Sulphur alloy drops in a flowing Oxygen-Helium mixture.

Figure 31: Iron-Carbon-Sulphur Alloy Drop during greatest 'boil' activity.
(Taken at 1000 frames/second)
Diameter is about 1¾ times normal size. Note 'bright' spots' appearing and dispersing. Striations are due to fume. (N.B. Top of image is cut off by viewing port)

disturbing their pressure or flow-rate. The pinch-cock at G was adjusted to make the resistance in the line the same as that in the other line to waste at F. Because only the ratio and not the absolute volumes of CO and CO_2 were required, the collecting vessel was merely flushed out with helium before each test. During the decarburisation experiment, the gases flowed through the collecting vessel and to waste at F. Just before the boil was due to begin, C was opened and D closed. After the sample had been cast, the levitation cell was purged with helium. The gases in the collecting vessel were then flushed by a stream of helium at 400 ml/min. through the absorption train. Results are shown in Table 16.

(b) Errors in Oxygen Contents of "Column-quenched" Samples:
Data in Table 15 showed that 0.03-0.04 % oxygen was measured in two samples that had been exposed to helium only and then cast in the argon-filled "quenching-column". It was important to test whether these figures constituted a "blank" that should be deducted from all oxygen contents.

The time available for purging the column was about ¼ - ½ minute longer than the time each specimen was held in helium prior to oxidation, which was usually one minute. Although the argon flowed at 1 litre/minute, it appeared that enough air might remain at the time of casting to oxidise the drop slightly (although all cast samples were free of oxide colours). Some samples were therefore held for 2 or 3 minutes in helium so that the column could be purged for longer times. Tests were repeated with the samples cast into the copper cup within the levitation cell. Some drops were additionally exposed to hydrogen for a few seconds after being melted in helium, to ensure that they were initially oxygen-free.

After a review of the first results, additional tests

were made in which the reaction was terminated by switching the gas flow back to pure helium; the sample was cast after 5 seconds in the helium to avoid oxidation during cooling.

Results are shown in Table 17.

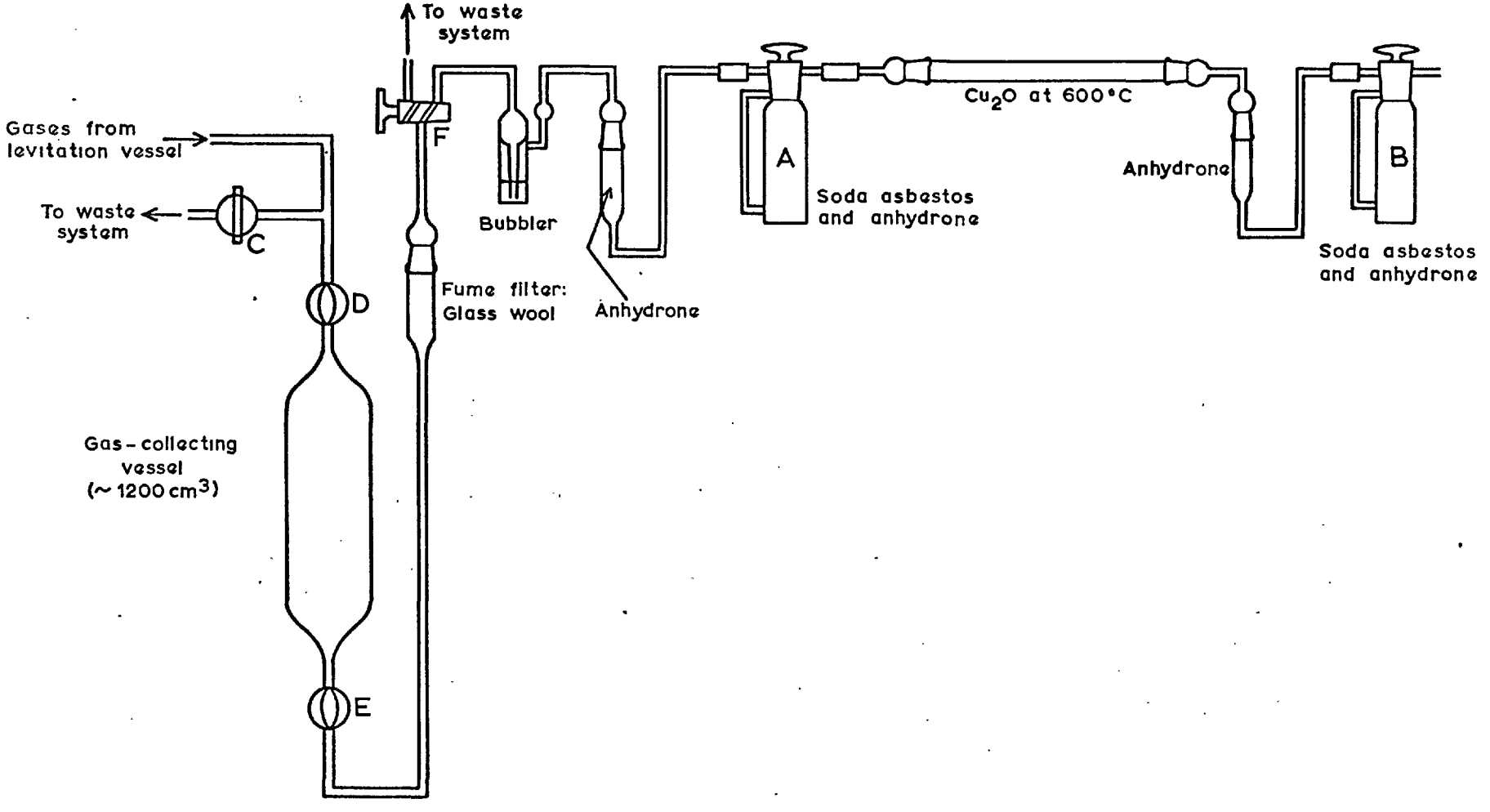

Fig. 32. Apparatus for measuring CO_2/CO ratios in gases from decarburization experiments

Table 16: Proportions of Carbon Dioxide to Monoxide in Gases evolved during decarburisation tests

"% CO convtd" = % converted to CO_2

Brackets indicate approx. figures.

Alloy	p_{O_2} atm.	Gas flow litr./min.	Temperature Range °C	Mean	Ratio CO_2/CO	% CO convtd.
Fe+3.9C	0.12	2	(1750-1830)	(1810)	0.55	36
			(1710-1810)	(1790)	0.55	36
			(1710-1795)	(1780)	0.59	37
ditto	0.25	2	(1710-1855)	(1810)	2.95	75
			1710-1850	1810	2.21	69
			1705-1850	1805	2.59	72
ditto	0.25	4	1670-(1820)	-	0.82	45
			1700-1830	1760	1.25	56
			1685-1810	1770	1.01	50
Fe+2.5C+ 0.8S	0125	2	1725-1865	1825	2.42	71
			1725-1870	1835	2.75	73
			1695-1860	1830	2.59	72
Ni+2.4C	0.02	2	1775-1825	1805	0.42	30
			1750-1820	1795	0.47	32
ditto	0.06	2	1805-1860	1845	0,86	46
			1805-1860	1840	0.79	44
ditto	0.12	2	1790-1895	1875	1.38	58
			1800-1900	1880	1.47	59
ditto	0.25	2	1790-1975	1920	4.9	83
			1795-1975	1925	4.2	81
ditto	0.25	4	1770-1975	1905	2.40	71
			1770-1975	1910	2.52	72
Ni+2.4C+ 0.8S	0.25	2	1815-2050	1990	7.8	89
			1820-2055	2005	8.9	90

Table 17: Comparison of Casting Methods etc. for Metal-Carbon Alloy Drops. (Oxygen contents)

Part A: Iron-based alloys

Method of Casting	Time in O_2/He	Pre-treatment: 1 minute in Helium	3 minutes in Helium	5 sec. approx. in H_2 & 3 min in He
copper cup in levitation vessel	0	0.000	0.012	0.000
		0.003	s 0.000	
	10	0.084	0.032	0.013
	15	0.026	0.035	0.033
		s0.026	s 0.035	
Steel mould in Argon-filled column	0	0.033	0.035	0.052
		0.047	0.039	0.047
	10	0.027	0.083	
	15	0.047	0.040	0.020
		s 0.046	0.036	
			0.061	

s: Fe/C/S alloy

All others are Fe/C alloy

Table 17: Comparison of Casting Methods etc. for Metal-Carbon Alloy Drops

(Oxygen contents)

Part B: Nickel-based alloys.

Note: All samples held for 2 minutes in Helium before exposure to O_2/He mixture

Numbers on left are times of exposure to O_2/He in seconds.

Copper cup in levitation vessel						Steel mould in Argon-filled column		
Cast in O_2/He			Cast after additional 5 sec. in helium					
$5\frac{1}{2}$	s	0.000	0		0.000	0		0.028
$9\frac{1}{2}$	s	0.009	5	s	0.000	11	s	0.037
$14\frac{1}{2}$		0.007	$5\frac{1}{4}$		0.000	14	s	0.030
$14\frac{1}{2}$	s	0.012	10	s	0.000	14		0.036
15		0.009	$10\frac{1}{4}$		0.000	$14\frac{1}{2}$		0.026
15		0.000	$14\frac{1}{2}$		0.000	$14\frac{1}{2}$	s	0.023
15		0.005	$14\frac{1}{2}$	s	0.007	15		0.033
16		0.007	15		0.013	16	s	0.043
			$16\frac{1}{2}$	s	0.000	$17\frac{1}{2}$	s	0.022

s: Ni/C/S alloy

All others are Ni/C alloy

V METHODS FOR MASS TRANSFER CALCULATIONS

When the rate-controlling step of a heterogeneous reaction is to be identified, it is important to compare the observed flux of a measurable species with that calculated from theoretical principles. This section sets out the principles that will be applied and describes experiments in which empirical constants needed for the gaseous-~~diffusion~~ transport expression were determined. Nomenclature is explained in Appendix 1.

1. Empirical Correlation of Data for Gaseous Mass Transfer

A purely mathematical analysis of the flow and convection processes around a heated sphere would be extremely complex. The model presented by the Boundary Layer Theory must be supplemented by empirical methods.

The theory gives the well-known expression for the total flux of A during counter-diffusion of species A and B:-

$$N_A = \frac{ak_g}{(1-\beta)\,RT} \text{Ln} \left[\frac{1 - (1-\beta)p_A^{\,b}}{1 - (1-\beta)p_A^{\,s}} \right] \quad \ldots(1)$$

where $N_B = -\beta N_A$

The problem is then one of obtaining a theoretical value for the ~~diffusion~~ mass transfer coefficient, $k_g = \frac{D_{AB}}{\delta}$. The diffusivity D_{AB} can be calculated from known properties of the gases but " δ " cannot be measured or calculated independently.

Several workers have shown how empirical expressions from the field of chemical engineering may be applied (1,4,5, 21-25). The approach of Steinberger and Treybal (51) has given the best agreement with observations. These workers studied the solution rates of benzoic acid spheres in flowing liquids and correlated their results, in addition to numerous

data by other workers on analogous systems of gaseous flow, by equating functions of dimensionless quantities:-

$$Sh = Sh_d + Sh_n + Sh_f$$

where Sh = Sherwood Number (see Appendix I)
Sh_d = contribution of radial molecular diffusion.
Sh_n = contribution of natural convection, due to a temperature difference between the sphere and the gas;
Sh_f = contribution of forced convection, due to the imposed flow velocity of the gas.

These terms may be expanded:-

$$k_g \cdot \frac{d}{D_{AB}} = 2.0 + \tfrac{1}{2} (\overline{Gr}.Sc)^{0.25} + nRe^{0.62}Sc^{0.31} \quad \ldots (2)$$

where d = diameter of sphere, cm.

n is a constant (S.& T. obtained 0.347)

The other dimensionless quantities are defined in Appendix 1. The literature sources for the gas properties and the methods of calculating values for binary and ternary mixtures are given in Appendix 2.

Although there is some doubt whether these three modes of transport do in fact operate independently and additively (52), Steinberger and Treybal showed that their expression fitted the experimental data with an average deviation of only 3%, in the range of Reynolds Numbers in which we are interested.

2. Determination of Empirical Constants

(a) Principles: Distin (1) and Forster (5) redetermined the value of "n" for the flow conditions in their levitation vessels. They measured the rates of weight loss from naphthalene-coated metal spheres, with the size, location and gas flow similar to those in levitation experiments. At room temperature, the natural convection term in equation (2) was zero, so that:-

$$\frac{Sh - 2}{Sc^{0.31}} = n.Re^{0.62} \quad \ldots\ (3)$$

Plotting the term on the left against $Re^{0.62}$ gave a straight line of slope "n", passing through the origin. The ~~diffusion~~ mass transfer coefficient "kg" used in calculating "Sh" was derived from the rate of the weight loss, dw/dt (g/s.):-

$$N_{NP} = \frac{1}{M_{NP}} \frac{dw}{dt} = \frac{k_G a}{R^G T} (p^s - p^b)_{NP}$$

which follows from equation (1) when β = zero and p_A (i.e. p_{NP}) is very small. In this expression, "p^s" is the vapour pressure (atm.) of naphthalene in equilibrium with the solid at temperature T(^oK) (53).

Both Distin and Forster assumed that "p^b", the partial pressure in the bulk gas, was zero but it will be shown that an allowance should be made for the vapour present there.

(b) Experimental Results: The writer's data, with a sphere representing a 1.6 g. metal drop and argon as the carrier gas, appeared to lie on a curve instead of a straight line (Fig. 33). This suggested that the exponent of "Re" and perhaps of "Sc" might need to be modified.

The experiments of Steinberger and Treybal were made in cylindrical tubes. Reliable correlations which were not affected by the ratio of sphere to tube diameter were obtained only when a "Sphere Reynolds Number", Re_s, was calculated from the average flow velocity in the tube. In the writer's levitation vessel, the Reynolds Number was based on the gas velocity in the supply jet, as this was the only velocity that could be calculated. Now, the gas stream impinges on the top of the sphere but velocities at other locations would be lower and it is reasonable to suppose that the exponent originally determined for "Re_s" would not be appropriate here.

The Schmidt Number, Sc, is the ratio of dynamic viscosity to diffusivity of the gas and should not be affected by this argument. Colburn (54) proposed an exponent of $\frac{1}{3}$ for "Sc" in mass transfer correlations and this has been widely followed in standard texts. Steinberger and Treybal commented that their experimental value of 0.31 was within one standard deviation of Colburn's value. The exponent of $\frac{1}{3}$ has therefore been retained in the following treatment.

From equation (3):-

$$\log \frac{Sh - 2}{Sc^{\frac{1}{3}}} = \log n + q \log Re \quad ...(4)$$

where "q" is the exponent of Re, to be determined. The transformed data should give a straight line of slope "q" and an intercept "n" at Re=1. Because we are dealing with dimensionless quantities, data for all carrier gases should lie on the same line, provided that the expression adequately represents the conditions. A few additional tests were made in helium and air to test this.

Figure 34 shows that a single line cannot be drawn for all of the gases. Although the points for air and helium are few, it appears reasonable to draw lines of the same slope through them. In the following section an important reason for the inadequate correlation is considered.

(c) Diffusivity of Naphthalene Vapour

Diffusivity data for the vapour in various gases are lacking and only an expression for the diffusivity in air has been found (55). Several empirical methods for calculating values have been proposed (56-58). Reid and Sherwood, in the second edition of their text (57b) reviewed these methods and favoured Hirschfelder's 'theoretical' method

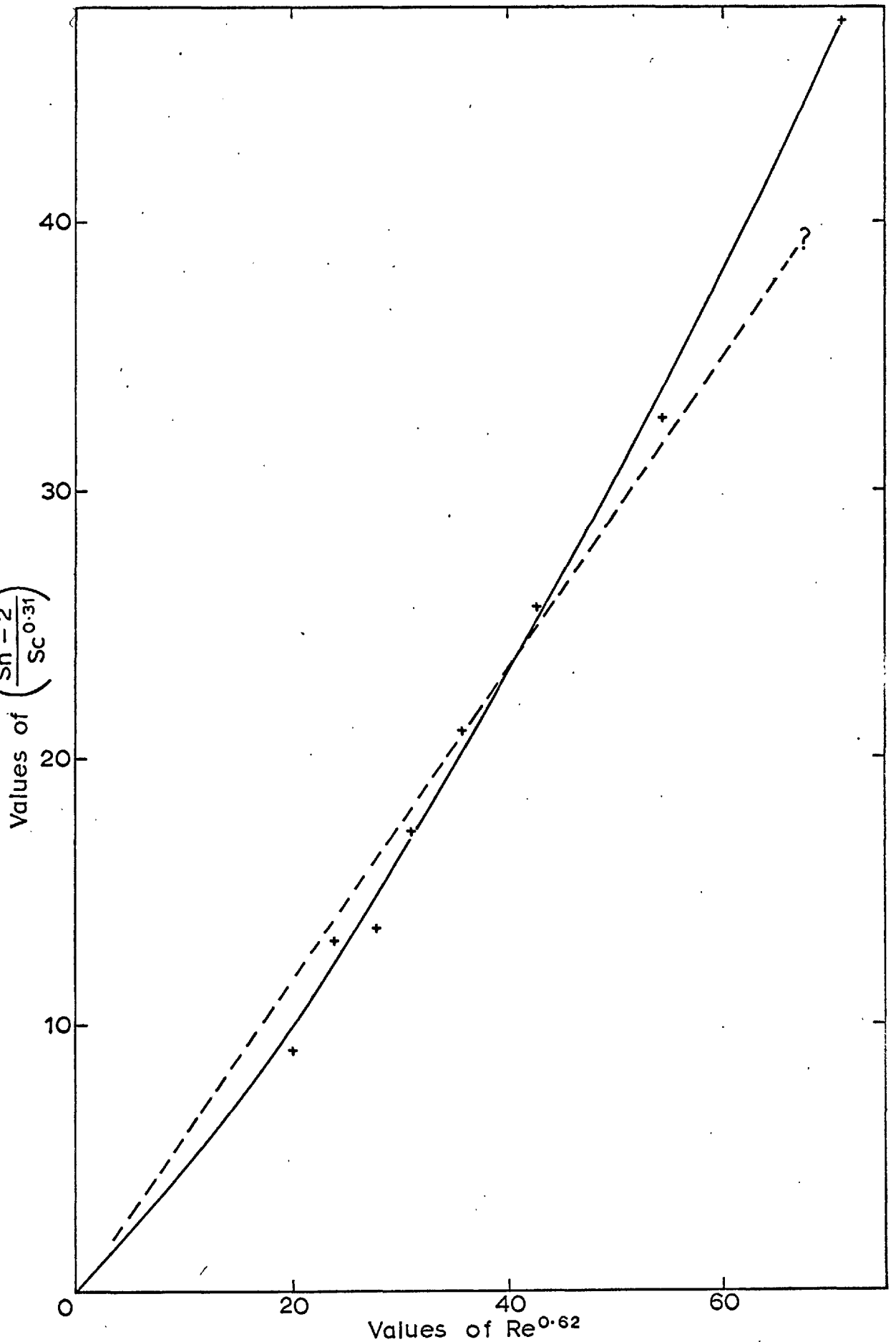

Fig. 33. Vaporization of Naphthalene in flowing Argon: Experimental results transformed by expression of Steinberger and Treybal.

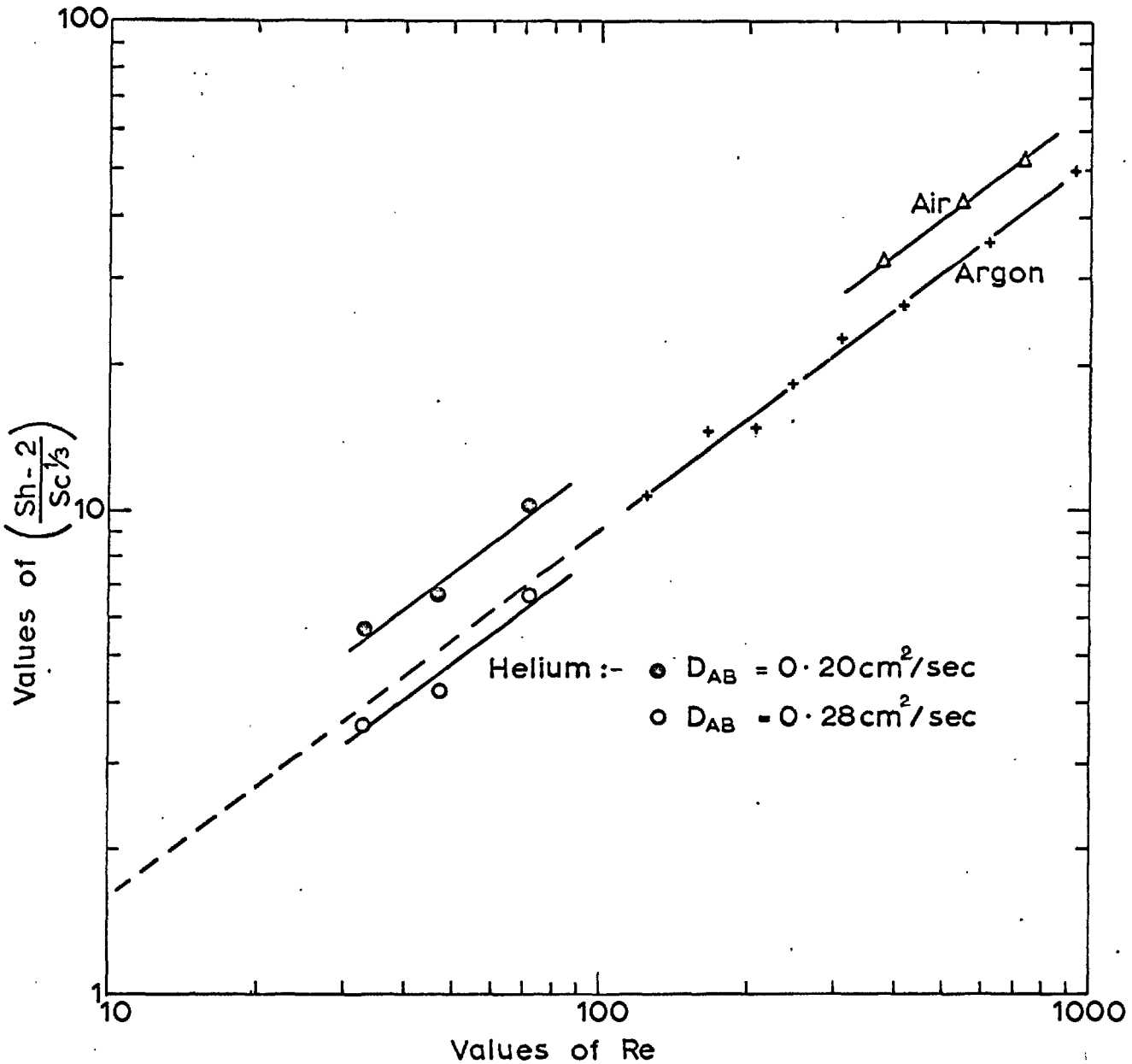

Fig.34. Vaporization of Naphthalene in flowing gases. Correlation of results in form of dimensionless quantities.

(56) which utilises the Lennard-Jones potentials and collision integrals for the gases. Even here, the potentials for the vapour must be estimated empirically from critical or molar volumes (57b). Table 18 shows diffusivity values calculated by various methods.

Table 18: Diffusivity of Naphthalene Vapour in Various Gases at 25°C. ($cm^2/s.$).

Method	Ref.	Ar	Air	He	H_2
Hirschfelder et al.	56	0.056	0.064	0.284	0.28
Wilke & Lee	58	0.056	0.0635	0.154	0.26
Reid & Sherwood (1st. edn.)	57a	0.057	0.0655	0.248	0.36
Mathers et al.	55	-	0.061	-	-

Values of 0.056 and 0.064 $cm^2/s.$ were accepted for argon and air respectively. For helium, separate sets of points were calculated for diffusivities of 0.28 and 0.20 $cm^2/s.$

(d) Constant and Errors: The slope of the argon line in Fig. 36 gives q = 0.76. The higher estimate of diffusivity for helium gives a line close to that for argon, which is taken as representing all the data; its intercept gives a value of n = 0.28. Then for metal drops of similar size in the levitation vessel:-

$$\frac{k_g \cdot d}{D_{AB}} = 2.0 + \tfrac{1}{2}(\bar{G}r.Sc)^{0.25} + 0.28Re^{0.76}Sc^{0.33} \qquad \ldots(5)$$

The uncertainty in the last term, measured as the gap between the argon line and that for air, is about 25%. The error in 'k_g' depends on the magnitude of the last term relative to the other two. With gas flows of 1-2 l/min. it is about 5-8%. rising to 15% at 8 l/min.

(e) Discussion of the correlation: It is possible that Steinberger and Treybal's expression does not take all relevant variables of the levitation system into account and that "n" is not a true constant. Distin found that "n" varied with sphere diameter. Forster obtained different values of the "constant" with different gases and the writer's data show the same effect when other effects have been compensated. The diffusivity data for naphthalene are not the sole source of error, since Figure 35 shows an appreciable difference between the lines for argon and air, in both of which the diffusivity of the vapour is known with reasonable certainty.

Ingebo (67) studied vaporization from spheres at temperatures up to 1000° and included the Peclet Number = (ReSc) in his forced convection term. When the present data were plotted as log(Sh-2) against log(ReSc), the correlation was not improved and the best line that could be constructed did not pass through the origin as required.

Expression (5) can however be used with the stated accuracy within the experimental range of Reynolds numbers. Extrapolations would be subject to unknown errors.

3. "Bulk Pressure" of a Reactive Gas

The model that provides the basis for expression (1) assumes the gaseous phase to be infinite in extent. The partial pressure of a component at the "bulk gas" end of the diffusion gradient remains the same as its value at the point where the gas flow enters the system and is not affected by utilisation or production of the component by the reaction.

The volume of the levitation cell is, in contrast, very limited and changes in the composition of the gas stream (the "bulk gas") may be large. We cannot assume that the value of "p^b" for a reaction product remains at zero. Calculations

must take account of the accumulation of the product in the gas stream and the consequent decrease in its concentration gradient between the gas stream and the reaction interface.

Mathematical analysis of the complex conditions in the levitation vessel is not practicable but a simpler case of changes in gas composition during flow across a flat interface has been worked out by the writer (Appendix 3).

For equi-molar counter-diffusion of a reactant A and a product B:-

Total flux of B, $N_b = -N_t \, x_B^{\,s} \left[\exp\left(\frac{-aZ}{N_t}\right) - 1 \right]$ ...(9)

where $Z = Pk_g/RT$

Similarly, for the absorption of A from a mixture with an inert gas:

$$N_A = N_t(x_A^{\,i} - x_A^{\,s}) \left[\exp\left(\frac{-aZ}{N_t}\right) - 1 \right] \quad ...(10)$$

provided that $x_A^{\,i}$, the mole fraction of A in the gas supply, is much smaller than unity.

A simpler approach is to assume that "$p_B^{\,b}$" varies linearly from its known value at the inlet to its calculable value at the outlet. For instance, if "$p_B^{\,b}$" is initially zero, its value at the outlet is:

$$(p_B^{\,b})_{max.} = \frac{N_B^r}{N_t + N_A^r + N_B^r}$$

$$= \frac{N_B^r}{N_t} \qquad \text{since } N_A^r = -N_B^r$$

Then, the mean value:

$$p_{B/av}^{\,b} = \frac{N_B^r}{2N_t}$$

Also, from equation (1), in the case of equi-molar counter-diffusion:-

Addendum to Section 3:

The data of Fig. 33 were plotted without this correction so that direct comparisons with the curves of Distin and Forster could be made. The resulting inconsistency between Figs. 33 & 34 is small and does not affect the form of each curve or the argument applied since the average bulk partial pressure of naphthalene was only about 10% of the vapour pressure at the solid surface at low flow rates and about 5% at high flow rates.

$$N_B^r = -aZ \left(p^b_{B/av} - p^s_B \right)$$

$$\frac{-N_B^r}{aZ} = \frac{N_B^r}{2N_t} - p^s_B = \frac{735}{L} N_B^r - p^s_B$$

where L is total flow in litres/minute at 25°C.

$$N_B^r \left(\frac{1}{aZ} + \frac{735}{L} \right) = p^s_B \qquad \ldots(11)$$

A similar expression can be worked out when a component is being absorbed from the gas supply.

If expressions (9) and (11) are tested with numerical values typical of conditions in levitation experiments, the differences between the alternative values of "N_B" are smaller than 1.5%.

The extent of the error where diffusion is not equimolar has not been worked out and the application of the above reasoning to spherical drops is subject to unknown errors. Nevertheless, the simple procedure of calculating the arithmetic mean value of the "bulk" partial pressure appears to be a step in the direction of reducing the errors and is employed in all calculations of gaseous ~~diffusion~~ transport in this thesis, including those for the naphthalene sphere experiments. in the revised correlation (Fig. 34).

4. Transport in the Metal Phase

Where atoms of a solute B are being transported by diffusion and convection through the hypothetical boundary layer of a liquid metal, the flux is expressed as:

$$N_B = -k_m a \left(\frac{n_B^b}{V} - \frac{n_B^s}{V} \right) \qquad \ldots.(6)$$

where k_m, the ~~diffusion~~ mass transfer coefficient of B in the metal phase, $= \frac{D_{B,m}}{\delta}$ cm/s.

This can be transformed to give:

$$\frac{d[B]}{dt} = \frac{-\rho_m \, ak_m}{W} \left([B]^b - [B]^s \right) \quad ...(7)$$

where $[B]$ is the concentration of the solute as a percentage.

When ~~diffusion~~ transport out of the metal phase is the rate-controlling step, it can usually be assumed that $[B]^s$ = zero and the rate is a first-order function of the "bulk" concentration:

$$\frac{d[B]}{dt} = - \frac{\rho_m ak_m}{W} \cdot [B]^b$$

By integration:

$$\text{Ln} \frac{[B]_1}{[B]_2} = \frac{\rho_m ak_m}{W} \cdot (t_2 - t_1) \quad ...(8)$$

where $[B]_1$ is the bulk concentration of B at time t_1, etc. Plotting $[B]$ on a logarithmic scale against a linear scale of "t" then gives a straight line. The same is true for any process that has first-order kinetics and does not apply only to ~~diffusion~~ transport in the metal phase.

VI DISCUSSION

1. Reduction of Metal/Oxygen Alloys by Hydrogen

(a) Rate-control by Gaseous Diffusion Step.

The early results showed, despite their scatter, that oxygen was removed from nickel much more rapidly than had been supposed and that the reaction rate was dependent upon the rate of hydrogen flow. Experiments with the high-oxygen samples confirmed that the rates were linear or very nearly so, down to fairly low oxygen levels.

From the data of Wriedt and Chipman (68) for the reaction:

$$H_2\ (g) + O_{Ni,\%} = H_2O\ (g)$$

the ratio $(p_{H_2O} / p_{H_2}) = 148\ [O]$ at 1625°C. Since $(p_{H_2O} + p_{H_2})_s = 1$ atm., $p^s_{H_2O}$ is close to 1 atm. and the concentration gradient of water vapour in the gas boundary layer is virtually constant until [O] is less than about 0.05%. A steady flux of H_2O is therefore expected. At 2000 - 2060°C, as in the tests with the high-oxygen samples, $(p_{H_2O}/p_{H_2})_s = 18\ [O]$ and divergence from a steady flux of H_2O should become evident when [O] is about 0.5%.

From iron, the equilibrium constant is much smaller and Wriedt and Chipman's data give a gas ratio equal to 2.4 [O] at 1710°C. At the oxygen saturation level of 0.35% (and also in the presence of free oxide, whose oxygen activity is the same as that of the saturated solution) $p^s_{H_2O} = 0.46$ atm. only. A steady flux of oxygen or water vapour is not expected. For the comparison of the theoretical and observed fluxes in experiments with iron drops (Table 19), calculations were made for the oxygen level of 0.35%.

The observed reduction rates for nickel were below

those predicted (Table 19), even when the effects of water vapour in the "bulk" gas were allowed for. The theoretical fluxes are believed to be realistic. The "naphthalene sphere" experiments showed that some uncertainties remain in the constants determined for the Steinberger and Treybal expression and hydrogen was not tested in those experiments. Even a fairly wide deviation of any data for hydrogen from the argon line should not affect the total Sherwood Number and thus the value of 'k_g' by more than a small fraction. Such errors should be smaller at lower flow-rates but the theoretical fluxes agree better with those observed at the higher flow-rates.

The points for iron drops at the lower rate of gas flow appear to fit a straight line, in spite of the expected dependence of the ~~diffusion~~ concentration gradient upon the oxygen content of the metal. This is perhaps fortuitous and results from the known errors in timing and casting technique. The line may then represent an "average" of the curve that should appear and its slope would probably be smaller than that calculated for 0.35% O. This may partly explain the very low flux ratio of 0.33.

At present no further explanation can be offered for the high predictions for the theoretical flux. Typical calculations have been independently checked. Errors in any one of the many quantities entering into the calculation of "k_g" should have a relatively small effect on the result. The diffusivity alone has a major effect. This was calculated by the method of Hirschfelder et al (59, 57b) and gave:-

$$D_{H_2/H_2O} = 8.0 \text{ cm}^2/\text{s. at } 1100^\circ\text{K},$$
$$10.8 \text{ cm}^2/\text{s. at } 1315^\circ\text{K},$$

these being the extremes of "film temperature" in the

Table 19: Reduction of Ni/O and Fe/O drops in Hydrogen Calculation of Fluxes

N.B. Brackets indicat approximate figures, based on few or scattered data.

	Ni: low initial %O			Ni: high %O		Fe	
H_2: litres/min	2.5	5	8	8	10	2.5	5
J: g.	1.84	1.75	1.75	2.0	2.0	1.79	1.79
Av. Temp. ^oC	1625	1625	1625	2000	2060	1710	1710
T_f ^oK	1100	1100	1100	1285	1315	1140	1140
N_{H_2} (mol/s) x 10^3	1.70	3.40	5.45	5.45	6.80	1.70	3.40
$-d[O]/dt$ (%/s)	0.35	(0.5*)	0.8	0.93	1.06	0.11	(0.33+)
N_{H_2O} exptl. (mol/s) x 10^3	0.4	(0.55)	0.87	1.16	1.33	0.12	(0.37)
% utilisation	24	(16)	16	21	20	7	11
Calculations of Theoretical N_{H_2O}							
(i) Assuming $p^b_{H_2O}$ = zero; using properties of pure H_2							
k_g (cm/s)	49	60	71	86	91	47	58
N_{H_2O} (mol/s) x 10^3	0.99	1.19	1.40	1.68	1.73	0.45+	0.55+
(ii) Assuming $p^b_{H_2O}$ = av. of inlet & outlet values; properties of H_2-H_2O mixture							
k_g (cm/s)	52	66	76	94	104	49	62
N_{H_2O} (mol/s) x 10^3	0.82	1.11	1.21	1.59	1.75	0.36	0.50
Ratio obs./theor flux ii	0.5	(0.5)	0.72	0.73	0.76	0.33	(0.74)

Notes: * Average of 3 estimates: 0.25, 0.42, 0.9 %/s. + Slope of initial steep part of curve.
Estimated flux when $[O]$ = 0.35% (see text)

experiments.

(b) Rate-Control by Diffusion in the Metal.

The evidence for rate-control by gaseous diffusion down to low oxygen levels implied that the transport of oxygen in the metal must be much faster than originally assumed. It is not clear, however, whether slow diffusion in the metal became the rate-controlling step at any time in these experiments.

We have seen that curvature of the lines in Figs. 9 and 11a can be accounted for, at least in part, ~~for~~ by decreases in $p^{s}_{H_2O}$. For a given value of k_g:-

$$\frac{d[O]}{dt} \propto \frac{K[O]}{1+K[O]}$$

where K is the equilibrium constant discussed in subsection (a). When $K[O] \ll 1$, $d[O]/dt \propto [O]$ but when $10 > K[O] > 0.1$, the relation is less simple. If the straight lines in Figs. 10 & 11b do indicate slow transport in the gas phase with first-order dependence on metal composition, transport in the metal must be still faster. If the slow transport of oxygen in the metal were rate-controlling at these oxygen levels, the effect should have been detected in the low-oxygen samples since the lower temperature should not greatly reduce the value of $k_{m(O)}$.

In either case, we can still use the slopes of the lines in Fig. 10 and 11b to give a conservative estimate of the value of $k_{m(O)}$, which is then not less than 0.2 cm/sec. for nickel and iron. The figure is 7 times larger than Distin's estimate of 0.032 cm/sec. for carbon in iron, and 100 times larger than his estimate for oxygen in iron.

(c) The "H_2O Boil"

No boiling action was seen in any drop except the one that was coated with zirconia particles, where nucleation

was evidently heterogeneous. For a boil to occur, even under these conditions, the pressure in the gas bubbles must be greater than atmospheric. Now, if the drop containing dissolved oxygen and hydrogen were at equilibrium with the mixture of vapour and hydrogen at the surface at each instant, the internal "pressure" of H_2O due to the solutes would be the same as $p^s_{H_2O}$, at a little below 1 atm. as long as the oxygen content were in excess of about 0.05%. The boiling action indicates, then, that [H] must be above this "equilibrium" value.

It follows that the gaseous hydrogen does not simply react with dissolved oxygen at the metal surface but that there is a balance between the rates of reaction and solution, depending upon the specific rates of the two processes (note also the "inflation" of the cast samples by water vapour, p. 42). The number of moles of hydrogen needed to reach the "equilibrium" concentration while the oxygen content is in the middle range is of the order of 1% of that forming H2O at the surface. For the higher concentrations inferred, the rate of solution is probably still small compared with that of chemical reaction but is nevertheless sufficient to allow the supersaturated condition with respect to H_2O to develop.

(d) Interfacial Turbulence.

The film provided evidence of eddying in the surface and this may have been caused by interfacial turbulence. Eddies of hydrogen in the gas may remove adsorbed atoms of oxygen locally from the surface and so cause large changes of surface tension over small distances and in short times. These would lead to movements of the metal itself.

A similar phenomenon is well-known in the chemistry

of organic and aqueous liquids as the Marangoni effect (69). Brimacombe (72, also cited in 81) observed it when an aqueous solution reacted with a mercury amalgam. Mass transfer rates in aqueous solution can be increased by eddying due to this effect (70, 71). A similar process might assist the transport of oxygen atoms to the metal surface and explain the high value of $k_{m(O)}$ above.

2. Reactions between Nickel and Oxygen

(a) Loss of Oxygen from Nickel-Oxygen Drops

The mass transfer expression, equation V:1, can be simplified when β = zero and the partial pressure of the reactive gas is small, to:-

$$N_a = \frac{-ak_g}{RT} (p_A{}^b - p_A{}^s)$$

Now $$p^s_{O_2} = K\,[O]^2$$

where K is the equilibrium constant for the reaction

$$2\,\underline{O}_{Ni,\%} = O_2\ (g)$$

It can then be shown that

$$\Phi[O] = \frac{[O]_i - [O]_t}{[O]_i \cdot [O]_t} = \frac{3200.K}{y.W}.\ t$$

Figure 35 shows this function plotted against time. The slope of each line: $\frac{d\Phi[O]}{dt} = \frac{3200K}{y\ W}$

where $y = \frac{1}{aZ} + \frac{735}{L}$ (see also Section V),

and the values of Z and thus K_g can be calculated. If $p_{O_2}{}^b$ is assumed to be zero, the term 735/L is omitted. Table 20 compares the observed and theoretical values of the mass transfer coefficient, k_g in place of the fluxes, which vary with the oxygen content of the metal.

Table 20: Loss of Oxygen from Nickel-Oxygen Drops

Experimental and theoretical mass transfer coefficients

Series	I	II	III
Gas flow: l/min	1He	2He	3He + 2 Ar
k_g theoret. cm/s.	37	43	42
k_g exptl. ($p^b_{O_2}$=zero)	43	33	35
k_g exptl. ($p^b_{O_2}$= av.)	92	41	42

The value of K was derived from data by Fischer and Ackermann (73) for the free energy of solution of oxygen in nickel. The experimental values for k_g are sensitive to errors in this free energy value and the choice of this set of data is discussed in Appendix 4. The use of a higher negative value for the free energy of solution would increase all the experimental values of k_g.

If allowance is made for oxygen accumulating in the gas stream, the values of k_g agree well for gas flows of 2 and 5 litres/min. but the discrepancy is large at 1 litre/min. The situation is reversed if the oxygen entering the gas stream is ignored.

Distin (1a) found that sulphur diffused out of liquid iron into inert gases much more rapidly than the theoretical value of k_g would allow and suggested that the reaction of sulphur with iron vapour might have the effect of steepening the ~~diffusion~~ concentration gradient. Turkdogan and his associates (78, 79) found that liquid iron vaporised more rapidly when the concentration of oxygen in a stream of gas was increased.

From Toop's data (2) we may estimate that the writer's nickel drops would give off about 30×10^{-8} moles of vapour per second in an inert gas stream. The fluxes of oxygen from the drop were of the order of 8×10^{-8} moles per second

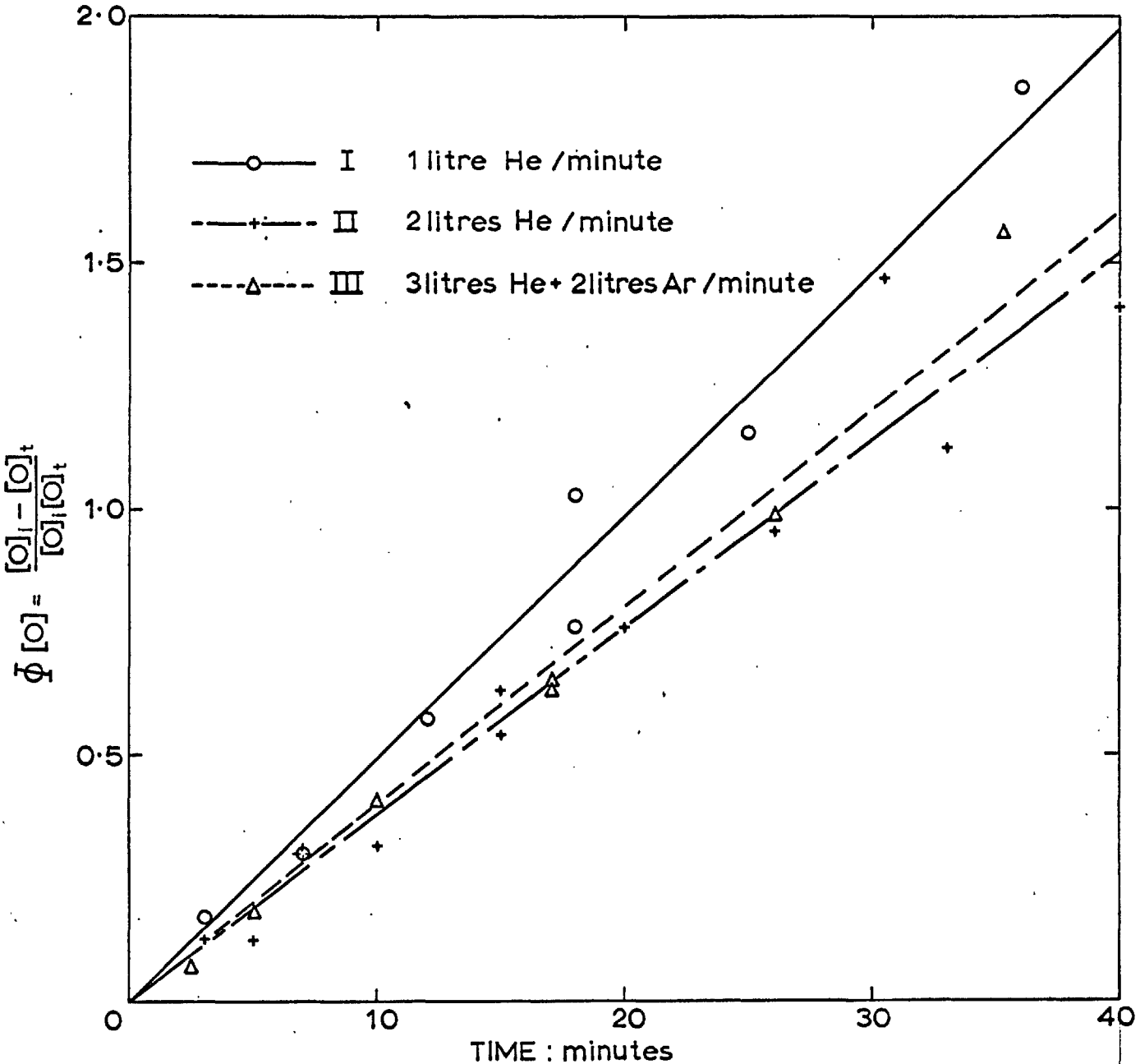

Fig. 35. Loss of oxygen from Nickel - Oxygen alloy drops in inert gases
Transformed variable based on oxygen content

and it is possible that some of this reacted with the nickel vapour. Calculations made assuming that $p^s_{O_2}$ = zero should then give the closer agreement for k_g. The pattern of agreement is inconsistent but the discrepancies are much smaller than those found by Distin and the occurrence of reactions with the vapour cannot be regarded as proven.

If the activity of oxygen in nickel deviates negatively from Henry's Law (for which Appendix 4 sets out some evidence), we should write:-

$$p^s_{O_2} = K.f_o^2[O]^2$$

where f_o is the Henrian activity coefficient

The concentration gradient would then be reduced (since f_o is less than unity) and the theoretical flux of oxygen at any time would be correspondingly smaller. This would have the same effect as a reduction in "k_g theoretical" in the comparisons made above and would suggest more strongly that the experimental rates were enhanced by reactions with the vapour.

(b) Oxidation of Liquid Nickel: low oxygen concentrations.

The observed fluxes of oxygen were smaller than those estimated theoretically although allowance was made for the depletion of oxygen in the 'bulk' gas (Table 21). The following tentative conclusions can be drawn:-

(i) Utilisation decreased as gas velocity increased (at constant oxygen concentration) because k_g changed very little as the supply of oxygen increased.

(ii) Flux ratios were higher for He + Ar mixtures than for those with He only, although temperatures were comparable. This suggests that interfering reactions, such as that with metal vapour, might be more effective in helium although it is difficult to see why this should be so. Alternatively the calculations of theoretical "k_g" might

be subject to greater errors for the very light gas.

(iii) If reaction with nickel vapour ~~was~~ were important the discrepancy should be larger at the higher temperatures but no such pattern is evident.

(iv) Increasing the partial pressure of oxygen appeared to increase the flux ratio although the effect was not uniform across the range (I, V & VI). Here again, it may be that the addition of a heavier gas in some way improved the precision of the estimates.

Another possible source of interference with absorption was the coating of silica or "slag" that was seen to form on some drops (Fig. 16) but it seems unlikely that this could account for fairly consistent reductions smaller than 3/1 in the absorption rate, or for the higher flux ratios in the presence of argon. Glen (4) reported that very thin silica coatings on copper reduced the absorption rate by factors of 10 or more but that the coatings were removed, probably by volatilisation, at temperatures above 1500°. The writer found that his results were more consistent when drops had been allowed to heat up to 1750°. Figure 16 b & c shows the thin films beginning to coalesce at an early stage of the oxidation. The frequent occurrence of slag as small spots may indicate that no coherent coating or barrier to absorption remained.

Reactions between nickel and oxygen were investigated for possible effects of surface activity upon the kinetics, but none can be discerned. If the rate of loss of oxygen from a drop were dependent upon the surface concentration of adsorbed atoms, the rate would remain almost constant down to oxygen levels below 0.05%, since surface coverage is thought to be virtually complete above that level. Similarly, adsorbed oxygen atoms could not constitute a

Table 21: Oxidation of pure Nickel (low oxygen concentrations)

Calculation of fluxes

L: total flow-rate, litres/minute (inert gases stated)

Weights: Series I: 1.84 g.; All others 1.60g.

N: Molar flux, moles/second.

No.	I	II	III	IV	V	VI
p_{O_2} atm.	0.008	0.008	0.008	0.008	0.020	0.040
L	1 He	3 He	3He+2Ar	5He+3Ar	1 He	1 He
Init. temp ^{o}C.	1690	1640	1680	1630	1700	1700
Max. temp.^{o}C.	1760	1720	1760	1720	1800	1820
T_f, ^{o}K	1155	1120	1170	1120	1175	1185
$10^6 \times N^t_{O_2}$	5.45	16.4	27.2	43.6	13.6	27.2
$10^3 \times d[O]/dt$ obs'vd.	3.13	4.80	9.03	8.92	7.65	19.9
$10^6 \times N^r_{O_2}$ obs'vd.	1.80	2.40	4.52	4.46	3.83	10.0
% Utilisation	33	15	17	10	28	37
k_g cm/s.	37	44	42	50	39.	39
$N^r_{O_2}$ theoret* $\times 10^6$	4.22	5.46	5.38	6.82	9.20	18.2
Obs'vd/theoret. $N^r_{O_2}$	0.43	0.44	0.84	0.67	0.42	0.55

* allowing for depletion of oxygen in the "bulk" gas.

Note: $p^s_{O_2} < 0.0002$ atm. when $[O] = 0.8\%$ and has been ignored in these calculations.

barrier to further solution of the gas, since kinetics would again be governnd by the surface coverage and there is no evidence of this.

(c) Oxidation of Liquid Nickel: high oxygen concentrations.

Oxygen could not be supplied to the metal surface more rapidly than transport processes carried it into the interior of the drop and it is clear that transport in the gas phase was rate-controlling in all experiments. This is unexpected for reactions in pure oxygen. The explanation may be that the oxygen had to diffuse in opposition to a flux of nickel vapour which would be high at these temperatures and may also have reacted with it in part.

For each set of conditions, a minimum value of $k_{m(O)}$ can be calculated. The observed rate of oxygen absorption $d[O]/dt$, can be equated to $\frac{\rho a k_m}{W}\left([O]^s - [O]^b\right)$. Now $[O]^s$ cannot be measured but we can obtain a conservative estimate for k_m by supposing that the ~~diffusion~~ concentration gradient was nearly steep enough to cause oxide to form. Then $[O]^s$ lies close to the saturation line on a temperature/composition diagram (Fig. 36). This line was plotted from the data of Bowers (49). The curves for the temperatures of nickel drops, calculated from the data in Fig. 15, indicate that the relation of observed temperature to oxygen content was similar for all nickel drops levitated in gas mixtures of high oxygen concentration. At about 1700° the difference $[O]^s - [O]^b$ was only 3%0 but although this gradient was small, no oxide formed. This figure was therefore used in calculating the values of k_m shown in Table 22.

As no oxide was observed at any time, the true value of k_m must be higher than the maximum estimate of 0.096 cm/s. This supports the estimates, from the hydrogen-reduction

experiments, of about 0.2 cm/s. and shows that high transport rates can occur where interfacial turbulence is absent, for rapid local changes in surface tension are not expected during the solution of oxygen in unalloyed nickel.

Table 22: Oxidation of Nickel Drops: High oxygen concentrations

No.	iv	v	vi	vii	viii	ix
p_{O_2} (atm.)	0.20	0.40	0.60	1.00	0.30	0.60
L (l/min)	5	5	5	5	5	5
O_2 suppld. (cm^3/s)	16.7	33.3	50.0	83.3	25.0	50.0
d[O]/dt (av)	0.276	0.725	1.52	2.2	0.52	1.80
Vol. Absorbed (cm^3/s)	4.22	11.1	23.2	33	6.75	27.5
% Utilisation	25	33	46	40	27	55
k_m(min)(cm/s)	0.012	0.032	0.068	0.096	0.026	0.080

p_{Ni} (1900°C) = 7.35 g/cm^3 (See Appendix 2)

Drop wt. = 2.00 g. (No. viii = 1.70 g)

Area = 2.03 cm^2 (No. viii: 1.82 cm^2)

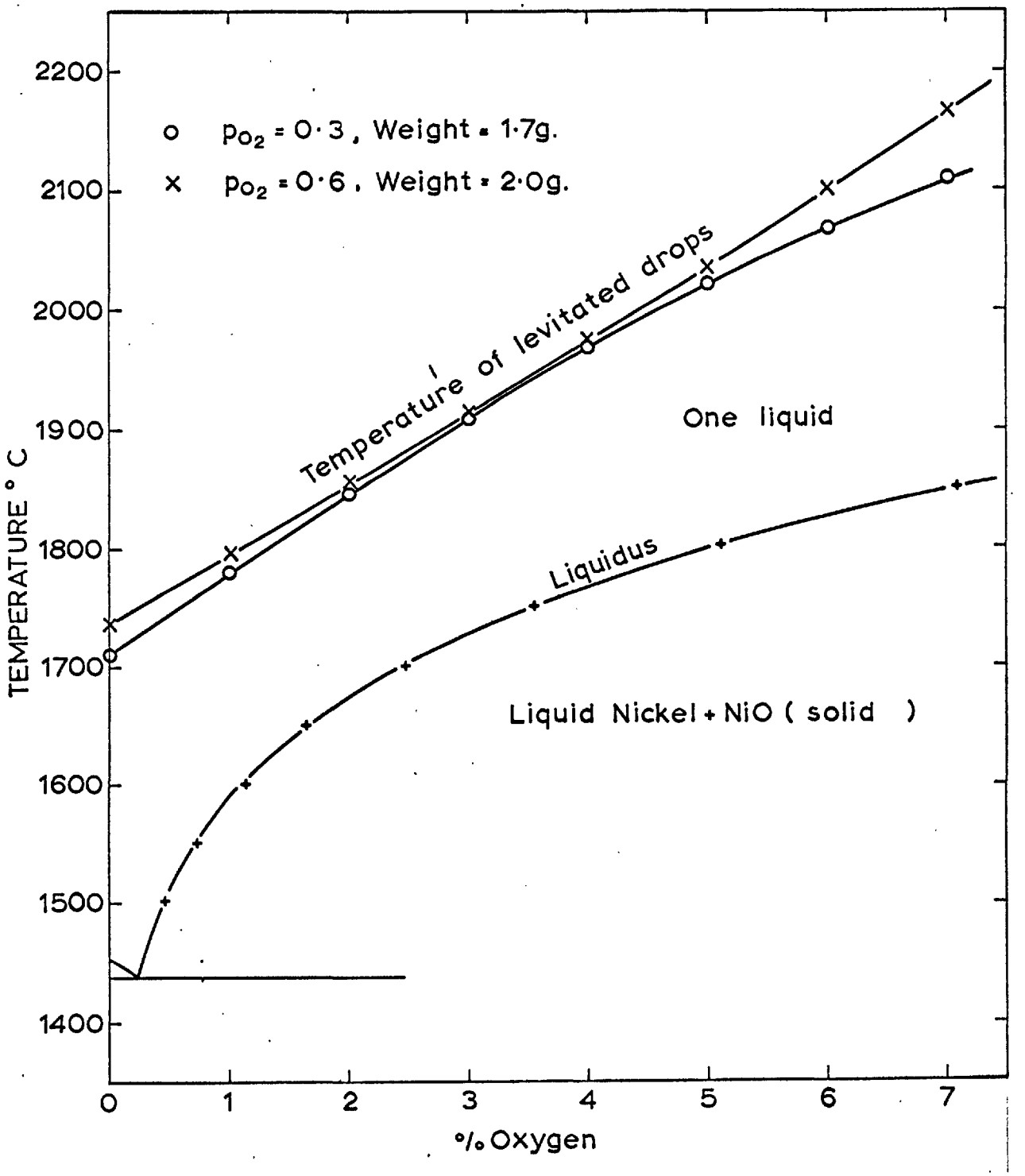

Fig. 36. Temperature rise during absorption of oxygen by nickel drops.

Page 133b: Correction.

The summation to give equation (1) should read:-

$$O_2(g) = 2\,\underline{O} \qquad \ldots(2)$$

$$2\,\underline{O} = 2\,\underline{O}_{ads} \qquad \ldots(3a)$$

$$\underline{S} = \underline{S}_{ads} \qquad \ldots(3b)$$

$$\underline{S}_{ads} + 2\,\underline{O}_{ads} = SO_2\,(g) \qquad \ldots(4)$$

The sum of the sulphur and oxygen contents is high enough to give virtually complete coverage of the surface at all times and some form of equilibrium must exist between reactions 3a and 3b. The "competition" for adsorption sites could be stated as the difference between 3a and 3b, giving equation 3 which still expresses an important limitation to the concentrations of reactants in the gas-forming reaction 4.

3. Oxidation of Nickel-Sulphur Alloys

(a) Initial Slow Desulphurisation: Evidence for Chemical Rate-Control.

The most interesting feature of the results is the delay before the steady oxidation of sulphur. This cannot be simply due to carbon because even the 0.06% present in some batches of nickel powder would be oxidised in less than half the "delay times" observed (from calculations based on the decarburisation experiments). The nickel "sponge" used in Series VI-IX contained only 0.005 %C.

The key to understanding this effect is in the rapid initial rise in the oxygen content. The data do not show whether this was in fact linear, as sketched in Figs. 12 a-d or whether the rate decreased more uniformly to the subsequent linear rate. It is clear however that the steady rate of oxygen absorption was attained at about the same time that the oxidation of the sulphur reached its linear rate.

The strong surface activity of both sulphur and oxygen has already been mentioned. The oxidation of dissolved sulphur by gaseous oxygen must include an important step in which adsorbed atoms of the two elements combine on the surface of the liquid.

The reaction: $\underline{S} + O_2(g) \longrightarrow SO_2(g)$ ...(1)

can be regarded as the sum of three reactions:-

$$O_2(g) = 2\underline{O} \qquad ...(2)$$

$$\underline{S}_{ads} + 2\underline{O} = \underline{S} + 2\underline{O}_{ads} \qquad ...(3)$$

$$\underline{S}_{ads} + 2\underline{O}_{ads} = SO_2(g) \qquad ...(4)$$

The rate of forming SO_2 is a function of the relative forward and backward rates of all these. For reaction (4), the rate equation is:

$$\frac{d[S]}{dt} = - ak' . [S]_{ads} . [O]^2_{ads}$$

where k' is the rate constant.

In the very early stages of an experiment the metal contains virtually no dissolved oxygen: $[O]_{ads}$ is very small (by equation 3) and the rate in equation (5) is low. Little of the gaseous oxygen arriving at the interface is used to form SO_2 and most instead dissolves in the liquid. The surface concentration $[O]_{ads}$ also increases and although this leads to a diminution in $[S]_{ads}$, the rate (5) increases. This continues until the rate becomes limited by the slow diffusion of SO_2 through the gas boundary layer.

(b) Linear-rate Oxidation

The middle period of the reaction was evidently controlled by a slow gaseous-diffusion step, since the rate of sulphur loss depended upon the flow-rate and composition of the gas stream and was independent of the alloy composition, at least down to low concentrations of sulphur.

The observed fluxes of SO_2 were only $\frac{1}{3}$ to $\frac{1}{2}$ of those calculated but the continuing absorption of oxygen makes comparisons difficult. It is not reasonable to calculate a 'total theoretical flux of oxygen' as a basis for comparison since the SO_2 has a slower diffusion rate which probably controls the overall rate. Under the conditions of Series IX:-

$$D_{O_2/SO_2+\ He} = 7.0\ cm^2/sec$$

$$D_{SO_2/O_2+He} = 5.0\ cm^2/sec.$$

The flux ratios for SO_2 ('a/b' in Table 23) were in general higher when the temperature was lower and again oxygen may have reacted with nickel vapour, although supporting evidence is lacking. Harvey (83) studied reactions of copper drops in O_2/N_2 mixtures at 1400-1600° where vaporisation should be strong but found no marked

Table 23: Oxidation of Nickel-Sulphur Alloy Drops: Comparison of Fluxes etc.

Note: All fluxes are stated as (mol/s) x 10^6; Brackets indicate approximate data

Series No.		I	III	V	VI	VIII	II	VII	IV	IX
p_{O_2}	atm.	0.008	0 008	0.008	0.008	0.008	0.020	0.020	0.008	0.025
L_{O_2}	litr/min	1	1	1	1	1	1	1	4	2.5
Initial % S		0.45	0.45	0.58	0.65	0.65	0.45	0.65	0.58	0.72
Av. metal temp.	°C	1700	1700	1690	1740	1760	1700	1740	1600	1740
Initial slow reaction	NO_2 to O	(1.6)	(1.6)	-	0.94	0.94	-	2.1	-	7.5
	% utilisn.	(30)	(30)	-	17	17	-	15	-	17
Linear reaction rate	10^3x d[S]/dt: %/s	2.22	2.50	2.88	2.09	2.09	5.6	4.3	6.0	13.0
	N_{SO_2} (a)	1.11	1.25	1.44	1.05	1.05	2.80	2.15	3.0	6.5
	N_{O_2} to O	-	(0.9)	-	0.23	0.23	-	0.92	-	4.3
	N_{O_2} total obsvd.	-	(2.2)	-	1.28	1.28	-	3.07	-	10.8
	% utilisation	-	(40)	-	24	24	-	24	-	25
	k_g theor.: cm/s	27	27	27	27	27	27	27	35	32
	N_{SO_2} theor. (b)	2.90	2.90	2.90	2.86	2.86	7.35	7.12	4.80	12.3
	Ratio: a/b	0.38	0.43	0.50	0.37	0.37	0.38	0.30	0.63	0.53
Final slow reaction	%S at change	-	0.084	-	0.20	0.16	0.25	0.25	0.17	0.30
	%O at change	-	(0.42)	-	(0.25)	(0.25)	-	0.37		(0.45)
	k_m(s): cm/s	-	0.0037	-	0.0013	0.0016	0.0028	0.0021	0.0045	0.0054

differences between observed and theoretical rates of oxygen absorption.

The total utilisation of oxygen during this period was generally smaller than with pure nickel under similar conditions. The slower diffusion of SO_2 in the gas boundary layer may account for the differences.

The fact that some of the gaseous oxygen arriving at the interface continued to dissolve indicates that the rate of absorption of oxygen was not much slower than that of the gas-forming reaction. Evidently there is a form of "competition" among the forward and backward rates of all the above reactions. The gas-forming reaction is not instantaneous (as often assumed in simple models) and the ratio $p^s_{SO_2}/p^s_{O_2}$ is probably smaller than the equilibrium ratio. If $p^s_{O_2}$ is higher than the equilibrium level, oxygen may dissolve more readily. This might explain the more rapid absorption of oxygen when the initial sulphur content was low (compare III with VI and VIII, Table 23) or the increase in the ratio N_{2O}/N_{SO_2} when the oxygen supply was larger:-

VI: 1740°, p_{O_2} = 0.008 atm., L=1, N_{2O}/N_{SO_2} = 0.23

VII: 1740°, 0.020 1, 0.43

IX: 1740°, 0.025 2.5 0.66

No "SO_2 boil" occurred because the contents of sulphur and oxygen were well below levels that would be in equilibrium with SO_2 at 1 atm. For the equation:

$$p^{eq}_{SO_2} = K\,[S]\,[O]^2$$

K is close to unity at 1500° (the free energy of solution of S was derived from the data of ref. 82). It can be shown that K will decrease with temperature unless the entropy of solution of S (as yet unknown) is more negative

than -9 cal/mol-^{o}K. The highest value of $[S][O]^2$ was only 0.064 (in Series IX) and $p^{eq}_{SO_2}$ must have been well below 1 atm. in all experiments.

When should the rate of diffusion of SO_2 become dependent upon the sulphur content? We can estimate that the equilibrium ratio:

$$(p_{SO_2}/p_{O_2})_s = 5000\,[S]\text{approx, at } 1500^{o}.$$

Data for the free energy of solution of sulphur at higher temperatures is lacking but the gas ratio probably remains high, so that $p^{s}_{SO_2}$ remains virtually constant and close to p_{O_2} for the inlet gas until the sulphur content is well below 0.01%.

(c) Kinetics at Low Sulphur Levels

The changes of slope in Fig.s 12a-d beginning between 0.3 and 0.1% must be caused by a change in the rate-controlling step (unless it could be shown that the factor of 5000 above falls to a value smaller than 10 at 1700-1800^{o}, which appears unlikely.

Figure 13 shows that the kinetics were close to first-order with respect to sulphur concentration. Slow transport of sulphur in the metal could not be the rate-controlling step since this should make the rate dependent solely upon the sulphur content irrespective of the other conditions (within a moderate temperature range) and all lines should have the same slope. The apparent values of $k_{m(s)}$, in the range 0.0013-0.0054 cm/sec are very low compared with $k_{m(O)} > 0.1$ cm/sec. These two facts indicate that some other step is rate-controlling.

As the sulphur content becomes depleted and the oxygen content increases, the concentration of adsorbed sulphur decreases steeply (by equation '3' in part 'a') and the

surface reaction (4) again becomes rate-controlling. When the oxygen supply is largerand the oxygen content higher, $[S]_{ads}$ is smaller (for a given sulphur content). The chemical reaction therefore becomes rate-controlling at a higher sulphur level.

It is difficult to reconcile the linear trends of the sets of points in Fig.13 with the different slopes of the lines. The oxygen supply was different for each series of experiments but remained constant during a given experiment. We would expect this to affect the chemical reaction only through the dissolved oxgyen content of the metal, yet that figure increased during the course of each test, and would be expected to change the slope of the line connecting $\log[S]$ with time. (See also p. 139)

If K_3 is the equilibrium constant for equation (3) above, substitution in the rate equation (5) gives:-

$$\frac{d[S]}{dt} = -\frac{ak'}{K_3}[S] \cdot \frac{[O]^4_{ads}}{[O]^2} \quad \ldots(6)$$

For simplicity, let $\frac{[O]^2_{ads}}{[O]} = f$

Now by analogy with the Langmuir isotherm for adsorption of gases, we may write for a solute:-

$$[O]_{ads} = \frac{q.\ b[O]}{1 + b[O]} \quad \text{mol./cm}^2$$

where $b = k_{ads}/k_{desorption}$ for dissolved oxygen,

q = number of moles to cover 1 cm^2 of surface.

Then $f = \left(\frac{qb}{1 + b[O]}\right)^2 . [O]$

If $b[O] \gg 1$, $f \propto 1/[O]$

If $b[O] \ll 1$, $f \propto [O]$

Between these extremes there may be a range where 'f' changes very little and from equation (6), $d[S]/dt \propto [S]$

The deviation of a few points to the right of the lines

at very low sulphur levels is consistent with this tentative explanation because the higher oxygen levels make 'f' and the reaction rate smaller. This does not, however, explain the steep slope for Series IX where the oxygen levels were highest.

Evidently the situation is more complex than this treatment assumes. The reactions proposed in part (a) represent only three ways of describing the highly dynamic relations among sulphur and oxygen atoms in dissolved, adsorbed and gaseous forms. Other equations could equally well be written, particularly those with activated species. Limitations such as the total area available for adsorption and so for the gas-forming reaction must also be considered.

In view of the variation of the rate of chemical reaction with the rate of oxygen supply, we may even consider that a form of 'mixed' kinetic control occurs, if the rate of supply of oxygen affects the balance of the various competing reactions described.

ADDENDUM to page 138:

The lines also had steeper slopes when the initial sulphur content was lower. (In Fig. 13, p. 51, compare line III: $[S]_i$ = 0.45% and lines VI & VIII: $[S]_i$ = 0.65%). Low initial sulphur contents are associated with faster absorption of oxygen (p. 136) and it appears that the high general oxygen level of Series III was the immediate cause of the higher rates of sulphur loss.

4. Decarburisation

(a) Linear-rate Oxidation.

Rate-control by slow gaseous diffusion has been confirmed by many workers (see Section II) and the straight lines in Figures 20 and 24 need little comment.

The theoretical fluxes were calculated assuming CO diffusing through O_2/He mixtures for gas compositions consistent with the observed figures for oxygen utilisation (Table 24). When the depleted "average bulk partial pressure" of oxygen is inserted in the general mass transfer equation (Section V, equation 1) the result can be expressed:-

$$\frac{-RT_f}{k_g} N^r_{\theta_2} = Ln\ (1 + p_{O_2}) + Ln(1 + j)$$

where p_{O_2} is the partial pressure of oxygen in the gas supply,

and $$j = 0.5\ N^r_{O_2} / (N_t - N^r_{O_2})$$

The second logarithmic term is small and varies only slowly as $N^r_{O_2}$ changes. The equation is solved by equating this term to zero at first and then using an iterative procedure.

The observed fluxes of CO appear to be in good agreement with the theoretical fluxes, except for those at the highest rates of oxygen supply. Baker and co-workers (23) found a similar anomaly and thought that the combustion of CO to CO_2 may have raised the film temperature and accelerated diffusion.

The diffusion of CO_2 is slower than that of CO. For the conditions of Ni:IV:-

$$D_{CO/He + O_2} = 5.0\ cm^2/s. \quad k_{g(CO)} = 39\ cm/s.$$

$$D_{CO_2/He + O_2} = 4.0\ cm^2/s. \quad k_{g(CO_2)} = 29\ cm/s.$$

Table 24: Oxidation of Metal/Carbon Alloy Drops

Comparison of Fluxes, etc. (Note: Fluxes are given as (mol/s) x 10^6)

	NICKEL					IRON		
No.	I	II	III	IV	V	I	II	III
p_{O_2} atm.	0.02	0.06	0.12	0.25	0.25	0.12	0.25	0.25
L Litres/min	2	2	2	2	4	2	2	4
10^2 x $d\underline{C}/dt$, %/S.	0.875	2.80	5.30	11.3	20.0	5.87	11.8	19.0
N_c^r (exptl.)	5.8	19.4	35.7	78	133	39	80	127
$D_{co/o_2 + He}$ $cm^2/s.$	6.7	6.35	5.8	5.0	5.0	5.8	5.0	5.0
k_g cm/s	39	39	39	37	45	38	36	45
N_{CO}^r (theor. i) p_{co}^b =zero	8.0	24.3	46.8	82.2	99.5	45.7	84.5	105
N_{co}^r (Theor.ii) p_{co}^b = av.	6.9	20.2	40.6	72.6	92.5	39.9	74.6	97
Flux ratio: exptl./theor ii	0.84	0.93	0.88	0.94	1.45	0.98	1.07	1.31
% Utilisation of O_2	21	24	22	23	20	24	24	19
% $\underline{C}$ at boil start	-	0.15	0.25	0.26	0.27	0.12	0.38	0.33
Apparent $K_{M(c)}$, cm/s.	-	0.022	0.025	0.052	0.089	0.060	0.038	0.071

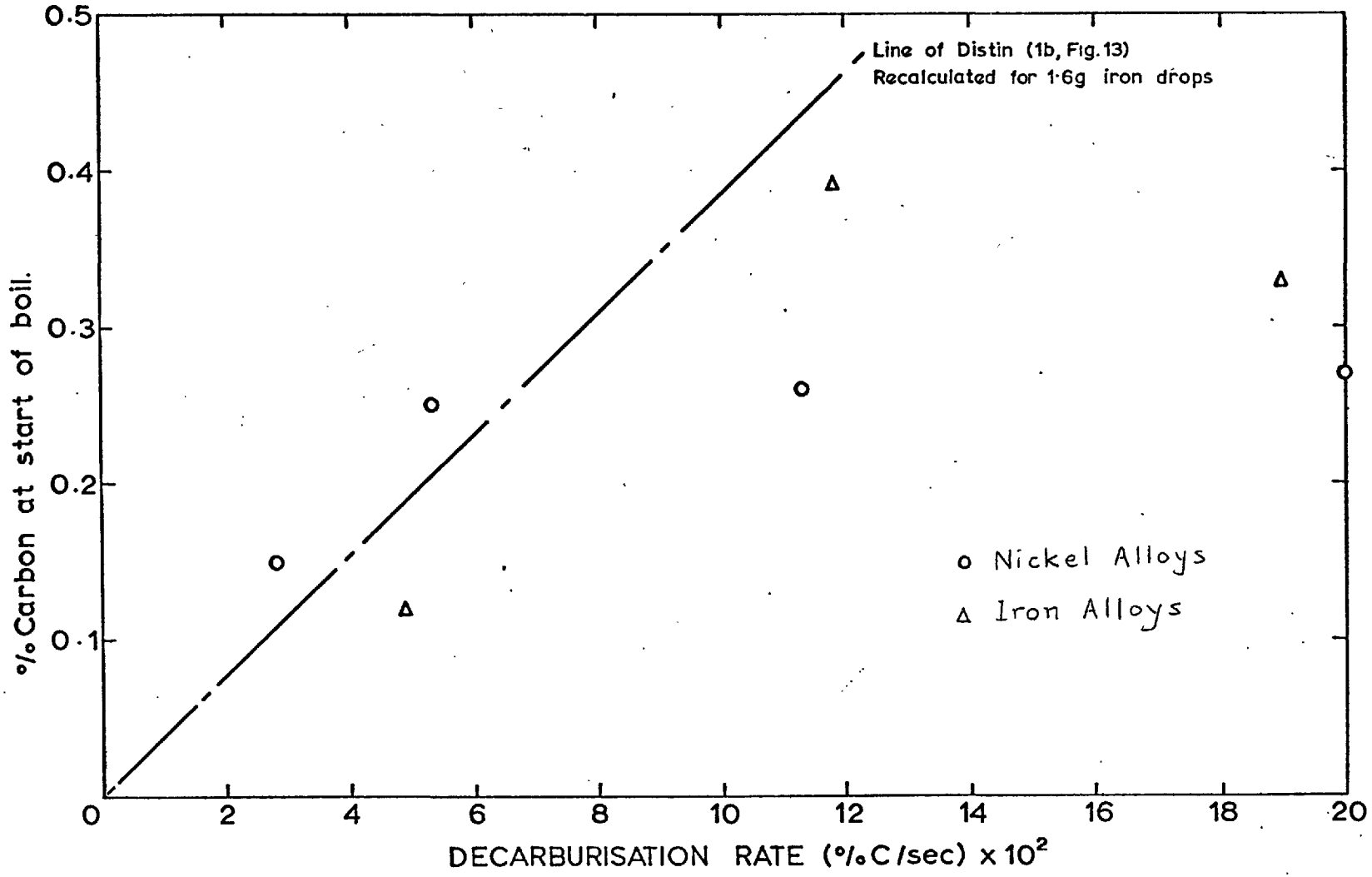

Fig. 37. Relation of %Carbon at CO boil to decarburisation rate.

Diffusion of the mixtures of CO and CO_2 might be slower than those calculated but it is not clear whether the same Boundary Layer Theory could be applied to conditions outside a flame front.

The proportion of oxygen utilised was about the same as in the desulphurisation experiments. The proportion of CO converted to CO_2 increased as the oxygen concentration in the gas increased, at constant gas velocity. Baker and co-workers (23), using 10% oxygen in helium, measured 0.33% CO_2 and 2.2% CO in their exit gases: a conversion of 13%. Their gases flowed at 5 litres/minute. The degree of conversion also decreased in the writer's experiments when the flow-rate was increased from 2 to 4 litres/minute and it appears that these data are not seriously at variance with Baker's. Distin, on the other hand, had a minimum CO/CO_2 ratio of 8 in pure oxygen, corresponding to 11% conversion. This conflicts with the writer's data, unless we suppose that the trend is reversed at some oxygen concentration between ·25 and 100%.

The proportions of CO_2 formed were consistently lower with iron than with nickel drops, but the lower metal temperature may have been a factor here. No flame front was seen in any experiment although it may have been inconspicuous because of fuming and the dilution by helium. The temperature of the metal may have affected the intensity of the oxidation of CO to CO_2 in the gas phase. It is also possible that CO_2 might be produced in addition to CO by reactions on the metal surface and that nickel favours this more strongly.

(b) Change in Rate-Controlling Step

The decarburisation curves show no clear evidence of a change in the rate. The occurrence of the boil and the

increase in the oxygen content at the same time, before all the carbon had been removed, suggests that the kinetic control of the reaction had changed.

The apparent values of a mass transfer coefficient $k_{m(C)}$ for ~~diffusion~~ transport in the metal phase were of the same order as those of Distin but were not constant. Figure 37 was plotted for comparison with Distin's diagram (1b:Fig.13). The data can be reconciled only if we suppose them to lie on curves for constant oxygen concentration whose slopes decrease as the decarburisation rates increase. Higher oxygen concentrations would then give curves of similar initial slope but with higher "plateaux".

We have shown that oxygen is transported very rapidly through the metal and a solute of similar atomic size is expected to diffuse at roughly the same rate, as Distin has argued. The total absence of oxide on the nickel drops and its delayed appearance on the iron drops do not accord with the model of carbon "starvation" at the drop surface. The hypothesis of kinetic control by the slow ~~diffusion~~ transport of carbon can therefore no longer be supported.

Consider instead the possibility of rate control by a surface chemical reaction. In contrast to sulphur, carbon is very weakly surface-active. Kozakevitch (45) reported that carbon depressed the surface tension of liquid iron only slightly. Halden and Kingery (46) could detect no effect at carbon levels up to 5%. Eremenko and Nizhenko (47) found that about 1%C in nickel lowered the surface tension from 1780 to 1700 dyn/cm. Stark and Filippov (cited by Semenchenko: 83) reported that carbon lowered the surface tension of iron from 1200 to 800 dyn/cm. but their alloys also contained up to 0.04% of oxygen.

Then in the reaction: $\underline{C}_{ads} + \underline{O} = \underline{C} + \underline{O}_{ads}$ ...(2) a

very small concentration of dissolved oxygen can drive the equilibrium strongly to the right. At the beginning of the reaction: $\underline{C}_{ads} + \underline{O}_{ads} = CO(g)$ ...(3) the absorption of an extremely small quantity of oxygen enables CO to be produced at the rate that is restricted only by slow ~~diffusion~~ transport away from the drop. A period of "initial slow reaction" is not observed because it is too short.

For the reaction (3) above, the rate equation is:-

$$d[C]/dt = -ak''[C]_{ads}[O]_{ads} \quad ...(4)$$

The specific rate k" must be much higher than k' for the SO_2 reaction because $[C]_{ads}$ is so small and $[O]_{ads}$ cannot exceed the value for complete surface coverage. The specific rate for oxygen absorption is the same as it was during desulphurisation and must be slow compared with that for the gas-forming reaction. We can now understand why so little oxygen is taken up by the metal during the period of linear-rate decarburisation.

When the carbon content is sufficiently depleted, the rate of the chemical reaction falls below the limiting rate of gaseous ~~diffusion~~ transport. Kinetic control of decarburisation at low carbon contents is therefore by a slow chemical reaction at the metal surface.

When the chemical reaction is slow enough to be rate-controlling, its rate is probably comparable with that for oxygen absorption. Less oxygen is being used to form CO, the element dissolves in the metal and conditions develop in which CO bubbles form within the liquid.

The surface area available for reaction (3) increases because of the distortion of the drops and the growth of the bubble surfaces. This helps to compensate for the low level of $[C]_{ads}$ and to increase the reaction rate again to that limited by gaseous ~~diffusion~~ transport. It is probably signif-

icant that the oxygen content does not rise sharply until the boil is finished since most of that available is still used to form CO.

(c) The "CO Boil"

The uncertainty in identifying the moment when a boil begins is small compared with the variations of several seconds recorded in Tables 12 and 13. The scatter of points for carbon content about the straight lines was also small and there was little change in decarburisation rate from one experiment to the next. We must conclude that there is no single "critical carbon content" at which the boil begins under a given set of conditions and also that the beginning is sensitive to unrecorded variations in the experimental conditions.

The matter of oxygen contents unfortunately remains in some doubt. From the data in Table 17 the following averages and estimates of error have been deduced:-

Table 25: Summary of Data on Oxygen "Blank" in Metal/Carbon Alloys

Seconds in O_2/He	Cast in levn. vessel (Cu cup)		Cast in argon filled-column
	Cast while O_2/He still flowing	Cast after 5 sec. in pur-He.	
0 - 6	Ni 0.000 Fe 0.006 $\pm$ .006	Ni 0.000	Ni 0.028 Fe 0.042 $\pm$ .010
14-17.5	Ni 0.010 $\pm$ .002 Fe 0.031 $\pm$ .005	Ni 0.005 + .008 - .005	Ni 0.030 $\pm$ .008 Fe 0.042 $\pm$.-2

The middle column might not represent the true conditions at the end of a reaction since O could continue to combine with C during the 5 sec. in He. Deducting figures in the first column from those in the third gives the following values:

Time (sec.)	Estd. oxygen pick-up, %		Estd. orig. %O
0 - 6	Ni	0.028	0.00
	Fe	0.036	0.006 ?
14-17.5	Ni	0.020	0.01
	Fe	0.010	0.03

In general, samples with less about 0.01% O gained about 0.03% when cast in the argon column; those already containing 0.02 - 0.03% gained less.

The original oxygen contents were lower than Distin's figure of 0.08% for iron but the difference may be due to the dilution of the O_2 by He in the writer's work. Again the oxygen content just before the boil was almost constant at all decarburisation rates for each metal.

The supersaturation of CO at the start of the boil can be estimated from the following expressions:-

Ni (about 2200°K): $p_{CO} = 5400\ [C][O]$ (ref. 86)

Fe (about 2100°K): $p_{CO} = 400\ [C]\ [O]$ (ref. 12)

Table 26: Estimates of CO supersaturation

	p_{O_2} atm.	L l/min	%C at boil	% O exptl.	p_{CO}	% O estd.	p_{CO}
Nickel	0.06	2	0.15	0.04	32	0.01	8
	0.12	2	0.25	0.035	47	0.01	14
	0.25	2	0.26	0.035	49	0.01	14
	0.25	4	0.27	0.035	51	0.01	15
Iron	0.12	2	0.12	0.05	2.4	0.03	1.5
	0.25	2	0.38	0.05	7.6	0.03	4.5
	0.25	4	0.33	0.055	7.3	0.03	3.9

From these data it appears that boiling can begin at quite low supersaturation levels of CO. The variations in the carbon level at the time of the boil, discussed in part (a) above, mean that there is no single 'critical supersaturation pressure', even under a given set of

experimental conditions.

The contrast between the uniform increase and decrease of boiling action in nickel drops and the short bursts of agitation seen in iron drops cannot easily be explained. It might be connected with the slightly lower purity of the iron powder but it is also possible that the low supersaturations of CO take time to "build up" again after each burst.

The most interesting feature of the boil in both metals was the succession of "bright spots". Robertson (87) has also observed these. Several tentative explanations can be offered:-

(i) The hollow curved surface exposed as a bubble bursts has an enhanced emissivity. This could only occur in the extremely short time that the first break occurs, so that the inside of a hollow sphere is viewed through a small aperture. An exposed curved surface has the same emissivity as a plane of the same apparent area which is perpendicular to the line of sight and should not appear brighter.

(ii) Metal oxides form transiently and redissolve. Experiments to oxidise liquid Ni in the absence of C were not successful and it is unlikely that oxide could form, even locally, when vigorous oxidation of carbon is proceeding. It is important to notice that "bright spots" also appeared in the film of the nickel-oxygen drop reduced in hydrogen (Fig. 16).

(iii) The heat evolved during the surface reaction causes local overheating which is not dispersed immediately Thermal diffusion and convection should immediately begin to 'blur' the edges of the hot zones and the persistence of fairly well-defined shapes would not be expected.

(iv) The reaction between adsorbed atoms gives rise to radiation of visible wavelengths, i.e. chemiluminescence. This is a highly speculative explanation and the literature mentions no precedents for liquid metals.

By elimination, only (iii) and (iv) are tenable. Both explanations support the hypothesis of surface chemical reaction, which we may imagine to proceed at the surface of new bubbles, as well as at the free surface of the drop. The effects become visible as soon as the bubble bursts and

are not immediately dispersed. Undoubtedly the same reaction also occurs on the outer surface of the drop but it is more diffuse and not distinguishable from the normal radiation.

(d) Initiation of the Boil

The research has not resolved the theoretical difficulty that is inherent in forming bubble nuclei of critical size. The data have shown that quite small supersaturations of CO can initiate boiling under conditions believed to be homogeneous.

Distin considered that iron oxide might assist nucleation. Kaplan and Philbrook (85a) also suggested this but later made calculations which showed that an iron/iron oxide interface could not serve as a nucleation site (85b). Certainly the present work has proved that bubbles can form in the absence of metal oxides and there was no evidence to link the "slag spots" with the boil. We might also mention that drops of iron and nickel could be supercooled in a hydrogen stream by 100° or more, demonstrating that no solid nuclei were present.

Kaplan and Philbrook (85b) suggested that "cavities swept into the levitated droplet from the surface serve as nuclei for bubble formation ". Robertson (87), had earlier worked out a similar idea in some detail, proposing that interfacial /turbulence caused by local changes in surface tension could set up vortices in the liquid. The low or even negative pressure at the centre of a vortex would then assist a bubble nucleus to reach critical size. No visual evidence to support this was seen in the high speed films except perhaps for the ripples just before boiling began and the small shapes resembling eddies shown in Figures 26:b, and 22:d.

The demonstrated importance of the surface activity of

oxygen suggests that the decrease in surface tension when the oxygen content begins to rise might assist bubble formation or even set up eddies and vortices. Against this, the addition of sulphur which kept the surface tension low throughout the decarburisation reaction had no marked effect on the time of boil.

The problem will probably be solved only by attention to the detailed structure and atomic bonding at the surface of very small bubbles and to the equilibria and kinetics of activated species in the various competing reactions.

(e) Other work on Chemical Rate-Control

Swisher and Turkdogan (32) found evidence of reaction rate control by a surface chemical reaction at carbon contents below 1%. They proposed that the slow dissociation of their oxidant, CO_2 in the presence of adsorbed oxygen on the metal surface could account for the observed changes in rate.

It has been shown above that low carbon levels can themselves cause low reaction rates when oxygen is the oxidant. It is perhaps not necessary to postulate a lsow dissociation step for CO_2. Swisher and Turkdogan related the dissociation rate and hence the oxidation rate to $(1-\theta_0)$, the fraction of the surface not occupied by adsorbed oxygen atoms. But $(1-\theta_0) = \theta_C$ approx. and the rate could equally well be related to the carbon content.

In spite of the chemical control of kinetics, the rate was still affected by the concentration of CO_2 in the gas stream and the authors were able to write rate equations that included p_{CO} as well as $(1-\theta_0)$. Possibly a process of this sort is responsible for the seeming "mixed control" of the last stages of desulphurisation.

Ghosh and Sen (88) have argued that all decarburisation

is chemically controlled. Their highest carbon concentration was only 1.1% and they may well have detected some of the effects just described but they rejected gaseous diffusion control solely on the grounds that the effective boundary layer of 3.5 mm was unrealistic in a gas velocity of 133 cm/s. But this velocity applied only to the stream confined in the supply jet, 10 cm. from the surface. For the writer's drops where the gas velocities were usually above 50 cm/s. in contact with the drop, typical values of D/k_g are 2 mm.

(f) Effect of Sulphur.

The linear rate of carbon oxidation was slightly lower when sulphur was present and there was a small change of slope 5-7 seconds after the reaction began. In about the same short period there was a slight loss of sulphur. Thereafter, no sulphur was oxidised from the nickel drops until the time of the boil when sulphur began to be rapidly removed before all of the carbon had been oxidised. In the iron drops there was no loss of sulphur after the 7 seconds mark. The decarburisation rate for iron slowed down abruptly at the time of the CO boil and then proceeded very slowly in spite of the rapidly-rising oxygen content.

Evidently there was a complex balance among the rates of the chemical reactions that have been discussed in connection with the desulphurising and decarburising experiments. We have argued that the specific rate for carbon oxidation in nickel is must higher than that for sulphur oxidation, which is in turn only a little higher than the specific rate for the solution of oxygen. The succesion of events described above could then be explained as follows:

(i) Initially the metal surface is occupied by adsorbed sulphur and a little carbon; no oxygen is present.

Sulphur "competes" with added oxygen for surface sites, so that the concentration of $\underline{O}_{ads}$ does not rise as rapidly as it does when only $\underline{C}_{ads}$ is present.

(ii) While the concentration of $\underline{O}_{ads}$ is low, the rate of oxidation of carbon is restricted and the oxidation of sulphur can proceed at a detectable but diminishing rate.

(iii) When the oxygen level is higher the rate of carbon oxidation becomes limited by the gaseous diffusion of CO and all the oxygen diffusing counter to this flux is used in forming CO.

(iv) When the carbon content is low, decarburisation becomes slow and oxygen becomes available to oxidise sulphur and to dissolve in the metal. Perhaps also the sulphur, by occupying part of the surface, further diminishes $[C]_{ads}$ and retards carbon oxidation.

Kozakevitch (45) reported that the effect of sulphur upon the surface tension of iron was greater when carbon was present because carbon raised the activity coefficient of the sulphur. This would make sulphur atoms more strongly adsorbed and increase the probability that they would react with oxygen.

The delay in forming oxide when Fe/S alloy drops were oxidised was probably due to the presence of small amounts of carbon in the iron powder. Evidently the specific rate for forming iron oxide is much greater than that for oxidising the sulphur and all the oxygen is used for oxidising the iron instead of the sulphur. The same effect was seen at the end of the reactions with Fe/C/S drops.

The "frothing" of the Ni/C/S drops and their spectacular expansion during boiling can only be due to the lowering of surface tension by the added sulphur.

The less spectacular performance of the Fe/C/S drops was consistent with the behaviour of the Fe/C drops but again cannot be explained, unless here again the low supersaturations of CO are responsible.

VII. CONCLUSIONS

1. The mass transfer coefficient for oxygen in levitated drops of liquid iron and nickel is at least 0.1 cm./s. and may be greater than 0.2 cm./s. Heterogeneous reactions involving dissolved oxygen are therefore very unlikely to be kinetically controlled by the slow transport of this solute in the metal. It has also been shown that the rates of oxidation of sulphur and carbon dissolved in iron or nickel drops are not controlled at any stage by slow transport in the liquid metal.

2. The gaseous products of heterogeneous reactions are formed by the chemical combination of atoms adsorbed on the surface of the liquid metal. The surface activities of the solutes are of particular importance in the kinetics of these reactions.

3. During the oxidation of sulphur from nickel-sulphur alloy drops, the rate-controlling step of the reaction changed twice:-

(a) Initially the chemical reaction between adsorbed atoms of sulphur and oxygen was slow because of the low concentration of adsorbed oxygen.

(b) When the concentrations of dissolved and adsorbed oxygen and hence the chemical reaction rate increased, the slow diffusion of SO_2 through the gaseous boundary layer became rate-controlling.

(c) When the sulphur content was about 0.3% the chemical reaction on the surface again became rate-controlling, this time because of the low concentration of adsorbed sulphur.

4. The specific rates of forming SO_2 and of dissolving oxygen with nickel-sulphur drops are similar. Oxygen continues to dissolve in the metal while SO_2 is being produced at the rate that is limited by slow gaseous diffusion.

5. Because carbon is very weakly adsorbed on liquid iron and nickel there is very little competition for the adsorption of oxygen atoms. A surface concentration sufficient to cause a rapid reaction is quickly reached at the beginning of decarburisation. The period of initial kinetic control by a slow chemical reaction is therefore too brief to be observed and the familiar process of carbon oxidation controlled by slow gaseous diffusion begins.

6. The specific rate of the CO reaction is much higher than that of the SO_2 reaction and of oxygen absorption, with the result that little or no oxygen is taken up by the metals while the decarburisation rate is controlled by the gaseous diffusion step.

7. At carbon levels below about 0.4%, the reaction is controlled by a slow surface chemical step because the concentration of adsorbed carbon is low. The evidence does not support earlier suggestions that the slow transport of carbon in the metal is rate-controlling.

8. When the surface chemical step begins to control the rate of carbon oxidation, gaseous oxygen becomes available to dissolve in the metal. The estimated supersaturation

of CO that occurred in these experiments at the start of the "boil" was below 10 atm. for iron-carbon drops and was probably below 20 atm. for nickel-carbon drops. High supersaturations of CO are therefore not believed to be necessary to initiate bubble formation.

9. No metal oxide appeared at any time during the oxidation of nickel-carbon drops. With iron-carbon drops the oxide appeared at least a second after the "CO boil" had begun. Oxides cannot therefore be responsible for nucleating CO bubbles.

10. Bright spots of light seen in high-speed films of "boil" reactions when CO bubbles burst are believed to constitute direct evidence of the vigorous chemical reaction at the metal/gas interface. Their precise cause is not clear: local emission of heat and chemiluminescence have been suggested.

11. Little sulphur is oxidised from nickel-carbon-sulphur drops until the time of the CO boil. With iron-sulphur and iron-carbon-sulphur drops, iron is oxidised in preference to the sulphur. The effects can be explained by the relative kinetics of reactions among oxygen, carbon and sulphur.

12. Experiments on the rates of transport of naphthalene vapour from solid spheres showed that the empirical mass transfer equation of Steinberger and Treybal does not accurately predict rates under all conditions of gas flow. Dilution of oxygen with helium also leads to inaccurate predictions for reaction rates with metal drops. It may be necessary to include other dimensions with or in place of 'n' in the "forced convection" term.

REFERENCES

1. (a) P.A. Distin, : Ph.D. Thesis, Univ. of London, 1967.
   (b) P.A. Distin, G.D. Hallet, F.D. Richardson, : J. Iron Steel Inst., 206, 1968, 821- 33.
2. (a) G.W. Toop, : Ph.D. Thesis, Univ. of London, 1963.
   (b) G.W. Toop, F.D. Richardson, : in "Advances in Extraction Metallurgy" (Inst. Min. Met., London 1968), 181.
3. W.A. Peifer, : J. Metals, 17 (1965) 487-494.
4. (a) C.G. Glen, : M. Phil. Thesis, Univ. of London, 1969.
   (b) C.G. Glen, F.D. Richardson, : in "Heterogeneous Kinetics at Elevated Temperatures" (Plenum Press, New York, 1970) 369-390.
5. A. Forster, : M.Phil. Thesis, Univ. of London, 1968.
6. G.D. Hallett, : M.Sc. Thesis, Univ. of London, 1964.
7. F.D. Richardson, W.E. Dennis, : Trans. Faraday Soc. 49 (1953) 171-9.
8. A. Rist, J. Chipman, : "Physical Chemistry of Steelmaking", (MIT/Wiley, New York, 1958), 3-12.
9. S. Ban-ya, S. Matoba, : "Physical Chemistry of Process Metallurgy", I (Interscience, New York, 1961) 373-402.
10. S. Marshall, J. Chipman, : Trans. A.S.M. 30 (1942) 695-741.
11. E.T. Turkdogan et al, : J. Iron Steel Inst., 181 (1955) 123-8.
12. T. Fuwa, J. Chipman, : Trans. AIME, 218 (1960) 887-891.
13. P. Wallet, : Iron & Steel, Oct. 1955, 463-7.
14. L.S. Darken, R.W. Gurry, : "Physical Chemistry of Metals" (McGraw-Hill, New York, 1953)
15. B.M. Larsen, L.O. Sordahl, : "Physical Chemistry of Process Metallurgy", II (Interscience, New York, 1961), 1141-77.

16. L. von Bogdandy, : (a) Arch. Eisenhüttenwes, 29 (1958) 329-337.
(b) "The Chipman Conference" (MIT Press, Boston, Mass., 1965) 156-165.

17. F.D. Richardson, : Iron & Coal Tr. Rvw., 24 Nov. 1961, 1105-1115.

18. N.A. Parlee, S.R. Seagle, R. Schumann, : Trans. AIME 212 1958, 132-8.

19. K. Niwa et al, : "Physical Chemistry of Process Metallurgy, II (Interscience, New York, 1961), 689-703.

20. W.D. Jamieson, C.R. Masson, : J. Am. Chem. Soc., 82 (1962), 4084.

21. L.A. Baker, N.A. Warner, A.E. Jenkins, : Trans. AIME, 230 (1964), 1228-1235.

22. L.A. Baker, R.G. Ward, : J. Iron Steel Inst. 205 (1967) 714-7.

23. L.A. Baker, N.A. Warner, A.E. Jenkins, : Trans. AIME, 239 (1967) 857-864.

24. L.A. Baker, : Can. Met. Quarterly, 7 (1968) 217-220.

25. A.E. Hamielec, W-K. Lu, A. McLean, : (a) ibid., 7 27-33.
(b) ibid., 7 220-221.

26. T. Fujii, T. Araki, : Tetsu-to-Hagané Overseas, 5 (1965) 290-302.

27. S.G. Whiteway et al, : Can. Met. Quarterly, 7 (1968), 211-215.

28. T. Fuwa, S. Matoba, : "Studies in Metallurgy for S. Matoba", (Tohoku Univ. 1969), 57-65.

29. K. Ito, K. Sano, : Trans ISI Japan, 8 (1968) 165-71.

30. K. Ito, K. Sano, : ibid. 9 (1969) 465-71.

31. K. Goto, M. Kawakami, M. Someno, : Trans. AIME, 245 (1969) 293-301.

32. J.H. Swisher, E.T. Turkdogan, : Trans. AIME, 239 (1967) 602-610.

33. R.G. Ward, : "An Introduction to the Physical Chemistry of Steelmaking" (Arnold, London, 1962).

34. A.V. Bradshaw, : "Le Vide", Nov/Dec. 1968, 376-415.

35. J.W. Cahn, J.E. Hilliard, : J. Chem. Phys., 31 (1959), 688.

36. A.E. Jenkins, B. Harris, L.A. Baker, : in "Metallurgy at High Pressures and High Temperatures", (Gordon & Breach, New York, 1964).

37. M.N. Dastur, N.A. Gokcen, : Trans. AIME, 185 (1949) 665.

38. A. Sieverts, : Z. phys. Chem., 77 (1911) 611.

39. D.R. Young, : Ph.D. Thesis, Univ. of London, 1965.

40. P.B. Brown, C.B. Alcock, : Metal Sci. J., 3 (1969), 116-120.

41. (a) C.E.A. Shanahan, : in "Determination of Gases in Metals", (Iron Steel Inst., Special Rpt. No. 68, London 1960) 75-92.

(b) C.E.A. Shanahan, : F. Cooke, : J. Iron Steel Inst., 188 (1958) 138-142

42. C.B. Alcock, L.L. Cheng, : J. Iron Steel Inst., 195 (1960) 169-173.

43. G. Ranque, : Rev. Mét., 39 (1942). 362.

44. C. Bodsworth, : "Phys. Chem. of Iron & Steel Manufacture" (Longmans, London, 1963), 381.

45. P. Kozakevitch, : Soc. Chem. Ind. Monograph No. 28 (1968), 223-245.

46. F.A. Halden, W.D. Kingery, : J. Phys. Chem. 59 (1955), 557-9.

47. V.N. Eremenko, V.I. Nizhenko, : Ukr. Khim. Zhurn. 26 (1960) 423-8.

48. R.J.W. Peters, C.R. Masson, S.G. Whiteway, : Trans. Faraday Soc. 61 (1965), 1745-53.

49. J.E. Bowers, : J. Inst. Met. 90 (1961) 321.

50. M. Hansen, K. Anderko, : "Constitution of Binary Alloys" 2nd edn. (McGraw-Hill, New York, 1958).

51. R.L. Steinberger, R.E. Treybal, : A.I.Ch. E. Jnl. 6 (1960), 227-232.

52. A. Acrivos, : ibid 4 (1958), 285-9.
53. - : "Handbook of Chemistry & Physics", 45th edn., (Chemical Rubber Co., Cleveland 1964), C 650.

54. A.P. Colburn, : Tr. Am. Inst. Chem. Engrs., 29 (1933), 174.

55. W.G. Mathers, A.J. Madden, E.L. Piret, : Ind. Eng. Chem., 49 (1957), 961-8, (citing E. Mack, 1925).

56. J.O. Hirschfelder, C.F. Curtiss, R.B. Bird, : "Molecular Theory of Gases & Liquids" (Wiley, New York, 1954).

57. R.C. Reid, T.K. Sherwood, : "Properties of Gases & Liquids" (McGraw-Hill, New York) (a) 1st edn., 1958 (b) 2nd. edn., 1966.

58. C.R. Wilke, C.Y. Lee, : (a) Ind. Eng. Chem. 47 (1955), 1253-7.
(b) cited in Ref. 57b : 530.

59. J.O. Hirschfelder, R.B. Bird, E. Spotz, : J. Chem. Phys., 16 (1948) 968.

60. J. Hilsenrath et al, : "The Thermal Properties of Gases" (Nat. Bureau Standards, Circ. No. 564, Washington, 1955).

61. J. Hilsenrath, Y.S. Touloukian, : Trans. Am. Soc. Mech. Engrs., 76 (1954), 967-983.

62. R.B. Bird, W.E. Stewart, E.N. Lightfoot, : "Transport Phenomena" (Wiley, New York, 1960).

63. A.D. Kirshenbaum, J.A. Cahill, : Trans. A.S.M., 56 (1963), 281.

64. S.Y. Shiraisi, R.G. Ward, : Can. Met. Quarterly, 3 (1964), 118.

65. G. Urbain, L.D. Lucas, : in "Phys. Chem. of Metallic Solutions and Intermetallic Compounds" II (NPL, London 1959) 4E.2-4E.10.

66. A.V. Grosse, A.D. Kirshenbaum, : J. Inorg. Nuclear Chem., 25 (1963), 331-4.

67. R.D. Ingebo, : Chem. Eng. Progress, 48 (1952), 403.

68. H.A. Wriedt, J. Chipman, : Trans. AIME, 206 (1956), 1195-9.

69. L.E. Scriven, C.V. Sternling, : Nature, 187 (1960) 186-8.

70. T.K. Sherwood, J.C. Wei, : Ind. Eng. Chem., 49 (1957), 1030-4.

71. W.J. Thomas, E.M. Nicholl, : Trans. Inst. Chem. Engrs., 47 (1969), T 325-331.

72. J.K. Brimacombe, : Ph.D. Thesis, Univ. of London, 1970.

73. W.A. Fischer, W. Ackermann, : Arch. Eisenhüttenwes, 37 (1966), 43-7.

74. E.S. Tankins, N.A. Gokcen, G.R. Belton, : Trans. AIME, 230 (1964) 820-7.

75. V.V. Averin, A.Y. Polyakov, A.M. Samarin, : Izv. Akad. Nauk SSSR (Tekhn.) (1957) No.8, 120.

76. J.F. Elliott, M. Gleiser, V. Ramakrishna, : "Thermochemistry for Steelmaking", II (Addison-Wesley, Reading, Mass., 1963), 515.

77. V.K. Semenchenko, : "Surface Phenomena in Metals and Alloys" (trans. N.G. Anderson) (Pergamon, London, 1961), 249.

78. E.T. Turkdogan, P. Grieveson, L.S. Darken, : J. Phys. Chem. 67,II (1963) 1647-54.

79. E.T. Turkdogan, : Trans. AIME 230 (1964), 740-753.

80. C.M. Diaz, F.D. Richardson, : Trans. Inst. Min. Met. 76 (1967) C 196-203.

81. F.D. Richardson, : Jernkontorets Ann., 153 (1969), 367.

82. C.B. Alcock, F.D. Richardson, : Acta. Met., 6 (1958) 385-395.

83. R.L. Harvey, : Imperial College, Univ. of London : Private communication, 1971.

84. W.A. Fischer, W. Ackermann, : Arch. Eisenhüttenwes, 37 (1966) 779-781.

85. R.S. Kaplan, W.O. Philbrook, : (a) Trans. AIME 245 (1969) 2195-2204.
(b) Paper read at AIME Annual Meeting, Feb 1970 (Abstract in J. Metals. Dec. 1969)

86. A.M. Samarin, : Jernkontorets Ann. 151 (1967) 181-196.

87. D.G.C. Robertson, : Ph.D. Thesis, Univ. of New South Wales, 1968.

88. D.N. Ghosh, P.K. Sen, : J. Iron Steel Inst. 208 (1970) 911-916.

Appendix 1: Nomenclature in Mass Transfer Calculations

General:

a	Area of reaction interface, cm^2
C_p	Specific heat at constant pressure, cal/g. - K^o
d	Diameter of liquid drop (assumed spherical), cm.
D_{AB}	Diffusivity in a binary mixture of A and B, cm^2/s.
g	Gravitational constant, 980.7 cm/sec^2
k	Thermal conductivity, cal/cm.s. ^oK
k_g, k_m	~~Diffusion~~ Mass transfer coefficient, in the gas or metal phase, cm/s.
Ln	Natural logarithm
M	Molecular weight
n_A	Number of moles of A.
N_A	Total flux of A, mol/s.
N''_A	Flux of A per unit area, mol/cm^2 - s.
N_t	Total flux of all gaseous species entering reaction vessel, mol/s.
P	Total pressure in the system, (assumed to be 1 atm in levitation experiments).
p_A	Partial pressure of A, (atm).
R	Gas constant, 82.06 cm^3. atm/mol.^oK
T	Temperature, ^oK
T_f	"Film temperature" = $(T_m + 298)/2$, ^oK
u	Velocity of gas stream, cm/s.
V	Volume, cm^3.
W	Weight of metal drop, g.
x_A	Mole fraction of A
δ	Effective thickness of boundary layer, cm.
η	Viscosity, g/cm.s.
ρ	Density, g/cm^3

Superscripts:

b	Bulk phase, remote from reaction interface
s	at reaction interface
r	used in or produced by the chemical reaction

(to distinguish a flux from that of the same species supplied to the reaction vessel).

Subscripts:

f "film" properties, estimated for T_f.

g Gas phase

m Metal phase

NP Naphthalene

Dimensionless Quantities:

Gr_H Grashof Number for heat transfer = $\frac{gd^3\rho_f^2}{\eta^2_f} \cdot \frac{T_m - 298}{T_f}$

Gr_M Grashof Number for mass transfer = $\frac{gd^3}{\eta^2_f} \cdot \rho_f (\rho^t - \rho^s)$

where ρ^s = density of gas at metal temperature.

$\overline{Gr}$ Compound Grashof Number = $Gr_M + (Sc/Pr)^{\frac{1}{2}} . Gr_H$

Pr Prandtl Number = $(C_p \eta / k)_f$

Re Reynolds No. = $\rho ud/\eta_f$

Sc Schmidt Number = $(\eta / \rho D_{AB})_f$

Sh Sherwood Number = $k_g d/D_{AB,f}$

(sometimes referred to as the Nusselt Number for mass transfer and written $Nu_{D,AB}$

Appendix 2: Sources of Transport Property Data, etc.

(a) Properties of Gases. (In a reference such as 56:533, the number after the colon refers to the page number).

Property	Single Species	Binary mixtures	Multicomponent mixtures
Viscosity, η	59, 60	56:533 57b:421	56: 533
Thermal condy. k	60, 61	57b:486	
Spec. heat. C_p	60 (He: 5R/2M)	(Weighted Arith. mean as an approx: k is not sensitive to errors in the Sh_n term).	
Density, ρ	60	$\rho = M/RT$ (for 1 atm). where M= weighted mean mol. wt.	
Prandtl No. Pr	60,61	Calc. from $Pr=Cp\,\eta/k$	
Diffusivity D_{AB}	-	56:539 57b:543 57b:523	

Lennard-Jones potential parameters:

σ,A	57b:632	Arith. mean	-
$\varepsilon/\kappa = T^*$	57b:632	Geometric mean	-

Collision integrals:

$\Omega_{1,1}$ (for D_{AB})	-	56:1126	-
$\Omega_{2,2}$ (for η)	-	56:1126	-

Notes:

1. For many problems concerning binary mixtures, one component (usually the reactant) was in large excess and the single-component values of η, k, C_p and ρ were used.

2. D_{AB} for binary mixtures has the virtually same value for all proportions (56). Values for multi-component mixtures were calculated for the proportions of each mixture.

(b) Density of Liquid Metals:

Nickel:

Cahill & Kirshenbaum (63); Shiraisi & Ward (64)

Iron:

Urbain, Lucas (65) - expression for specific volume.

Grosse, Kirshenbaum (66)

The two curves cross at about 1560^{o} but diverge by as much as 0.13 at 1800^{o}. This error is however not very significant in the calculations of "d" (for estimates of k_g); a mean value was used.

Appendix 3 Partial Pressure of a Product from a Flat Reaction Interface: Effect on Diffusion Rate

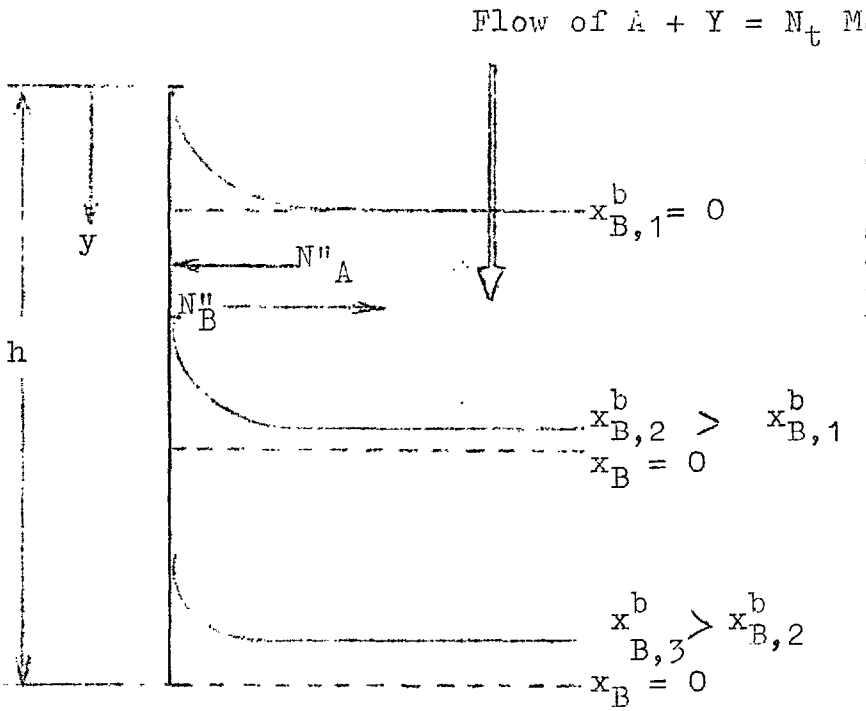

Consider a gas mixture of a reactive component A and a non-reactive component Y flowing across a reaction interface of length h and width w; the reaction product is B. Assume equi-molar counter-diffusion of A and B.

Under steady-state conditions:-

x^s_A and x^s_B, the mole fractions of the two components at the interface, are constant,

x^b_B and N''_B vary with y but not with time,

$p_i = Px_i$ atm. (where i represents any component)

At any distance 'y' from the leading edge:-

Flux of B per unit area: $$N''_{B,y} = \frac{-k_g}{RT}(p^b_B - p^s_B)$$

$$= \frac{Pk_g}{RT}(x^s_B - x^b_B)$$

For simplicity, write $Z = Pk_g/RT$

At a slightly greater distance $(y + \delta y)$:

$$x^b_{B,y+\delta y} = x^b_{B,y} + \frac{N''_{B,y} \cdot w.\delta y}{N_t + N^r_A + N^r_B}$$

where N_A^r is the rate of removal of A (mol/sec) from the gas between y=0 and $(y + \delta y)$, etc.

But $N_A^r = -N_B^r$ and

$$x^b_{B,y+\delta y} - x^b_{B,y} = \delta x^b_B$$

Therefore $$\delta x^b_B = \frac{N''_{B,y}}{Nt} w.\ \delta y$$

Therefore $$\frac{\delta x^b_B}{y} = w \frac{N''_{B,y}}{N_t} \qquad ...(1)$$

Also between y and $(y + \delta y)$:-

$$\delta N''_{B,y} = Z(x^s_B - x^b_{B,y+\delta y}) - Z(x^s_B - x^b_{B.y})$$

$$= Z\ (x^b_{B,y} - x^b_{B,y} + \delta y)$$

$$= -Z.\ \delta x^b_B$$

Then, $$\frac{\delta N''_{B,y}}{\delta x^b_B} = -Z \qquad ...(2)$$

Combining (1) and (2):-

$$\frac{\delta N''_{B,y}}{\delta y} = -Zw\frac{N''_B}{N_t}$$

$$\int \frac{dN''_{B,y}}{N''_B} = \frac{-Zw}{N_t}\int dy + c$$

* At $y = 0$, $N''_{B,y} = N''_{B,\max}$; Then $c = \mathrm{Ln}N''_{B,\max}$

$$\mathrm{Ln}\left(\frac{N''_{B,y}}{N''_{B,\max}}\right) = \frac{-Zw}{N_t}.y$$

$$N''_{B,y} = N''_{B,\max}\exp\left(\frac{-Zwy}{N_t}\right)$$

Then the total flux of B from the interface,

$$N_{B,\text{total}} = \int_0^h N''_{B,y}\, w\, dy$$

$$= -wN''_{B\max}\frac{Nt}{Zw}\left[\exp\left(\frac{-Zwy}{N_t}\right)\right]_0^h$$

* $\mathrm{Ln}\ N''_{B,y} = -\frac{Zw}{N_t}.y + c$

$$= N''_{B,\,max} \cdot \frac{N_t}{Z} \left[\exp\left(\frac{-aZ}{N_t}\right) - 1 \right]$$

But $N''_{B,max}$ = flux at y=0, where $x_B^b = 0$

$$= Z x_B^s$$

Then $N_{B,\,total} = -N_t \, x_B^s \left[\exp\left(\frac{-aZ}{N_t}\right) - 1 \right]$

Appendix 4: The Activity and Free Energy of Solution of Oxygen in Liquid Nickel

The following expressions for free energy of solution have been proposed in recent years:-

Authors	Ref.	ΔG°(cal/g.-atom)	Exptl. temp range, $^{\circ}C$
Averin et al	75	-18064 + 1.03 T	1475- 1630
Bowers	49	-19000+ 1.49 T	1453 -1697
Tankins et al.	74	- 11920 - 2.28 T	1550
Fisher, Ackermann	73	- 25270 + 3.93 T	1460-1700

The values of the free energy agree well at 1825$^{\circ}K$ but diverge at higher temperatures:-

Authors	ΔG°_{1825}	ΔG°_{2000}
Averin et al.	-16185	-16000
Bowers	-16280	-16020
Tankins et al.	-16080	-16480
Fischer, Ackermann	-16090	-15410

Tankins et al made their equilibrium measurements at one temperature only and with oxygen contents up to 0.3%. Deducing that the oxygen activity followed Henry's Law, they also calculated the saturation contents of oxygen in nickel for various temperatures. Bowers measured saturation contents directly and obtained consistently higher values. This suggests that there is a negative deviation from Henry's Law; from the differences we can calculate that:

$\log f_o = -0.18\ [O]_{Ni}$ approximately.

Bowers measured equilibria over a range of temperatures and oxygen contents (0 - 1.0 %) but also took no account of possible non-Henrian behaviour. By a fresh statistical treatment of his experimental data, we can fit a plane instead of the existing curve:-

If K is Bower's equilibrium constant

$$= p_{CO_2} / p_{CO}\ [O]$$

and K' is a corrected constant = $p_{CO_2} / p_{CO} f_o[O]$
(where f_o is the Henrian activity coefficient)

Then: $\log K = \log K' + \log f_o$

$$= \frac{A'}{T} + B + c\,[O]$$

$$= \frac{9087}{T} - 3.353 - 0.28\,[O]$$

The two estimates of "c" are in line with the value -0,20 for oxygen in iron quoted by an authoritative text (76). Young found that oxygen in copper also showed a negative deviation from Henry's Law (39, cited in 80). Then at infinite dilution the free energy of solution is corrected to lower negative values closer to those of Fischer and Ackermann. The same reasoning could be applied to the expression of Tankins et al.

The German workers used an electrochemical method of measuring activities. They did not find any positive evidence of non-Henrian behaviour although their highest oxygen content was only 0.18%. In this range, any errors due to deviations from Henry's Law would be very small.